Nanotoxicology: Pulmonary Toxicity Studies on Self-Assembling Rosette Nanotubes

A Thesis Submitted to the College of Graduate Studies and Research in partial fulfillment of the requirements for the degree of Doctor of Philosophy in the

Toxicology Graduate Program
University of Saskatchewan
Saskatoon, SK, Canada

William Shane Journeay

Keywords: nanotoxicology, lung inflammation, nanomedicine, nanotechnology

Permission to Use

In presenting this thesis in partial fulfillment of the requirements for a Postgraduate degree from the University of Saskatchewan, I agree that the Libraries of this University may make it freely available for inspection. I further agree that permission for copying of this thesis in any manner, in whole or in part, for scholarly purposes may be granted by the professor or professors who supervise my thesis work or, in their absence, by the Head of the Department or the Dean of the College in which my thesis work was done. It is understood that any copying or publication or use of this thesis or parts thereof for financial gain shall not be allowed without my written permission. It is also understood that due recognition shall be given to me and to the University of Saskatchewan in any scholarly use which may be made of any material in my thesis.

Requests for permission to copy or to make other use of material in this thesis in whole or part should be addressed to:

Chair of the Toxicology Group
Toxicology Centre
University of Saskatchewan
Saskatoon, Saskatchewan, S7N 5B3
Canada

Abstract

A growing demand for information on the human health and environmental effects of materials produced using nanotechnology has led to a new area of investigation known as nanotoxicology. Research in this field has widespread implications in facilitating the medical applications of nanomaterials but also in addressing occupational and environmental toxicity concerns. Improving our understanding of these issues also has broad appeal in the stewardship of nanotechnology and its acceptance by the public. This work represents some of the early research in the field of nanotoxicology. Using a variety of *in vivo* and *in vitro* models, as well as cellular and molecular techniques I first studied a possible role for the novel cytokine endothelial monocyte activating polypeptide-II (EMAP-II) in acute lung inflammation in rats (Chapter 2). This work demonstrated a significant increase in total EMAP-II concentration in lipopolysaccharide inflamed lungs as early as 1h post-treatment ($P<0.05$). Increased numbers of monocytes and granulocytes were also observed in lungs treated with mature EMAP-II relative to control rats ($P<0.05$), and the recruitment of cells did not occur via upregulation of either Interleukin-1β or Macrophage inflammatory protein-2. I further studied whether mature EMAP-II can be induced in pulmonary nanotoxicity studies by exposure to rosette nanotubes (RNT) (Chapters 3-5). In the first *in vivo* experiments in mice on the RNT(**1**)-G0 (Chapter 3) I showed an acute inflammatory response at the 50 μg dose by 24h, but this response was resolving by 7d post-exposure as evidenced by a decreased number of cells in the bronchoalveolar lavage fluid ($P<0.05$) and from histological examination. The results of this study indicated that water soluble and metal-free rosette nanotubes can demonstrate a favorable acute pulmonary toxicity profile in mice. Subsequently, I studied

the responses of the pulmonary epithelium using the human Calu-3 cell line (Chapter 4). This experiment indicated that RNT(**2**)-K1 neither reduces cell viability at 1 or 5 μg/ml doses nor does it induce a dose-dependent inflammatory cytokine response in pulmonary epithelial cells *in vitro*. My final experiment (Chapter 5) studied the human U937 pulmonary macrophage cell line since the macrophage is one of the key defense mechanisms to encounter RNT in the lung environment. The data indicate that this cell line lacks a robust inflammatory response upon exposure to RNT and that when RNT length is changed by altering the conditions of nanotube self-assembly, cytokine release into the supernatant is not affected profoundly. Although, EMAP-II is upregulated in a lipopolysaccharide model of lung inflammation, it does not serve as a good marker of RNT exposure. The data indicate that RNT have a favourable toxicity profile and these experiments provide a framework upon which rosette nanotubes can be investigated for a range of biomedical applications. Furthermore, in light of media and scientific reports of nanomaterials showing signs of toxicity, this work demonstrates that a biologically inspired nanostructure such as the RNT can be introduced to physiological environments without acute toxicity.

Acknowledgements

My time in Saskatoon and at the University of Saskatchewan would not have been possible without the encouragement and guidance of many people.

I would like to thank my supervisor Dr Baljit Singh. Few, supervisors would accept the risk in allowing a student to pursue an area of research foreign to both of us. Furthermore, I was given the intellectual freedom to develop this area of work and I look forward to watching it grow at the University of Saskatchewan.

Secondly, I would like to thank Dr Barry Blakley who played a major role in the process that led to me choosing the University of Saskatchewan's toxicology graduate program. His endless wisdom, experience in toxicology and professional guidance has helped me tremendously.

Dr Niels Koehncke. It could not have been better timing for me to meet you when I arrived here, as our similar interests in occupational and aerospace medicine added the perfect touch to my training. I look forward to continuing our relationship as I navigate through the medical world in the coming years.

I would also like to thank Dr Vikram Misra for his timely contribution to my committee and for allowing me to gain insight into the relationship between viruses and nanostructure design. I also thank Dr Rajendra Sharma for serving on my committee.

I also thank the Natural Sciences and Engineering Research Council of Canada and the Canadian Institutes of Health Research for selecting me for doctoral scholarships to fund my education.

My transition to a PhD would not have been as smooth without solid preparation in my Masters work. For that I thank Dr Glen Kenny and Dr Frank Reardon of the University of Ottawa for their excellent scientific mentorship.

Finally, I would like to thank my parents for their endless support.

Table of Contents

List of Figures

List of Abbreviations

ALI	Acute lung inflammation
BALF	Bronchoalveolar lavage fluid
CNT	Carbon nanotubes
ELISA	Enzyme-linked immunosorbent assay
EMAP-II	Endothelial monocyte-activating polypeptide-II
HRN	Helical rosette nanotubes
HRP	Horse Radish Peroxidase
H&E	Hematoxylin and Eosin
ICAM-1	Intercellular adhesion molecule-1
IL-1β	Interleukin-1 Beta
IL-8	Interleukin-8
LPS	Lipopolysaccharide
MCP-1	Monocyte chemoattractant protein-1
MIP-2	Macrophage-inflammatory protein-2
MWNT	Multi walled carbon nanotubes
NASA	National Aeronautics and Space Administration
RNT	Rosette nanotubes
SEM	Scanning electron microscopy
TEM	Transmission electron microscopy
TPA	12-*O*-tetradecanoylphorbol 13-acetate
SWNT	Single walled carbon nanotubes
TNF-α	Tumour necrosis factor-alpha
TLC	Total leukocyte count
qRT-PCR	Quantitative real time reverse-transcriptase polymerase chain reaction

Preface

This dissertation details the first work on the pulmonary toxicity of novel self-assembling rosette nanotubes. The experiments are interdisciplinary in nature and represent some of the preliminary studies in the burgeoning field of nanotoxicology. The ongoing theme in these chapters is the development of inflammatory responses in lung tissue. It begins with a known model of lipopolysaccharide-induced lung inflammation in Chapter 2, and progresses to a pulmonary *in vivo* assessment of rosette nanotube toxicity in Chapter 3. In Chapters 4 and 5 the inflammatory responses of two specific lung cell lines after exposure to rosette nanotubes are profiled.

The data has been organized as manuscripts for publication in scientific journals and therefore some overlap may occur in the introductory sections of each chapter. Additionally, an abstract is included at the beginning of each experimental chapter. At present Chapter 2 has been published in *Inflammation Research*, Chapter 3 is submitted to *ACS Nano* and Chapter 4 has been accepted in the journal *SMALL.* Chapter 5 is in preparation for publication and an additional piece of this work was requested and published in the journal *Integrated Environmental Assessment and Management* as a 'Learned Discourse'. It should also be noted that a number of important activities outside the research program have been generated from this work including invited presentations on nanotoxicology to: United States Environmental Protection Agency, Health Canada, American Industrial Hygiene Association, the Alberta Occupational Health Nurses Association, and CIHR Nanomedicine Symposium. Additionally, I contributed to an international team project on micro and nanotechnologies in the space industry while

representing Canada at the International Space University Summer Session Program in Strasbourg, France 2006.

Chapter 1 provides the background information on nanotechnology and the context for the development of nanotoxicology. Chapter 2 presents data on a rat model of acute lung inflammation and identifies for the first time that endothelial monocyte-activating polypeptide-II (EMAP-II) is upregulated in response to LPS and that it is chemotactic for inflammatory cells *in vivo.* These findings provided the basis to study EMAP-II as a possible marker, in addition to the use of established markers of inflammation, of rosette nanotube induced inflammation. Chapter 3 presents the first *in vivo* pulmonary toxicity data on the water soluble rosette nanotubes in mice. Chapter 4 profiles the isolated inflammatory profile of pulmonary epithelium using the human Calu-3 cell line. Chapter 5 includes data on the responses of the human U937 pulmonary macrophage cell line after exposure to rosette nanotubes and tests the effect of nanotube length on cytokine secretion. Chapter 6 discusses the interrelationship of these chapters in the context of nanotoxicology research and provides future avenues of study for the rosette nanotubes.

CHAPTER 1

Introduction and Review of Literature

1.1 Background

Nanotechnology bridges scientific disciplines such as chemistry, biology, physics and engineering, and provides a wide range of applications on the nanoscale in broad areas of society. In fact nanotechnology is projected to be so ubiquitous in the world it is considered a disruptive technology. A disruptive technology is one that permeates all areas of industry and can eventually lead to the demise of firms not utilizing such applications (Christensen, 1997). The wide impact of a disruptive technology, can be exemplified by the advent of personal computers. Thomas Watson stated in 1943, 'There is a worldwide market for maybe five computers'.

Today, the next big thing is really small and our ability to work at the molecular level will undoubtedly facilitate the discovery of new or improved value-added products in which our very understanding of their function depends on nanoscale, biology, chemistry and physics. As with any new technology that moves as fast as nanotechnology the societal impacts are being debated. A central issue is the potential human and environmental costs and benefits of this technology. These impacts are being portrayed in both a positive and negative light. On one hand, nanotechnology is being hailed for green energy as well as improved drugs and diagnostic ability for diseases such as cancer. However, these benefits are being tempered by some groups raising concern over occupational, environmental and consumer health effects from nanomaterial exposure.

At the core of this debate is our knowledge that materials on the nanoscale do possess some unique physicochemical properties which are of prime interest. Whether or not they lead to novel toxicities, and to what degree humans and the environment will be exposed to them, is difficult to answer given the paucity of nanotoxicology data and the lack of personnel presently qualified to tackle such issues. Conversely, an understanding of how to exploit the novel properties of nanoscale materials for societal benefit will be paramount to the maturation of nanotechnology.

Regardless of the purported use of nanomaterials, the toxicologist with a sound knowledge of the technology will be a key to overcoming such barriers as scalability of the nanostructure, commercialization and public acceptance. A broad understanding of the basic sciences and knowledge of the value-added properties of nanotechnology will be required. The following work combines the fields of molecular biology, chemistry, and pulmonary biology to address toxicity questions related to novel self-assembling nanotubes.

1.2 Nanotechnology

1.2.1 What is nanotechnology?

The advancement of technology in the past decade has allowed scientists to explore the design of materials on a much smaller scale than ever before. Thus, nanoscience has resulted in a greater focus on the unique interactions and behaviour of nanoscale materials and has subsequently fuelled the field of nanotechnology. Nanotechnology has generated vast interest in the scientific and general community and some have termed it the “nanotechnology revolution”, or the next industrial revolution

(Donaldson *et al.*, 2004) and even today's version of the space race (Hood, 2004). Nanotechnology can be defined as "… the manipulation, precision placement, measurement, modeling or manufacture of sub-100 nanometer scale matter…" (Meyer *et al.*, 2001). Other factors which can characterize nanotechnology according to the US National Nanotechnology initiative include: a) research and technology development at the atomic, molecular or macromolecular levels in the length scale of approximately 1-100 nanometer range; b) creating and using structures, devices and systems that have novel properties and functions because of their size; and c) the ability to control or manipulate on the atomic scale (Karluss & Sayre, 2005). Others have defined a nanoscale material as "those structured components with at least one dimension less than 100nm" (Royal Society, 2004). The capability to exploit the properties of nanoscale materials is what drives the development of nanotechnology. Such properties include altered conductivity, chemical reactivity and optical activity when in the nanoscale format (Hood, 2004). Thus, the ability to engineer and exploit matter at the nanoscale has far reaching implications for materials science, electronics and medicine to name a few. The medical applications are particularly promising as the use of nanotechnology to study phenomena and treat disease at the cellular and molecular level develops.

1.2.2 Nanomaterials

It is important to note that nanomaterials per se are not a new concept. In fact materials on the nanoscale have been present in the environment for centuries and include sea salt, by-products of forest fires and volcanic eruption. There is also increasing production of anthropogenic particulate from diesel fuel combustion and industrial emissions (Donaldson *et al.*, 2005). Early investigations of particles tended to focus on

micro-sized components however the past decade has seen the examination of ultrafine or nanoscale particles (1-100nm) as a contributor to observed health effects during episodes of high air pollution (Oberdorster *et al.*, 1995; Seaton *et al.*, 1995). Thus, many terms have been used in recent literature such as nanoparticles, nanosized particles, nanomaterials, nanoscale materials and ultrafine particles. The term 'ultrafine' primarily stems from studies on particulate matter or those related to occupational hygiene. The 'nano' terms allude to the nature of modern engineered materials derived from nanotechnology that are manufactured with certain specifications in laboratory or industrial environments (Karluss & Sayre, 2005). Careful consideration is being given to issues of nomenclature and defining nanotechnology in different disciplines, as it will significantly effect the regulatory actions towards new products.

Presently, nanotechnology-related activities are abundant internationally, although Canada does not have a federal nanotechnology strategy in place. Nanomaterials are already used in a wide range of products such as sunscreens, composites, medical devices and catalysts with approximately 500 products on the market claiming to be 'nanotechnology' based. This field is in its relative infancy but the quantity of nanomaterials manufactured is expected to increase tremendously in the next five years with a projected ten billion dollar global demand for nanoscale materials, tools and devices by 2010 (Hood, 2004), while others estimate a one trillion dollar market for nanotechnology by 2015 (Nel *et al.*, 2006). At present nanoscale silicates, metal oxides, quantum dots and fullerenes are the most plentiful and commercially viable (Aitken *et al.*, 2006). With such an enormous demand for materials comes a need for workers to mass produce the materials thus presenting a new challenge to the occupational medicine

and health regulatory communities to develop policies and safety measures to ensure proper implementation of their handling.

1.2.3 Carbon nanotubes

There is a general tendency to consider all nanoparticles as spherical in shape however nanomaterials may be nano sized in only one dimension and significantly larger in another. Thus, a subclass of nanoparticles can be considered high aspect ratio nanoparticles and includes nanotubes, nanorods and nanowires (Oberdorster *et al.*, 2007). Carbon nanotubes (CNT), which have a large length to diameter aspect ratio, are one of the most studied nanomaterials because of their novel physicochemical properties which include high surface area, high mechanical strength yet ultra-light weight, rich electronic properties and chemical and thermal stability (Ajayan, 1999). Two common types of CNT are the single-walled carbon nanotubes (SWNT) which are formed by a cylindrical sheet of graphite with a diameter of 0.4-2 nm, and the multi-walled carbon nanotubes (MWNT) which have multiple concentric graphite cylinders with increasing diameter ranging from 2-200 nm (Dresselhaus *et al.*, 1996). Single-walled nanotubes have received attention primarily as a possible inhalation toxicant (Lam *et al.*, 2004; Warheit *et al.*, 2004; Shvedova *et al.*, 2005), and carbon nanotubes in general also have potential for biomedical applications (Bianco & Prato, 2003; Martin & Kohli, 2003; Bianco, 2004; Lin *et al.*, 2004; Polizu *et al.*, 2006). In order for CNT to be used for biomedical applications they typically need to become soluble and or functionalized with the additional of surface molecules (Georgakilas *et al.*, 2002; Pantarotto *et al.*, 2003; Hudson *et al.*, 2004; Lin *et al.*, 2004). Indeed, the compatibility of water soluble carbon nanomaterials such as fullerenes and SWNT are functionalisation dependent (Sayes *et al.*, 2004; Sayes *et al.*,

2005). The ability to functionalize nanomaterials has raised the possibility of 'engineering in' the properties of a nanomaterial that confer reduced toxicity. The experiments herein were directed towards the toxicity evaluation of the rosette nanotubes and therefore experimental comparisons with other classes of nanotubes were not conducted.

1.2.4 Rosette nanotubes

Self-assembled rosette nanotubes (RNT), are a novel class of biologically inspired nanotubes that are naturally water soluble upon synthesis (Fenniri *et al.*, 2001; Fenniri *et al.*, 2002a; Fenniri *et al.*, 2002b). 'Biologically inspired' refers to an approach within nanotechnology that attempts to mimic self-assembly mechanisms provide by nature to synthesize new structures. In this, context, the RNT are obtained through the self–assembly of the G∧C motif, a self–complementary DNA base analogue featuring the complementary hydrogen bonding arrays of both guanine and cytosine. The first step of this process is the formation of a 6–membered supermacrocycle (rosette) maintained by 18 hydrogen bonds, which then self–organizes into a tubular stack defining an open central channel of 1.1 nm diameter and several micrometers of length (Fenniri *et al.*, 2001; Fenniri *et al.*, 2002a; Fenniri *et al.*, 2002b; Raez *et al.*, 2004; Moralez *et al.*, 2005; Johnson *et al.*, 2007). Upon self-assembly, in principle any functional group covalently attached to the G∧C motif could be expressed on the surface of the nanotubes, thereby offering versatility in functionalization of the RNT for specific medical or biological applications. For preparation and characterization details of the nanotubes studied in this work see the methods section of each chapter.

1.2.5 Nanoparticle synthesis

In the life sciences, nanotechnology has spawned new creativity in drug delivery and biomaterials to enhance interactions at the cellular and molecular level. While chemists use nanotechnology to seek new ways of encapsulating important compounds for biomedical applications, nature has already provided us with a number of nanoscale materials for use in nanotechnology. Nanoscale structures of virus-like particles are complex and have been fine-tuned for eons of evolutionary processes. These natural assemblies can come in different shapes, sizes and have varying properties and thus can be applied in nanotechnology for use in materials science, engineering, and as building blocks for chemistry, electronics and biomedical applications (Singh *et al.*, 2006a). Specific properties of virus-like particles that make them attractive for nanotechnology are their uniform structures and particle sizes, potential for mutagenesis to manipulate the proteins, particle stability, accessibility to the particle interior, and ease of production (Singh *et al.*, 2006a). The use of virus structures and virus-like particles allows for natural starting structures on the nanoscale, which are uniform in composition. Biological entities such as viruses and DNA underscore the nanofabrication process known as self-assembly. Self-assembly is the basis of formation of the rosette nanotubes and can also be considered a bottom-up process. Conversely, top-down approaches begin with bulk material to arrive at the desired nanostructure.

1.3 Nanotoxicology – "science of engineered nanodevices and nanostructures that deals with their effects in living organisms" (Oberdorster *et al.*, 2005b)

Particle and fiber toxicology is a relatively mature field of study. Correlations of exposure to various particulates and the manifestation of disease were already being made early in the 20th century. One of the classic examples is that of asbestos. In 1924, Cooke published a paper in the British Medical Journal relating asbestos exposure to fibrosis of the lungs (Cooke, 1924). However, it was not until the 1970s that legislative action occurred for occupational exposures. This example is commonly used by opponents to the rate of nanotechnology development, who suggest that a similar consequence to nanomaterial exposure might be experienced.

The industrial revolution also stimulated research into the field of particle toxicology with particular focus on coal dust, diesel particles and various forms of quartz (Borm, 2002; Borm & Tran, 2002). In the 1980s an association between ambient particulate matter and human health became apparent, while the specific emphasis on ultrafine particles was linked to cardiovascular events in the early 1990s (Seaton *et al.*, 1995). Thus a significant body of literature exists on ultrafine particles and therefore serves as a launch point for our understanding of nanoscale materials (Oberdorster *et al.*, 2005b).

It is because of the data on ultrafine particulate matter toxicity that concerns over nanomaterials have developed. The key difference between ultrafine particulates and nanomaterials is the range of compositions. Ultrafine particulate is usually combustion derived and contains a mixture of carbon and metals which adsorb to the particle surface. Nanomaterials, while having some overlap with the nature of ultrafine particles, tend to be more focused on structures which exploit novel properties conferred at the nanoscale

or those that have been engineered at the nanoscale for a specific purpose. It is the possibility of generating large quantities of new nanostructures (within the confines of entropy) which has led to the development of nanotoxicity research. At present the ability to produce nanostructures using a top-down method is the most mature, while bottom-up approaches are developing rapidly. The rosette nanotube in this work is a bottom-up approach and is produced via self-assembly.

Materials on the nanoscale exhibit a range of attractive properties for new products and applications but also confer unique challenges for toxicity evaluation (Nanotoxicology, 2004). Such physicochemical characteristics include: size, surface area, number of particles and reactivity. By virtue of the physical size of nanostructures, their potential to interact with biological receptors is altered. Moreover, as particle size decreases a greater proportion of atoms and molecules are displayed on the surface rather than the interior of the material (Nel *et al.*, 2006). The increase in surface area determines the potential number of reactive groups on the particle surface (Nel *et al.*, 2006) and thus the reactivity of the particle may be enhanced. One example of increased activity of particles at the nanoscale is that of gold which shows a spike in reactivity below the 100 nm size (Daniel & Astruc, 2004). This also highlights the issue of nomenclature and toxicity testing, such that two particles both considered as gold may display different dose-response relationships based on the size dependent properties. Such properties also have significant implications for determining occupational exposures and interpretation of toxicity data for risk assessment purposes. To this end, I attended a workshop titled '*Developing experimental approaches for the evaluation of toxicological interactions of nanoscale materials*' in Gainesville, Florida in November 2004. The results of this

workshop helped shaped the current framework for nanotoxicology testing, and the recommendations have generally been upheld in a key publication encapsulating the suggested testing guidelines (Oberdorster *et al.*, 2005a). The present work represents the first toxicity data on a self-assembling nanotube and contains elements of a tiered nanotoxicology screening strategy, proposed at the above workshop.

1.4 Lung inflammation and inflammatory cell recruitment

Inhalation toxicology is deeply rooted in not only our understanding of the toxicant or drug properties but their interaction and kinetics within the lung environment. The respiratory tract is a primary route of exposure to environmental pathogens and its structure and function have evolved as an intricate first line of defense for both innate and adaptive immunity (Nicod, 2005). From a toxicological perspective the interrelationship between the environment and the lung has a long history ranging from chronic occupational exposures, acute lethal incidents of hydrogen sulphide exposure, as well as cardiovascular morbidity and mortality observed in subsections of the population with cardiovascular and respiratory diseases during episodes of high air pollution (Oberdorster *et al.*, 1995; Seaton *et al.*, 1995). Clinically, the acute lung inflammatory response is of great concern in septic patients (Piantadosi & Schwartz, 2004). The acute inflammatory response in the lung is typified most commonly by activation of resident alveolar macrophages, as well as epithelial and endothelial cells. In addition, an influx of monocytes and neutrophils occurs (Kobayashi, 2006). While the inflammation pattern, time course and long-term effects may differ between toxicants, inflammatory stimuli lead to the induction of pro-inflammatory chemokines and cytokines such as IL-8, IL-1β,

TNF-α (Driscoll *et al.*, 1997; Driscoll, 2000; Goodman *et al.*, 2003), and by extension the downstream pleiotropic effects of these cytokines further amplify the inflammatory cascade. Additionally, reactive oxygen species produced by invading neutrophils cause damage to the blood-air barrier leading to edema formation (Abraham *et al.*, 2000b; Ning *et al.*, 2004).

A pivotal cellular process in pulmonary toxicology is the alveolar macrophage response to particulate that is inert in nature (Lehnert, 1992; Kobzik, 1995; Dorger & Krombach, 2000, 2002). This is important because if one considers that a gram negative bacterial component such as lipopolysaccharide (LPS) binds to a specific Toll-like receptor-4 leading to the activation of macrophages, it leads to the question how do alveolar macrophages become specifically activated by inert particulate such as silica or asbestos? Alveolar macrophages not only bind certain bacteria to produce proinflammatory mediators but they also phagocytose the material, digest it through chemical breakdown, thereby initiating and then resolving the pro-inflammatory signal (Bowden, 1984; Savill *et al.*, 1989; Duffield, 2003). Furthermore, there has been substantial evidence that macrophages phagocytose apoptotic cells such as neutrophils and upon engulfing an apoptotic cell they become quiescent and the proinflammatory signal is shut off (Savill *et al.*, 1989). Uptake of foreign agents or inert particles (apoptotic bodies) induces a proinflammatory or anti-inflammatory signal that is dependent upon a variety of molecular factors (Duffield, 2003). A unique aspect of phagocytosis of inhaled silica or asbestos fibers is the inability of alveolar macrophages to digest them leading to macrophage rupture and the release of proteolytic enzymes, and chemoattractants such as MIP-2 leading to an influx of neutrophils (Laskin & Pendino,

1995). Under the low-stress of moderate particle load, the alveolar macrophages deliver the particles to the mucociliary escalator for expectoration or swallowing. With high exposures, the capacity of the alveolar macrophage to deliver particles to the mucociliary escalator can be overwhelmed and the proinflammatory signal would persist (Lehnert, 1992; Oberdorster *et al.*, 1994). Therefore, the biologically strategic positioning of the alveolar macrophage to engulf and remove foreign material may cause an initial inflammatory response but ultimately rescues the most sensitive alveolar and interstitial regions of the lung from particle burden (Lehnert *et al.*, 1985; Lehnert, 1992; Kobzik, 1995; Kreyling *et al.*, 2006). While it was previously considered that interstitialization of inert particles was minimal, it has become a greater issue with increased atmospheric ultrafine particulate matter and with the impending boom of nanomaterial production. Even though much of the toxicity from nanoparticles is due to oxidative stress (Xia *et al.*, 2006), there is some evidence to suggest that the alveolar macrophage may not be as efficient at detecting and engulfing the smaller particles. Whether this is a chemotactic recognition problem or biomechanical constraint remains to be determined (Renwick *et al.*, 2001; Moller *et al.*, 2002; Renwick *et al.*, 2004).

The mechanisms of neutrophil and monocyte recruitment are incompletely understood. Although the major steps of neutrophil influx into inflamed lungs are well characterized, those operating in monocyte recruitment are far from elucidated. Monocyte chemoattractant protein-1 (MCP-1) is known to promote monocyte recruitment into lungs (Maus *et al.*, 2001; Maus *et al.*, 2002). However, it was found that MCP-1 may require the presence of neutrophils to exert its full actions (Janardhan *et al.*, 2006). Therefore, because the resolution of inflammation and the maintenance of alveolar macrophage

populations requires migration of new monocytes into the alveoli, it is important to understand the mechanisms that regulate recruitment of monocytes into the lungs. Following the findings that MCP-1 alone may not be sufficient to induce migration of monocytes in acute lung inflammation, I focused my attention on a novel antiangiogenic molecule called endothelial monocyte-activating polypeptide-II (EMAP-II). EMAP-II is well recognised as a regulator of angiogenesis, but its inflammatory properties such as the ability to recruit monocytes in lung inflammation remain unknown. Therefore, I decided to investigate expression and function of EMAP-II in lung inflammation with an intent to study its expression in lungs exposed to rosette nanotubes.

1.5 Pulmonary toxicology of nanomaterials

Given the large base of literature on inhalation toxicants such as ultrafine particles, it is generally accepted that nanomaterials may have the propensity to become airborne during production or handling in the industrial environment. Conversely, pulmonary delivery of therapeutics holds promise for treating disease (Pison *et al.*, 2006), and therefore an understanding of the fate of particulate nanostructures in the lung is required. Indeed, nanotoxicology research will not only provide data for safety evaluation of engineered nanostructures and devices but will also help to advance the field of nanomedicine by providing information about their undesirable properties and means to avoid them (Kagan *et al.*, 2005; Oberdorster *et al.*, 2005b).

One of the first properties unique to nanostuctures in the realm of inhalation toxicology is the relation of size and deposition pattern. The particles with a diameter below 0.1 μm (100 nm) show increasing deposition in the alveolar region of the lung

(ICRP, 1994). This area of the lung is highly vascular, and therefore particles entering this region may have a greater probability of translocating to the interstitium or blood as preliminary studies show that such translocation although minimal can occur (Nemmar *et al.*, 2001; Kreyling *et al.*, 2002; Nemmar *et al.*, 2002; Oberdorster *et al.*, 2002). The extent and toxicological significance of extrapulmonary particle translocation continues to be a source of debate (Ghio & Bennett, 2007; Oberdorster & Elder, 2007; Semmler-Behknke *et al.*, 2007). It should also be noted that the pulmonary deposition patterns for nanotubes are unknown at present.

Another novel issue that has been raised in the study of nanoparticles in the lungs is the correct dose metric. This was first highlighted by exposing rats to 20 and 250 nm TiO_2 which suggested that surface area and not mass or particle number was the best metric to express the dose-response data (Oberdorster, 2000). In workshops on this issue (Nanotoxicology, 2004) and in the literature (Wittmaack, 2007) the appropriate metric continues to be sought after and it is likely that the answer will not be uniform for all nanostructures which further complicates the issue of metrics in nanotoxicology. Despite this challenge, adequate characterization data, and reporting of the mass, surface area and particle number will allow for analysis of these issues as the field matures. Developing new nanostructures and attributing specific nanotechnology-added properties to biological responses will ride a fine line between scientific objectivity and teleology.

1.5.1 *In vivo* pulmonary toxicology studies of nanotubes

Concern over possible adverse human health effects of engineered nanomaterials was in large part initiated by the first pulmonary toxicology study on single-walled carbon nanotubes at the NASA Johnson Space Center (Lam *et al.*, 2004). This particular

study had some criticism over the doses chosen but considering it was the first paper of its kind, their observations served as a building block for future studies of SWNT in the lungs. Moreover, this work began to highlight some of the difficulties in toxicological experimentation with nanoscale materials. Subsequent *in vivo* studies (Warheit *et al.*, 2004; Shvedova *et al.*, 2005; Mangum *et al.*, 2006) have been performed on the SWNT with a few key conclusions being submitted. These studies showed granuloma formation in the lungs of mice and the debate continues over the toxicological significance of this response. It is possible that granuloma formation may be a protective response to encapsulate the aggregated nanotubes and that it leads to pathology of no toxicological significance. Secondly, the evidence from this work suggests that SWNT produce a unique fibrogenic response in the lungs of C57/BL mice (Shvedova *et al.*, 2005). Specifically, it was observed that in addition to a fibrogenic response associated with the deposition of nanotube aggregates, fibrosis was also apparent in alveolar septa distant from deposition sites of aggregates and in the absence of persistent inflammation. Another key factor in SWNT toxicity in the lungs is the metal content of the tubes which can lead to significant oxidative stress (Donaldson *et al.*, 2006), and this is further exacerbated by batch to batch variation of the nanotubes.

The interest in SWNT toxicology is driven by concerns over occupational exposure during production and handling of the material. This is also of immediate interest because the SWNT are likely to be produced in commercial amounts as is occurring in ton quantities at select plants in Japan. To this end, one preliminary study on the propensity of SWNT to become airborne during laser ablation production at the NASA Johnson Space Center showed that levels of material in the air appear to be low

unless intentionally agitated vigorously (Maynard *et al.*, 2004). At present, adequate technology to measure airborne SWNT alone does not exist, nor have the pulmonary deposition patterns of SWNT been resolved. It should also be noted that the airborne content of SWNT will be dependent on engineering processes. Laser ablation synthesis is a combustion reaction whereas the chemical vapour deposition method of nanotube synthesis is a more controlled process (Awasthi *et al.*, 2005). Regardless of production method, a concern still exists over exposures throughout the lifecycle of SWNT, particularly as commercial quantities are being produced and handled. Given the lack of data on workplace exposures and therefore realistic aerosol exposures on animals, current toxicity data must be treated cautiously. The present work is the first to examine the effect of a water-soluble self-assembling nanotube on the pulmonary system and provides a framework for the feasibility of using nanostructures for pulmonary biomedical applications such drug delivery (Hung, 2006; Moghimi & Kissel, 2006; Pison *et al.*, 2006).

1.5.2 *In vitro* studies of nanotoxicity

Just as epidemiology, human clinical and animal studies provide strong approaches to evaluating pulmonary toxicological response to particles, *in vitro* approaches are also used (Devlin *et al.*, 2005). When investigating mixtures of a toxicant such as air pollution an integrated interpretation of these approaches is used to answer research questions. The ideal goal in particle toxicology would position *in vitro* screening tests at the base of a tiered testing strategy. Moreover, the data gleaned from such studies would ideally be predictive of *in vivo* responses. Recent work suggests that their predictive value for *in vivo* responses is not accurate for some particle types (Sayes *et al.*,

2007b). It is likely due to the complex interplay of cellular and molecular responses involved in the lung inflammatory response, which involves the interaction of lung biology with exposure to and fate of toxicants. While *in vitro* nanotoxicology studies may not adequately predict the global *in vivo* responses or possible pathology, they are essential to answering some of the fundamental questions pertinent to toxicology such as specific cellular responses including cytokine activation, nanoparticle uptake, sub cellular fate, signaling pathways and induction of oxidative stress and associated reactive oxygen species.

The present work has examined inflammatory activation in two cellular targets likely to encounter nanotubes during pulmonary exposure; the epithelium and macrophages. Specifically, we studied the human Calu-3 epithelial cell line and the human U937 human macrophage cell line, in an effort to study the qualitative contribution to the acute inflammatory response *in vivo.*

1.6 Objectives and working hypothesis

Objectives:

Chapter 2 **–** To determine the expression and function of endothelial monocyte-activating polypeptide-II in lipopolysaccharide-induced acute lung inflammation.

Chapter 3 – To study the acute pulmonary responses after exposure to self-assembling nanotubes in mice.

Chapter 4 **–** To determine the time course of epithelial cell activation from direct exposure to rosette nanotubes *in vitro.*

Chapter 5 – To determine the inflammatory activation of human U937 macrophages after exposure to rosette nanotubes and to determine the effect of nanotube length on cytokine secretion.

Working hypothesis:

Self-assembling nanotubes will demonstrate a favorable pulmonary toxicity profile *in vivo* and *in vitro* due to their biologically inspired and water soluble architectures.

CHAPTER 2

Expression and function of endothelial monocyte-activating polypeptide-II in acute lung inflammation

2.1 Abstract

I tested the hypothesis that total endothelial monocyte-activating polypeptide-II (EMAP-II) expression (proEMAP/p43 and mature EMAP-II) is up-regulated in lipopolysaccharide (LPS)-induced acute lung inflammation (ALI) and that mature EMAP-II induces monocyte/macrophage and granulocyte recruitment *in vivo.* Thirty-five 10 week old, male Sprague-Dawley rats were instilled intratracheally with 250μg of *E. coli* LPS (N=15) or saline (N=5) or 20μg of mature EMAP-II (N=5). Total EMAP-II was quantified using an enzyme linked immunosorbent assay (ELISA) and the protein was localized with light and electron microscopic immunocytochemistry in lungs of rats at 1, 3 and 12h (n=5/group). Enzyme linked immunosorbent assay showed increased total EMAP-II concentrations ($p<0.05$) in lungs from LPS-treated rats compared to control animals. Compared to the control rats, light and electron microscopic imunocytochemistry localized total EMAP-II in monocytes/macrophages and alveolar septa at 1 and 3 h and in vascular smooth muscles at 12 h post-LPS treatment. Instillation of mature EMAP-II increased lung monocytes/macrophages and granulocytes compared with control animals ($p<0.05$). However, compared to the LPS treatment, mature EMAP-II instillation did not induce expression of IL-1β and Macrophage inflammatory protein-2 ($p<0.05$) and provoked less vigorous recruitment of monocytes/macrophages. I conclude that endothelial monocyte-activating polypeptide-II expression is increased in LPS-induced ALI, and that intra-tracheal instillation of mature EMAP-II induces recruitment

of monocytes/macrophages and granulocytes into the lungs without stimulating IL-1β or MIP-2 expression.

2.2 Introduction

Acute lung injury (ALI) is a clinical condition that involves a complex inflammatory response, and in its most severe clinical manifestation is called acute respiratory distress syndrome (Abraham *et al.*, 2000a). The disease may be caused by acute chemical exposures or be the consequence of systemic infections. The pathophysiology of ALI is marked by epithelial and endothelial cell damage, cytokine and reactive oxygen/nitrogen species release, inflammatory cell sequestration and activation and prothrombotic events. An influx of neutrophils and monocytes into the lung occurs, which is a classical histological feature of acute lung inflammation (Abraham *et al.*, 2000a). The acute inflammatory response is multifactorial and yet more molecules playing a role in ALI are still being considered. While significant data exist on molecules that regulate entry of neutrophils into inflamed lungs, relatively little is understood of the mechanisms governing migration of monocytes. For example, recently it was shown that a potent chemokine MCP-1 alone is not sufficient to stimulate recruitment of monocytes in a rat model of LPS-induced lung inflammation (Janardhan *et al.*, 2006).

Mature endothelial monocyte-activating polypeptide II (EMAP-II) is a 22kDa protein, originally isolated from supernatants of methylcholanthrene A-induced fibrosarcoma cells (Kao *et al.*, 1992). Mature EMAP-II is derived from a precursor proEMAP-II/p43 molecule which is a part of the macromolecular aminoacyl-tRNA

synthetase complex (Quevillon *et al.*, 1997; Shalak *et al.*, 2001; Ivakhno & Kornelyuk, 2004). There is recent evidence that proEMAP-II/p43 of hamster, rat and sheep origin has a molecular weight of 43kD while that of humans is 34 kD (Quevillon *et al.*, 1997; Murray *et al.*, 2004). The immunohistological expression of aminoacyl-tRNA synthetase is ubiquitous in the human body, while the p43 component is cleaved and secreted under specific conditions (Knies *et al.*, 1998; Shalak *et al.*, 2001; Matschurat *et al.*, 2003). However, the expression of mature EMAP-II is even more restricted (Murray *et al.*, 2000). Specifically, mature EMAP-II is highly expressed in the developing murine lung and remains low during adult life (Schwarz *et al.*, 1999). Murray and colleagues observed occasional weak cytoplasmic staining of endothelial cells and alveolar macrophages, and a generally negative parenchyma and pneumocytes in human lungs (Murray *et al.*, 2000).

Although mature EMAP-II influences the physiology of angiogenesis, lung development and neural injury, there is evidence that proEMAP-II/p43 is also directly secreted from mammalian cells and stimulates fibroblast proliferation, wound repair, production of pro-inflammatory cytokines, expression of ICAM-1 and adhesion of monocytes (Ko *et al.*, 2001; Park *et al.*, 2002; Park *et al.*, 2005). It has also been shown *in vitro* that the physiological stimulants of mature EMAP-II expression include apoptosis (Knies *et al.*, 1998) and hypoxia (Matschurat *et al.*, 2003). The *in vitro* data show that EMAP-II up-regulates expression of P-selectin and E-selectin, causes release of von Willebrand factor, induction of tissue factor in endothelial cells and monocytes, and is chemotactic for monocytes and neutrophils (Kao *et al.*, 1994). Kao and colleagues (Kao *et al.*, 1992) demonstrated in the murine foot pad model that injection of mature EMAP-II provokes an inflammatory response typified by neutrophil infiltration and

edema. Subsequently, they observed an arrest of circulating leukocytes and other inflammatory cells in the pulmonary vasculature after systemic infusion of EMAP-II (Kao *et al.*, 1994). To date the expression and role of EMAP-II in acute lung inflammation has not been investigated and *in vivo* data are limited.

I hypothesized that total EMAP-II expression (proEMAP/p43 and mature EMAP-II) is upregulated in lipopolysaccharide (LPS)-induced ALI and that the mature EMAP-II is capable of inducing monocyte/macrophage and granulocyte recruitment *in vivo.* To test this hypothesis, I conducted experiments to 1) examine expression of total EMAP-II at various time points in an LPS model of ALI and 2) to evaluate the ability of mature EMAP-II to recruit monocytes/macrophages and granulocytes into the lungs after its intratracheal instillation.

2.3 Materials and Methods

2.3.1 *Animals*

All animal protocols in this study were approved by the University of Saskatchewan Committee on Animal Care Assurance, and each experimental procedure was conducted according to the Canadian Council on Animal Care Guidelines. A total of thirty-five 10 week old, specific pathogen free, male Sprague-Dawley rats were procured from Charles River Laboratories, Canada. The animals were acclimatized for a period of 1 week in the animal care unit prior to experimentation, and were randomly assigned to treatment groups. Rats were fed standard rat chow and weighed 350-500 g at the time of experiments.

2.3.2 *Induction of acute lung inflammation*

Rats (N = 15) were anesthetized by intraperitoneal administration of xylazine (20 mg/kg) and ketamine (100 mg/kg). The trachea was exposed surgically and rats were treated with *E. coli* LPS (250μg ; intratracheally) and euthanized at 1, 3 and 12 hours (n = 5 each) post-treatment. Control animals (n = 5) were prepared in the same manner and treated with 250μl of endotoxin-free saline intra-tracheally instead of the LPS and euthanized at 6 hours.

2.3.2 *Lung collection and processing*

Lungs for histology and immunohistochemistry were fixed in 4% paraformaldehyde for 16 hours. Lungs used for quantification of cells were filled with 4% paraformaldehyde at 23 cm H_2O pressure. Pieces of the lobes were later processed through ascending grades of ethanol and then embedded in paraffin. Tissue blocks were then cut into 5 μm sections for light microscopy. Lung samples for immunoelectron microscopy were fixed in 2% paraformaldehyde containing 0.1% glutaraldehyde for 3 hours at 4°C. These samples were dehydrated in ascending grades of alcohol and embedded in LR white resin followed by polymerization under UV light at -1°C for 48 hours. The tissue blocks were cut into 80-100nm sections.

2.3.4 *Antibodies and reagents*

The monoclonal antibody against the 22kD portion of EMAP II (mouse anti-human EMAP II) was purchased from Bachem California Inc, USA. This antibody will recognize both the proEMAP/p43 and mature EMAP-II proteins as it recognizes the C-terminus segment of the complex. The ED-1 antibody, which recognizes mononuclear phagocytic (monocytes and macrophages) cells, was purchased from Serotec Inc. The

mouse anti-rat granulocyte antibody was bought from PharMingen. Secondary HRP conjugated secondary antibodies were obtained from Dako Diagnostics Canada and the peroxidase substrate color development kit was purchased from Vector Laboratories, USA. Recombinant EMAP-II was purchased from Cell Sciences Inc., Canton, MA, USA. Endotoxin free saline and bovine serum albumin were purchased from Sigma-Scientific, USA. The EMAP-II and MIP-2 (macrophage inflammatory protein-2) ELISA kits were purchased from Medicorp Inc, Montreal, PQ, Canada; a distributor for Biosource, USA. Interleukin-1β ELISA detection and capture antibodies were purchased from R&D Systems.

2.3.5 *Enzyme linked- immunosorbent assay (ELISA)*

Frozen lung samples were homogenized in lysis buffer [150 mM sodium chloride, 1% NP-40, 0.5% sodium deoxycholate, 0.1% SDS, 50 mM TRIS (pH 8.0), 5 mM EDTA, and protease inhibitor cocktail (100 µl/10 ml)]. Homogenates were collected after centrifuging the samples at 25,000 g for 20 minutes. For quantification, samples in duplicates, from 3 rats for each time point were used. Because a commercial antibody that would exclusively detect the mature form of EMAP-II does not exist our ELISA recognizes both proEMAP/p43 and mature EMAP-II. The minimum detectable concentration of hEMAP-II is <100 pg/mL. Interleukin-1β and MIP-2 were quantified by sandwich ELISA using antibody pairs and recombinant standards purchased from R&D Systems and Biosource respectively.

2.3.6 *Immunohistochemistry*

The immunohistochemical protocol has been described previously (Janardhan *et al.*, 2004). Briefly, tissue sections were deparaffinized and rehydrated followed by

treatment with 5% hydrogen peroxide to quench endogenous peroxidase. Sections were treated with pepsin (2 mg/ml in 0.01 N hydrochloric acid) for 45 minutes to unmask the antigens and with 1% bovine serum albumin to block non-specific binding. Sections were incubated with primary antibody against EMAP-II (1:50) for 60 minutes followed by appropriate HRP conjugated secondary antibodies; normal mouse/goat–biotin in BSA (1:100) and streptavidin-HRP (1:300) for 30 minutes each. This EMAP-II antibody has previously been used by the Schluesener group to detect EMAP-II with immunocytochemistry (Schluesener *et al.*, 1997). Additional lung sections were incubated with mouse anti-granulocyte (1:50) or anti-monocyte/macrophage ED-1 antibody (1:400) for 60 minutes followed by an appropriate HRP conjugated secondary antibody in BSA (1:100 for granulocytes) for 30 minutes. The antigen–antibody complex was visualized using a color development kit. Control tests consisted of staining without primary antibody or with normal mouse IgG instead of primary antibody.

2.3.7 *Immunogold electron microscopy*

Ultrathin sections (80 – 100 nm) were incubated with 1% bovine serum albumin to block non-specific sites. This was followed by incubations with EMAP-II (1:50) antibody for 60 minutes and appropriate 15 nm gold-conjugated secondary antibodies (1:100) for 30 minutes. Sections were stained with uranyl acetate and lead citrate and examined in a Philips 410LS transmission electron microscope at 60 kV. Control sections were labeled without primary antibody or with normal serum instead of primary antibody.

2.3.8 *Endothelial monocyte-activating polypeptide-II (EMAP-II) instillation experiment*

To investigate whether mature EMAP-II was capable of recruiting monocytes/macrophages into the lungs, Sprague-Dawley rats (n = 5) were treated with 20μg of recombinant EMAP-II in 250μL of endotoxin-free saline intratracheally. The animals were euthanised at 6 hours post-instillation. Additionally, control rats were instilled with either endotoxin free saline (n = 5) or 250μg of LPS and euthanized at 6 hours for comparison with the mature EMAP-II treated animals.

2.3.9 *Quantification of monocytes/macrophages and granulocytes*

To evaluate whether instillation of mature EMAP-II resulted in monocyte/macrophage and granulocyte recruitment into the lungs, tissue sections were stained for ED-1 antibody (1:400) and rat anti-granulocyte antibody (1:50). To compare the numbers of monocytes/macrophages and granulocytes in the lungs between the EMAP-II treated and control groups, ED-1 and granulocyte positive and cells were counted in tissue sections in 10 random fields of view (40X) per section. The cells were counted in 0.076 mm^2/section (two sections/lung; 40 fields/animal = total lung area per animal 0.304 mm^2). The cell counting was performed in a blinded manner.

2.3.10 *Statistical analysis*

The ELISA data were compared using a one-way ANOVA. When a significant difference was noted Tukey's Post-hoc test was performed. Cells counts between the control and EMAP-II treated lungs were compared using a paired t-test. Differences were considered significant at $p<0.05$.

2.4 Results

Endothelial monocyte-activating polypeptide-II (EMAP-II) expression in lungs

2.4.1 *Enzyme linked immunosorbent assay (ELISA) for total Endothelial monocyte-activating polypeptide-II (proEMAP/p43 and mature EMAP-II)*

I used an ELISA to determine concentrations of total EMAP-II (proEMAP-II/p43 & mature EMAP-II) in lungs from the control and LPS-treated rats (Figure 2.1). An increase in total EMAP-II concentration was detected at 1 ($p=0.001$), 3 ($p=0.002$), and 12 hours ($p<0.001$) post-LPS treatment when compared with saline-treated control animals. However, no difference was observed between the 1, 3 and 12 hour points after the LPS treatment.

2.4.2 *Light and electron microscopic immunohistochemistry for total endothelial monocyte-activating polypeptide-II*

Compared to the control rats (Figure 2.2A), the LPS-treated rats showed a typical inflammatory response in their lungs (Figure 2.2B). Lung sections were stained with an antibody that recognizes both proEMAP/43 and mature EMAP-II. The staining for total EMAP-II was absent in lung sections from control rats (Figure 2.2C) but present in the LPS-treated rats (Figures 2.2 D-F). Total EMAP-II antibody stained alveolar septa including the septal monocytes/macrophages at 1 hour (Figure 2.2D) and 3 hours (Figure 2.2E) and the vascular smooth muscle cells at 12 hours (Figure 2.2F) post-LPS treatment. No positive reaction was observed when sections were treated with normal mouse IgG as an immunohistochemical control (see inset in Figure 2.2C). Immuno-gold electron microscopy confirmed EMAP-II staining in the septal cells and intravascular monocytes in inflamed lungs (Figure 2G).

2.4.3 *Mature endothelial monocyte-activating polypeptide-II instillation experiment*

To determine if mature EMAP-II is capable of inducing monocyte/macrophage and granulocyte recruitment, the peptide was instilled intra-tracheally in 5 rats. Histopathology showed septal congestion in lungs from EMAP-II treated rats compared to saline-treated control rats (Figure 2.3A-B). ED-1 antibody was used to identify monocytes/macrophages (Figure 2.3C-D), which showed more ED-1 positive cells in EMAP-II treated rats (Figure 2.3D) compared to the controls (Figure 2.3C). No positive reaction was observed when slides were treated with normal mouse IgG as an immuno-histochemical control (See inset in Figure 2.3C). Lungs from rats treated with mature EMAP-II revealed an increase in the numbers of monocytes/macrophages compared to the saline-treated controls (26 ± 4 versus 10 ± 2 / 0.304 $mm^{2;}$ p=0.0003; Figure 2.3E). Lung sections from rats treated with mature EMAP-II also showed more granulocytes than those from saline-treated animals (44 ± 4 versus 25 ± 2 / 0.304 mm^2; Figure 2.3F).

2.4.4 *Enzyme linked immunosorbent assay for Interleukin-1β and Macrophage inflammatory protein-2*

We used ELISA to compare the concentration of IL-1β and MIP-2, proinflammatory mediators, in lung homogenates from rats at 6 hours after treatment with either LPS, EMAP-II or saline. No detectable levels of IL-1β were observed in the EMAP-II treated or saline-treated control animals. Macrophage inflammatory protein-2 levels were not different between control and EMAP-II treated animals. In the LPS treated animals, however, IL-1β and MIP-2 concentrations were greater than the control (p=0.0005) and EMAP-II (p=0.006) groups (Figure 2.4A-B).

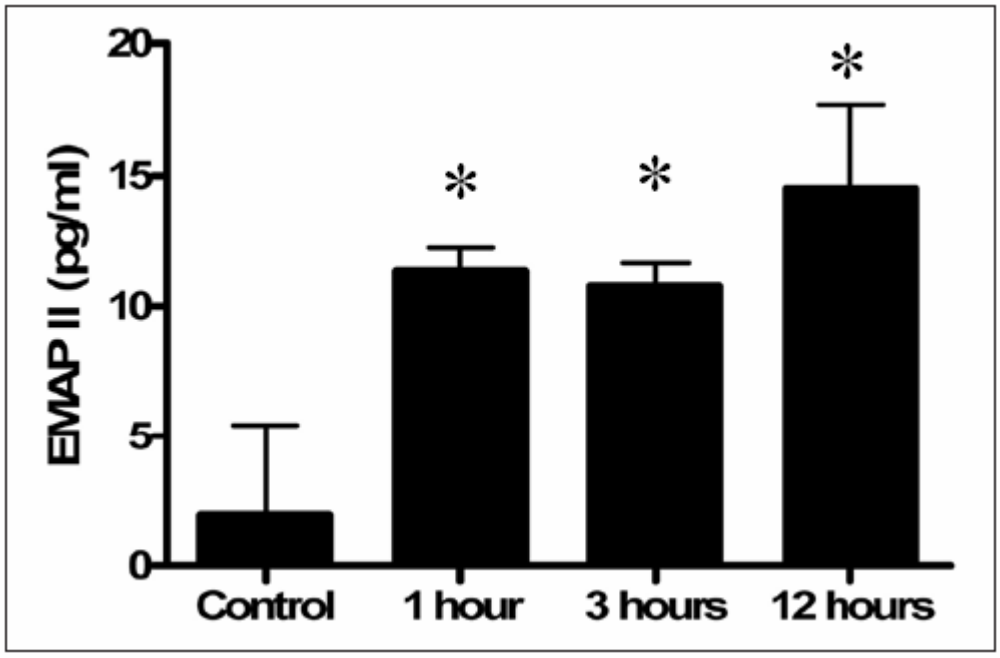

Figure 2.1 Endothelial monocyte-activating polypeptide-II concentrations in lungs as determined by Enzyme linked- immunosorbent assay: Compared to the control rats, Endothelial monocyte-activating polypeptide-II concentrations were significantly more (*:P<0.001) in lung homogenates from rats at 1 hour, 3 hour and 12 hours post-LPS treatment. Data are expressed as pg/mL of lung homogenate extract from approximately 100mg of wet lung tissue. Values are means ±SD

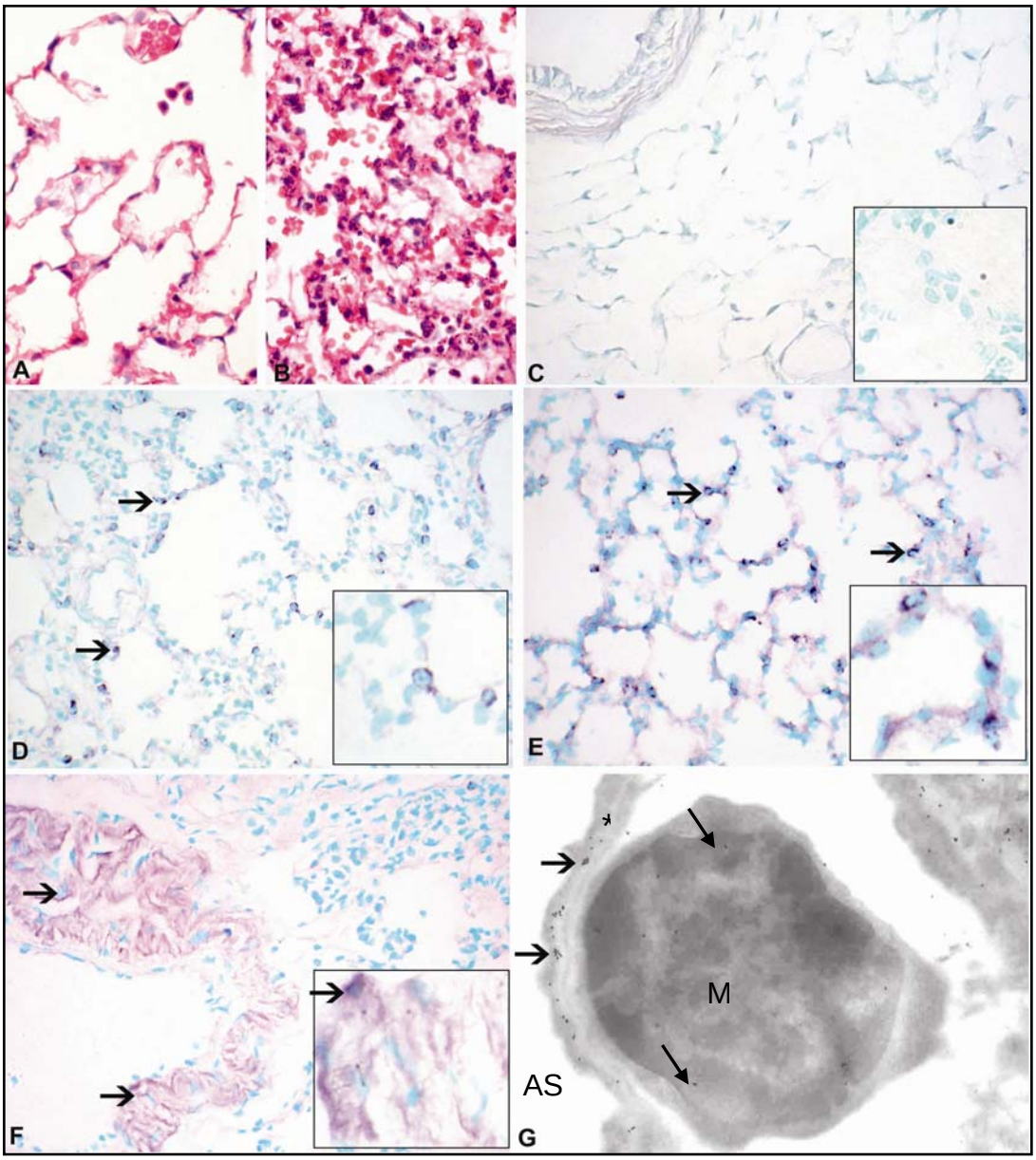

Figure 2.2 Endothelial monocyte-activating polypeptide-II expression in lungs: Hematoxylin-eosin stained lung sections from control rats (**A**) show normal histology while signs of acute inflammation (**B**) were observed at 3 h post-LPS treatment. Staining for Endothelial monocyte-activating polypeptide-II was absent in lung sections from control (**C**) rats but was observed (arrows) at 1 h (**D** and inset), 3 h (E and inset) and 12 h (F) post-LPS treatment. Immuno-gold electron micrograph (**G**) shows Endothelial monocyte-activating polypeptide-II labeling (arrows) in alveolar septal cells (asterisks) lining the alveolar space (AS) and an intravascular monocyte (M). Original magnification: **A-F**: X40; Insets: X100; **G**: X10000.

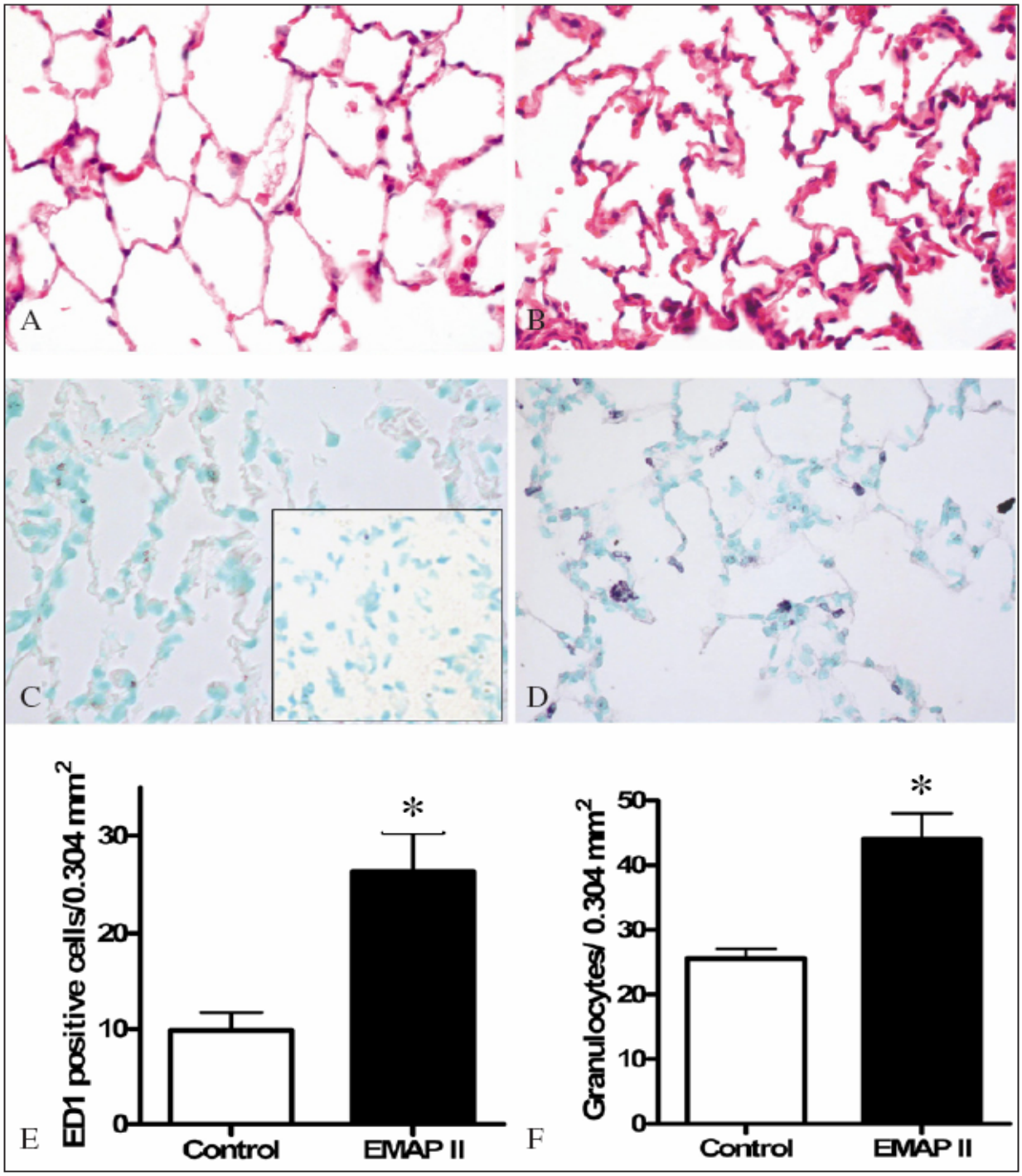

Figure 2.3 Intra-tracheal instillation of mature endothelial monocyte-activating polypeptide-II. Hematoxylin-eosin stained lung sections from the control (**A**) rats showed normal histology while those from mature endothelial monocyte-activating polypeptide-II treated rats (**B**) showed congestion in alveolar septa. Lung sections from control rats (**C**; inset is a normal mouse IgG control) have less ED-1 positive cells compared to those from Endothelial monocyte-activating polypeptide-II treated rats (**D**). Quantification revealed an increase (*: P=0.0003) in the numbers of ED-1 positive cells (**E**) and granulocytes (**F**) at 6 hours post-Endothelial monocyte-activating polypeptide-II instillation. Original magnification: 40X

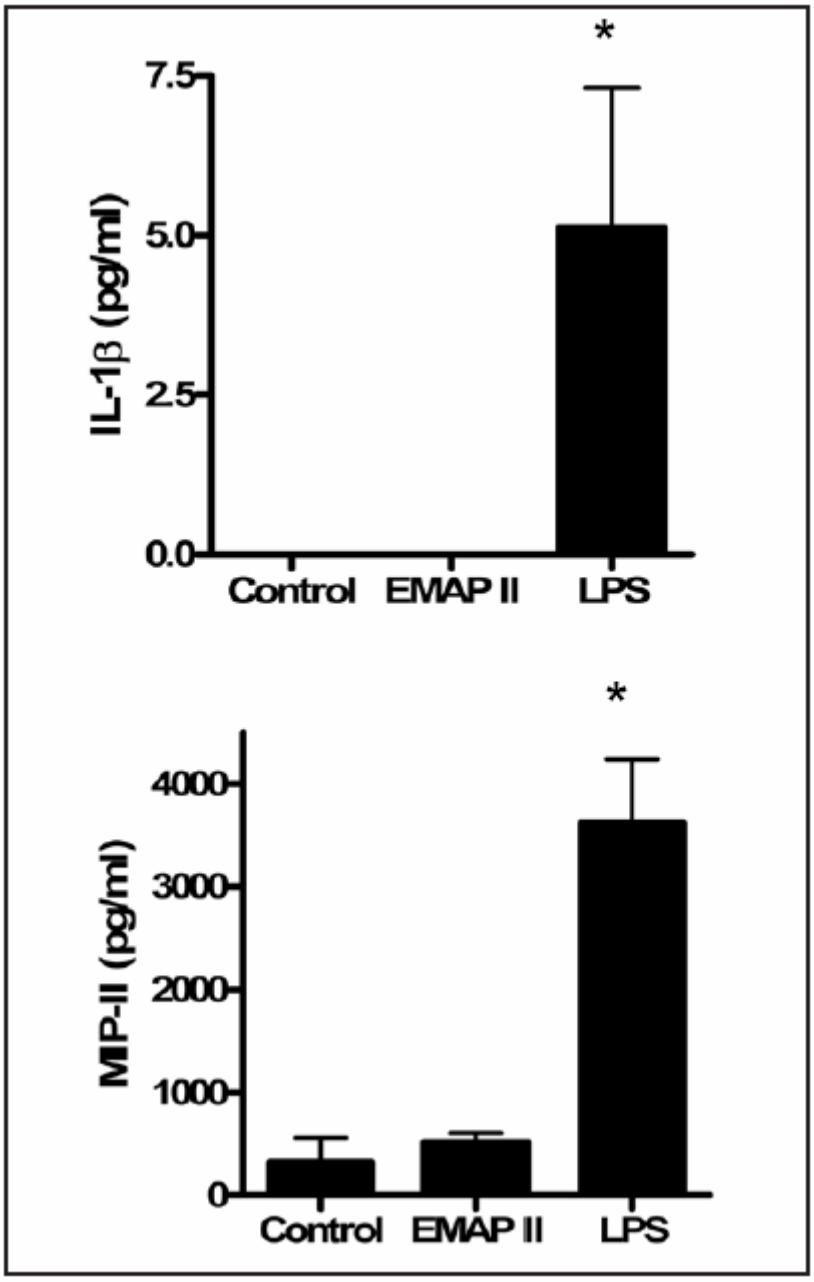

Figure 2.4 Concentrations of Interleukin-1β (**A**) and Macrophage inflammatory protein-2 (**B**) in lungs: Enzyme linked- immunosorbent assay showed increased concentrations of Interleukin-1β and Macrophage inflammatory protein-2 in lung homogenates from rats treated with lipopolysaccharide (*: $P<0.05$) compared to those given Endothelial monocyte-activating polypeptide-II or the saline. Values are means ±SD.

2.5 Discussion

These experiments have resulted in the following observations: 1) LPS challenge causes rapid induction of EMAP-II expression (proEMAP/p43 and mature EMAP-II) which is localized in septal endothelial cells and epithelial cells, mononuclear phagocytes and vascular smooth muscle cells in the lungs and 2) intratracheal instillation of mature EMAP-II provokes recruitment of monocytes/macrophages and granulocytes into the lungs without altering the lung expression of IL-β or MIP-2. Therefore, the total increase in expression of EMAP-II in acute lung inflammation may, in concert with other known molecules, stimulate recruitment of monocytes/macrophages and granulocytes.

First, I employed an ELISA to find that LPS challenge rapidly induces an increase in lung concentrations of total EMAP-II compared to the normal rats. Because the antibody used in ELISA detects the mature (22kD) as well as proEMAP/p43 forms of EMAP-II, both the forms may have contributed to the increased concentrations of this cytokine. ProEMAP-II/p43, an integral component of the synthetase complex, is released under various conditions of cell activation and is pro-inflammatory (Knies *et al.*, 1998; Shalak *et al.*, 2001; Matschurat *et al.*, 2003). ProEMAP-II/p43 is processed into a 22 kD mature form of EMAP-II (Shalak *et al.*, 2001). Therefore, I directly localized both proEMAP/p43 and mature EMAP-II in lungs from LPS-treated and control rats with light and electron microscopy. Compared to a near absence of EMAP-II in lungs from control animals, total EMAP-II was localized to alveolar septa and intravascular monocytes at 1 and 3 hours and to vascular smooth muscles at 12 hours after the LPS treatment. Taken together, these data show increased lung expression of total EMAP-II, contributed to by both the mature and proEMAP/p43 forms, within 1 hour of LPS-treatment. Previous

immunohistochemical data have shown increased expression of EMAP-II in the developing murine lung followed by lower expression in adult life (Schwarz *et al.*, 1999) (Murray *et al.*, 2000). Therefore, my observations of sparse EMAP-II expression in lungs from control rats are similar to the previously reported data. However, this is the first data on the sharp increase in the expression of total EMAP-II in inflamed lungs. This work adds to data showing other pathologic conditions where EMAP-II is upregulated including in infant bronchopulmonary dysplasia (Quintos-Alagheband *et al.*, 2004), in a rat model of myocardial infarction (Thompson *et al.*, 2004), and after chemical and hypoxic stress in prostate adenocarcinoma cells (Barnett *et al.*, 2000).

My experiments do not directly address the specific mechanisms of increased expression of EMAP-II in LPS-induced acute lung inflammation. However, it is known that mature EMAP-II is upregulated by both apoptosis (Knies *et al.*, 1998) and hypoxia (Matschurat *et al.*, 2003) *in vitro*. In support of such a mechanism, it has been shown that the prevention of lung epithelial cell apoptosis by administration of the angiotensin-II receptor antagonist saralasin, simultaneously down-regulated EMAP-II expression as shown by Western blot (Lukkarinen *et al.*, 2004). Thus, an increased number of apoptotic events secondary to LPS induced lung inflammation may have contributed to increased total EMAP-II expression. Studies using intratracheal instillation or inhalation of LPS, similar to our studies, have shown apoptosis in endothelial cells as well as bronchial and alveolar epithelium within 2-6 hours (Fujita *et al.*, 1998; Vernooy *et al.*, 2001). Therefore, while it is not known whether LPS can induce apoptotic events at 1 hour to cause increased expression of EMAP-II, it is certainly possible 3 hours following LPS instillation. This may be a contributing factor to my observations of increased expression

of EMAP-II as early as 1 and 3 hours. However, extrapolation from *in vitro* studies to our *in vivo* LPS model is preliminary given the paucity of *in vivo* EMAP-II data under inflammatory conditions. As recently discussed in a review by van Horssen et al.(van Horssen *et al.*, 2006), the mechanisms responsible for processing of proEMAP/p43 to mature EMAP-II are dependent upon the experimental model and assay environment employed. The authors of the van Horssen et al. review particularly highlighted the conflicting data on the role of caspases in EMAP-II maturation.

It has been shown (Tsai *et al.*, 2004) that the time course of EMAP-II release ranges from 8 to 20 hours after induction of apoptosis and 20-28 hours of hypoxia *in vitro*. It is also known that the proform of EMAP-II undergoes intracellular proteolytic cleavage to its mature form prior to release (Kao *et al.*, 1994). My immunohistology data and ELISA data suggest that the LPS-induced rapid increase in total EMAP-II is contributed to by both the proEMAP/p43 and mature EMAP-II forms. Furthermore, because there was very little or no staining for mature EMAP-II in normal lungs, it appears that a precursor to proEMAP-II/p43 and mature EMAP-II is processed within 1 hour of the LPS stimulus. It is not known whether proEMAP/p43 is always present in the cytoplasm awaiting cleavage and secretion (Tas & Murray, 1996). It is obvious that additional time-course studies are required to examine changes in the forms of EMAP-II as well as specific cleavage events over time during acute lung inflammation.

In an attempt to determine the *in vivo* potential of mature EMAP-II to recruit inflammatory cells, I instilled pure EMAP-II into the airways. I did these experiments because of the apparent correlation between the recently observed early rapid recruitment of monocytes/macrophages (Janardhan *et al.*, 2006) and the expression of total EMAP-II

in inflamed lungs in my present experiments. Mature EMAP-II instillation resulted in a significant increase in the number of monocytes/macrophages and granulocytes at 6 hours after its instillation, thus demonstrating that mature EMAP-II has the *in vivo* capability to recruit mononuclear phagocytes and granulocytes. This is plausible given previous work that has shown that mature EMAP-II is chemotactic for monocytes and neutrophils *in vitro* and promotes migration of inflammatory cells in the foot pad model (Kao *et al.*, 1992). There is also evidence that systemic administration of mature EMAP-II induces arrest of circulating leukocytes and other inflammatory cells in the pulmonary vasculature (Kao *et al.*, 1992). Recently, it was reported that there is a novel early recruitment of monocytes/macrophages at 3 hours in addition to neutrophil migration at 6 hours after intratracheal instillation of LPS (Janardhan *et al.*, 2006). Compared to the intra-tracheal instillation of LPS, EMAP-II provoked a less vigorous recruitment of monocytes/macrophages. Therefore, it is possible that EMAP-II is one of the many chemotactic signals induced by LPS to stimulate migration of monocytes/macrophages and granulocytes into the lungs. Distinct features of my experiments were instillation of mature EMAP-II directly into the lungs compared to systemic infusion in previous experiments and the immuno-morphometric quantification of recruited monocytes/macrophages and granulocytes. Based on the *in vivo* potential of mature EMAP-II to promote recruitment of inflammatory cells, it suggests that increased expression of mature EMAP-II in inflamed lungs may have similar functions.

Currently, the chemotactic signals induced by mature EMAP-II following its intra-tracheal instillation are not known. Therefore, I sought to probe whether mature EMAP-II may recruit mononuclear phagocytes and granulocytes through the stimulated

expression of a proinflammatory cytokine IL-1β and MIP-2. These molecules were targeted because IL-1β is critical in the early phase of acute lung inflammation while MIP-2 promotes recruitment of monocytes and granulocytes (Goodman *et al.*, 2003). To address this, I examined IL-1β and MIP-2 expression by ELISA at 6 hours after either EMAP-II or LPS instillation. I chose this time point because of significant recruitment of monocytes/macrophages and neutrophils in the LPS model of lung inflammation (Janardhan *et al.*, 2006). My data show similar lung concentrations of IL-1β and MIP-2 in the saline or EMAP-II treated rats although the latter showed significant recruitment of monocytes/macrophages and granulocytes at 6 hours. In contrast, IL-1β and MIP-2 were markedly increased in the LPS treated lungs, which have large numbers of neutrophils and monocytes/macrophages, compared to the control or EMAP-II-treated rats. These data suggest that mature EMAP-II instillation does not induce expression of IL-1β or MIP-2 to manifest its effects on recruitment of monocytes/macrophages and granulocytes. Further studies are needed to elucidate EMAP-II induced signaling pathways that result in inflammatory cell recruitment, such as the induction of other cytokines such as TNF- α, IL-8, MIP-1α and MIP-1β. It is possible however, that EMAP-II may have direct chemotactic effects *in vivo*.

2.6 Summary

In conclusion, I report a rapid upregulation of total EMAP-II expression following intratracheal instillation of LPS in rats. Secondly, mature EMAP-II promotes septal recruitment of monocytes/macrophages and granulocytes in lungs *in vivo*. Finally, in contrast to LPS, intra-tracheal instillation of mature EMAP-II into the airspace did not

induce IL-1β or MIP-2 expression relative to control lungs. I propose to use EMAP-II as a marker to understand monocyte recruitment in subsequent experiments focusing on the toxicology of rosette nanotubes. Future, studies should examine the role of EMAP-II in acute lung inflammation through antibody blocking experiments.

CHAPTER 3

Novel self-assembling rosette nanotubes show low acute pulmonary toxicity *in vivo*

3.1 Abstract

Nanotubes are being developed for a large variety of applications ranging from electronics to drug delivery. Common carbon nanotubes such as single-walled and multi-walled carbon nanotubes have been studied in the greatest detail but require solubilization and removal of catalytic contaminants such as metals prior to being introduced to biological systems for medical application. The present work represents the first *in vivo* inflammatory characterization of a novel class of self-assembling rosette nanotubes, which are biologically inspired, naturally water soluble and free of metal content upon synthesis. Upon pulmonary administration of this material we examined responses at 24h and 7d post exposure. An acute inflammatory response is triggered at high doses by 24h post-exposure but an inflammatory response is not triggered by a 5 μg dose. Lung inflammation observed at the 50μg dose at 24h was resolving by 7d as supported by bronchoalveolar lavage cell counts and histological examination. This work suggests that novel nanostructures with biological design may negate toxicity concerns for biomedical applications of nanotubes. This study also demonstrates that self-assembling rosette nanotube structures may be an alternative to traditional nanotube compounds and represent low pulmonary toxicity, likely due to their biologically inspired design, and their self-assembled architecture.

3.2 Introduction

Nanotechnology is a rapidly evolving interdisciplinary research area offering great potential for applications to such fields as electronics, materials science, drug delivery, medical imaging and diagnosis. It has been estimated that nanotechnology will have a market of $1 trillion by 2015 (Nel *et al.*, 2006). New nanomaterials and nanodevices are being developed with the intention of improving everyday life (Roco, 2004), but efforts are also being devoted to understand the possible toxicity and health implications of engineered nanomaterials. Knowledge of such factors is also considered a potential barrier to public acceptance, commercialization and future development of nanotechnology, and therefore warrants more research.

Materials at the nanoscale possess some unique physicochemical properties (Nel *et al.*, 2006) which make them attractive for their intended use but may also confer challenges upon those evaluating their potential toxicity. Indeed, some of the concerns about possible toxicity of engineered nanomaterials have been raised from our understanding of ultrafine particle toxicity research (Oberdorster *et al.*, 2005b; Kreyling *et al.*, 2006). At present the majority of research on engineered nanomaterials has focused on those which are anticipated to be produced in commercial quantities in the near future such as carbon nanotubes. The toxicity and biocompatibility of these materials (Fiorito *et al.*, 2006; Smart *et al.*, 2006) and the relevance to occupational health (Donaldson *et al.*, 2006; Lam *et al.*, 2006) have been reviewed elsewhere.

Carbon nanotubes (CNT) are one of the most studied nanomaterials because of their novel physicochemical properties which include high surface area, high mechanical strength yet ultra-light weight, rich electronic properties and chemical and thermal

stability (Ajayan, 1999). Two common types of CNT are the single-walled carbon nanotubes (SWNT) that are formed by a cylindrical sheet of graphite with a diameter of 0.4-2 nm, and the multi-walled carbon nanotubes (MWNT) that have multiple concentric graphite cylinders with increasing diameter ranging from 2-200 nm (Dresselhaus *et al.*, 1996). Single walled nanotubes have received attention primarily as a possible inhalation toxicant in their raw form (Lam *et al.*, 2004; Warheit *et al.*, 2004; Shvedova *et al.*, 2005), but carbon nanotubes also have potential for biomedical applications (Bianco & Prato, 2003; Martin & Kohli, 2003; Bianco, 2004; Lin *et al.*, 2004). In order for CNT to be used for biomedical purposes they typically need to become soluble with the addition of surface molecules (Georgakilas *et al.*, 2002; Pantarotto *et al.*, 2003; Hudson *et al.*, 2004; Lin *et al.*, 2004). Indeed, the *in vitro* toxicity of carbon nanomaterials, such as fullerenes and SWNT, has been shown to be dependent upon the degree of surface functionalization (Sayes *et al.*, 2004; Sayes *et al.*, 2005).

Self-assembled rosette nanotubes (RNT) are a novel class of biologically inspired nanotubes that are naturally water soluble upon synthesis (Fenniri *et al.*, 2001; Fenniri *et al.*, 2002a; Fenniri *et al.*, 2002b). The RNT are obtained through the self–assembly of the G∧C motif, a self–complementary DNA base analogue featuring the complementary hydrogen bonding arrays of both guanine and cytosine (Figure 3.1). The first step of this process is the formation of a 6–membered supermacrocycle (rosette) maintained by 18 hydrogen bonds, which then self–organizes into a tubular stack defining an open central channel 1.1 nm across and several micrometers long (Figure 3.1) ((Fenniri *et al.*, 2001; Fenniri *et al.*, 2002a; Fenniri *et al.*, 2002b; Raez *et al.*, 2004; Moralez *et al.*, 2005; Johnson *et al.*, 2007). Upon self-assembly, in principle any functional group covalently

attached to the G∧C motif could be expressed on the surface of the nanotubes, thereby offering versatility in functionalization of the RNT for specific medical or biological applications. Moreover, the RNT are void of any metals in the synthetic process, which confers potential advantage to their biocompatibility given reports on the role of metals in particle-induced oxidative stress (Ghio *et al.*, 1999; Donaldson *et al.*, 2006). Several hydrophilic RNT have been reported, displaying chiroptical (Fenniri *et al.*, 2002a; Johnson *et al.*, 2007) and hierarchical (Moralez *et al.*, 2005) tunability, high thermal stability (Fenniri *et al.*, 2002b; Moralez *et al.*, 2005) and entropically–driven self–assembly behaviour (Fenniri *et al.*, 2002b) in polar solvents.

Compound **1** (Figure 3.1) was previously shown to undergo self-assembly into RNT by NMR spectroscopy, circular dichroism (CD) spectroscopy, variable temperature UV-vis melting studies, dynamic light scattering (DLS), tapping mode atomic force microscopy (TM-AFM), and transmission electron microscopy (TEM). In agreement with the calculated average diameter of 3.8 nm, TEM images of RNT(**1**)-G0 featured a diameter of 4.0 ± 0.3 nm (Moralez *et al.*, 2005).

Compound **1** was designed relative to other compounds (Moralez *et al.*, 2005) so that upon self-assembly (a) the functional group density and net charge are reduced by a factor of two (b) the thermal stability of the corresponding RNT is enhanced as a result of preorganization, increased amphiphilic character, and greater number of H-bonds per module (12 instead of 6), (c) the corresponding twin rosettes are preorganized and maintained by 36 H-bonds instead of 18, and (d) the resulting RNT(**1**)-G0 is sterically less congested and experiences reduced electrostatic repulsion on its surface. These design criteria made RNT(**1**)-G0 far more robust relative to its singe base congeners

(Moralez *et al.*, 2005), even in boiling water.

To date, RNT have only been investigated for application to biomaterial interfaces in the field of orthopedics and specifically as a way to promote osteoblast adhesion *in vitro* (Chun *et al.*, 2004; Chun *et al.*, 2005). No data exist on the *in vivo* responses to exposure of these specific nanotubes and furthermore there are no studies on the responses to functionalized nanotubes in the lungs. I have chosen to evaluate the pulmonary responses because of the variety of potential applications of RNT including drug delivery (Hung, 2006) and the relative paucity of toxicity information on functionalized self-assembling nanostructures. Furthermore inflammatory physiology in the lung is well characterized, and is therefore a good model organ for studying the possible immunologic responses to RNT.

3.3 Materials and Methods

3.3.1 *Animals*

All animal protocols in this study were approved by the University of Saskatchewan Committee on Animal Care Assurance, and each experimental procedure was conducted according to the Canadian Council on Animal Care Guidelines. A total of forty-two 6-8 week old, specific pathogen free, male C57BL/6 mice were procured from Animals resource unit at the University of Saskatchewan, Canada (n=6 per group). The mice weighed 25-30g. The animals were acclimatized for a period of 1 week in the animal care unit prior to experimentation, and were randomly assigned to treatment groups.

3.3.2 *Rosette nanotube(1)-G0 preparation and characterization*

The nanotubes were formed by mixing 1 mg of compound **1** in 1ml of nanopure, sterile water and heating at 90ºC for ~30 min. The self-assembly process is quantitative, thus 1mg of compound **1** yields 1 mg of RNT(**1**)-G0 (Figure 3.1). Based on scanning and transmission electron microscopy, the length of the nanotubes is polydisperse. But the synthetic protocol employed here yields tubes that are several microns long. Without a heating protocol the tubes range from 50-200 nm in length. Regardless of the length, RNT(**1**)-G0's outer diameter is ~4 nm. Their calculated surface area is ~10^4 m^2/g. The aggregation state of RNT(**1**) is pH-dependent: as the protonation state of the lysine changes, the nanotubes aggregate in a parallel fashion (Moralez *et al.*, 2005). At low pH they are well dispersed however their status upon being introduced to the lung environment is unknown.

3.3.3 *Experimental overview*

Mice were studied at different doses of RNT(**1**)-G0 at two time points. The first experiment was conducted by treating C57/BL mice with RNT(**1**)-G0 intratracheally (5, 25, 50 µg in 50 µl of nanopure water /mouse). Two control groups included mice treated with 50 µl of nanopure water, or 50 µg of lysine in 50 µl of nanopure water. The lysine group was used as control for the lysine component of the nanotube surface. These mice were euthanized at 24h. In a second group of mice, we examined the effect of 5 and 50 µg doses at 7 days post instillation. This experiment was selected based on our 24h time point results. I wished to test if a 5 µg dose triggered an inflammatory response by 7d and whether the inflammatory response measured in our 50 µg group resolved by 7d. Thus an intermediate dose of 25 µg was not studied at the 7d time-point. Doses were chosen

based on the range used by other studies investigating SWNT pulmonary responses (Shvedova *et al.*, 2005).

I evaluated the extent of the inflammatory response by examining the bronchoalveolar lavage (BAL) total and differential cell counts as well as the peripheral blood total leukocyte count (TLC). Changes in lung permeability were assessed using BAL fluid protein as a marker. The chemokine macrophage inflammatory protein-2 (MIP-2) and the cytokines interleukin -1beta (IL-1β) and tumor necrosis factor-alpha (TNF-α) were measured in the BAL fluid and lung homogenate. Changes to the mRNA levels of MIP-2, IL-1β and TNF-α were also assessed using quantitative real time reverse transcriptase polymerase chain reaction (qRTPCR). Histological evaluation of the lavaged lung tissue was performed using the Hemotoxylin and Eosin staining technique.

3.3.4 *Lung collection, processing, histology and cell counts*

Mice were euthanized (1mg xylazine and 10 mg ketamine / 100 g) and blood, BAL fluid and lung samples were collected. Blood was collected by cardiac puncture for total leukocyte counts. A BAL was performed by washing the whole lung with 3 ml (1ml x 3 washes) of ice cold Hanks Balanced Salt Solution(Sigma Chemicals Co., St. Louis, MO). Total cell count was performed using a standard hemocytomter. Sixty µl of BAL fluid was used for a cytospin preparation on which the polymorphonuclear and monocyte differential counts were performed. Blood was collected by cardiac exsanguination and processed for evaluation on total leuckocyte count on the hemocytometer. One lung was fixed in 4% paraformaldehyde for 16 hours. Lungs used for quantification of cells were filled with 4% paraformaldehyde at 23 cm H_2O pressure. Pieces of the lobes were later processed through ascending grades of alcohol and then embedded in paraffin. Tissue

blocks were then cut into 5 μm sections for light microscopy. Hematoxylin and eosin stained sections were used for histopathological evaluation.

3.3.5 *Enzyme linked- immunosorbent assay (ELISA) for Macrophage inflammatory protein-2, Interleukin-1β, Tumor necrosis factor-α and Endothelial monocyte-activating polypeptide-II*

Enzyme linked- immunosorbent assay was conducted on both the BAL fluid and the lung tissue. For lung tissue analysis, frozen lung samples were homogenized in lysis buffer [150 mM sodium chloride, 1% NP-40, 0.5% sodium deoxycholate, 0.1% SDS, 50 mM TRIS (pH 8.0), 5 mM EDTA, and protease inhibitor cocktail (100 μl/10 ml)]. Homogenates were collected after centrifuging the samples at 25,000 g for 20 minutes. For quantification, samples in duplicates, from 3 mice for each treatment were used. Interleukin-1β, TNF-α and MIP-2 were quantified by sandwich ELISA using antibody pairs and recombinant standards purchased from R&D Systems. For the lung homogenate analysis each well was loaded with 20μg of protein. Endothelial monocyte-activating polypeptide-II was assayed as per Section 2.3.5.

3.3.6 *BAL fluid total protein assay*

Total protein in the BALF supernatant was quantified using an assay kit from Bio-Rad Laboratories as per the manufacturer's protocol. The protein assay is based on the Bradford method of protein quantification. Protein concentration values were calculated from a standard curve using bovine serum albumin (BSA) concentrations ranging from 0 to 1.0 mg/ml.

3.3.7 *RNA isolation and quantitative real time reverse-transcriptase polymerase chain reaction (qRTPCR)*

Total RNA was extracted from the lungs of mice by using TRIzol reagent (Invitrogen, Ontario, Canada) followed by treatment with RNase-free DNase (Qiagen, Ontario, Canada) and purification on RNeasy mini columns (Qiagen) according to the manufacturer's instructions. Integrity of RNA was confirmed by agarose gel electrophoresis and RNA was quantified by spectrophotometric analysis. The mRNA was reverse transcribed at 42°C for 40 min by using StrataScript QPCR cDNA synthesis kit (Stratagene, USA) and universal oligo dT primer as per manfacturer's instructions. This cDNA was used for QRtPCR analysis for the expression of TNF-α; (GenBank Accession No. NP_038721), MIP-2; (GenBank Accession No. X53798), and IL-1β; (GenBank Accession No. NP_032387) genes using Brilliant SYBR Green QPCR kit (Stratagene, USA). The glyceraldehyde-3-phosphate dehydrogenase gene (GAPDH; GenBank Accession No. XR004536) was used as the reference housekeeping gene. The reactions were performed using the primer pairs; 5'-ATGAGCACAGAAAGCATG-3' and 5'-GGGAACTTCTACTCCCTT-3' for TNF-α, 5'-ATGGCCCCTCCCACCTGC-3' and 5'-ACTTCTGTCTGGGCGCAG-3' for MIP-2, 5'-ATGGCAACTGTTCCTGAA-3' and 5'-GCCACAGCTTCTCCACAG-3' for IL-1β and 5'-TGCATCCTGCACCACCAACTG-3' and 5'-GGGCCATCCACAGTCTTCTGG-3' for GAPDH. A negative control reaction consisted of all the components of the reaction mixture except RNA. Real-time PCR analysis was performed using the MX3005PLightCycler (Stratagene). The cDNA was denatured at 95°C for 5 minutes. This was followed by amplification of the target DNA through 45 cycles of denaturation at 95°C for 1 min, annealing at 55°C for 30 seconds

and elongation at 72°C for 30 seconds. Relative expression levels were calculated after correction for expression of GAPDH using MxPro software.

3.3.8 *Data analysis*

Statistical analysis was carried out with SigmaStat® statistical software. Values represent the means ± SD. Comparisons between 24h treatment groups were performed using a one-way ANOVA. When significant main effects were observed, a Tukey's post hoc test was performed. Differences were considered significant when $P < 0.05$. An unpaired Student's t-test was used to examine differences between 24h and 7d for the doses of 5 μg and 50 μg.

3.4 Results

3.4.1 *Bronchoalveolar lavage fluid and blood cell counts*

The total number of cells observed in the BALF showed a dose dependent effect in the 24h treatment groups. The Control, Lysine, and 5 μg treatment groups did not differ from each other, while the 25 μg and 50 μg showed an increase in the total cell count over these groups ($P < 0.001$). The 25 μg and 50 μg also differed from each other (Fig. 3.2A; $P < 0.001$).

The 5 μg dose of RNT(**1**)-G0 did not trigger an inflammatory response when the 24h and 7d responses were compared. However in the 50 μg treatment group a reduction in the total cell count was observed at 7d when compared to 24h (Fig. 3.2A, $P = 0.001$).

The absolute PMN and monocyte counts were greater in the 25 μg and 50 μg than the Control, Lysine, and 5 μg groups at 24h (Fig. 3.2B-C; $P < 0.001$). The 50 μg group also had a greater absolute numbers of PMN and monocytes than the 25 μg group (P =

0.002 and P < 0.001). There was no difference in the absolute number of PMN and monocytes between the 24h and 7d groups when the mice were administered 5 μg of RNT(**1**)-G0 (P = 0.103 and P = 0.901). However when the mice were treated with 50 μg of RNT(**1**)-G0, the 7d group demonstrated a decreased number of PMN (P = 0.01) and monocytes (P = 0.001) relative to the 24h time-point.

Total leukocyte counts in the blood did not differ between any groups at 24h. The 5 μg and 50 μg dose groups did not differ between the 24h and 7d time-points (Fig. 3.3).

3.4.2 *Bronchoalveolar lavage fluid total protein assay*

Protein levels in the lavage fluid were greater in the 50 μg treatment group than all the other groups at 24h (Fig. 3.4; P = 0.07). When comparing the 5 μg dose at 24h and 7d, no difference was observed in protein concentrations in the lavage fluid (P = 0.838) nor did the 50 μg dose group differ between 24h and 7d (Fig. 3.4; P = 0.827).

3.4.3 *Enzyme-linked immunosorbent assay (ELISA) for Tumor necrosis factor-α, Interleukin-1β, Macrophage inflammatory protein-2, and Endothelial monocyte-activating polypeptide-II*

Lavage fluid analysis

An ELISA was performed on both the lavage fluid and on tissue homogenate. The cytokines IL-1β, TNF-α, and EMAP-II were found to be below detectable levels in the lavage fluid. The MIP-2 levels were recorded in the lavage fluid. However, levels did not differ between groups at 24h, or between time points for the doses of 5 μg and 50 μg (Fig. 3.5).

Tissue homogenate analysis

At 24h, levels of TNF-α in the lung tissue of mice treated with 5 μg and 25 μg of RNT(**1**)-G0 were greater than both the Control ($P = 0.004$ and $P = 0.04$) and Lysine ($P < 0.001$ and $P = 0.003$) treated mice (Fig. 3.6A). The 50 μg did not differ from control but did differ from the Lysine treated group ($P = 0.005$). No differences were detected between nanotube treatment groups at 24h (Fig. 3.6A). The amount of TNF-α approached a statistically significant decrease between 24h and 7d in the 5 μg groups ($P = 0.056$), and did not differ in the 50 μg group ($P = 0.231$).

The IL-1β levels (Fig. 3.6B) did not differ between the Control and Lysine treated groups. While the 5 μg group showed a greater amount of IL-1β than both the Control and Lysine groups, the 25 μg and 50 μg levels were only significantly greater than the Lysine group. Levels did not differ between the nanotubes groups at 24h. At 7d, IL-1β concentration in the tissue was lower than at 24h when mice were treated with 5 μg ($P = 0.029$). In the 50 μg treatment, levels did not differ between 24h and 7d ($P = 0.260$).

The MIP-2 levels did not differ between all treatment groups at 24h (Fig. 3.6C). When comparing MIP-2 levels in the 5 μg groups at 24h and 7d no difference was detected, however in the 50 μg group levels of MIP-2 were higher at 24h than at 7d ($P < 0.001$).

3.4.4 *Quantitative real time reverse-transcriptase polymerase chain reaction (qRTPCR) for tumor necrosis factor-α, interleukin-1β and macrophage inflammatory protein-2*

When compared to control lungs the lysine and 5 μg groups showed a ~3 fold reduction in TNF-α mRNA (Fig. 3.7A; $P < 0.001$), while the 25 μg group was the same

as control lung and the 50 μg group had a ~2 fold increase in TNF-α mRNA at 24h. In the 5 μg group the level of TNF-α mRNA at 7d did not differ from control lungs (P =0.378), while the 50 μg treatment group had a ~2 fold lower level of mRNA than control (P = 0.02). The IL-1β transcription was increased relative to control lungs in all nanotube treated groups at 24h, however the lysine treated group did not differ from the control group (Fig. 3.7B; P < 0.001). At 7d, mRNA remained elevated above control in the 5 μg (P = 0.004) and 50 μg (P = 0.025) treatment groups. The MIP-2 mRNA was reduced at 24h relative to control in the Lysine, 5 μg and 25 μg treated lungs (Fig. 3.7C; P < 0.001) and approached statistical significance in the 50 μg treatment group at 24h (P = 0.058). At 7d, the 5 μg treated lungs did not differ from control (P = 0.528) however the 50 μg treatment group showed a significant reduction in mRNA levels at 7d (P < 0.001).

3.4.5 *Histology*

When compared to Control (Fig. 3.8A), 5 μg (Fig. 3.8B) and Lysine (not shown) treated lungs, the 25 μg (not shown) and 50 μg (Fig. 3.8C) treated lungs showed septal thickening, edema and influx of cells at 24h. When examined at 7d post-instillation (Fig. 3.8D), the 50 μg treated lungs showed less septal congestion and influx of cells relative to the 24h lungs (Fig. 3.8C). There was perivascular dilatation at 24h in lungs exposed to 25 & 50 μg doses but not in the other treatment groups or time points (data not shown). No evidence of granuloma formation was apparent.

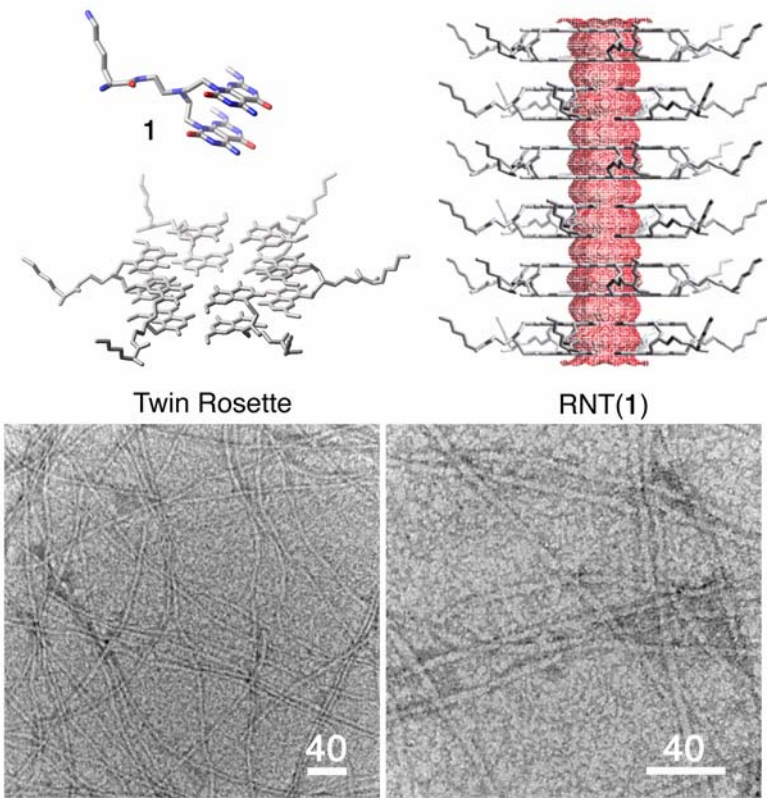

Figure 3.1 Rosette nanotubes assembled from compound **1** and corresponding transmission electron micrographs. Scale bars in nm.

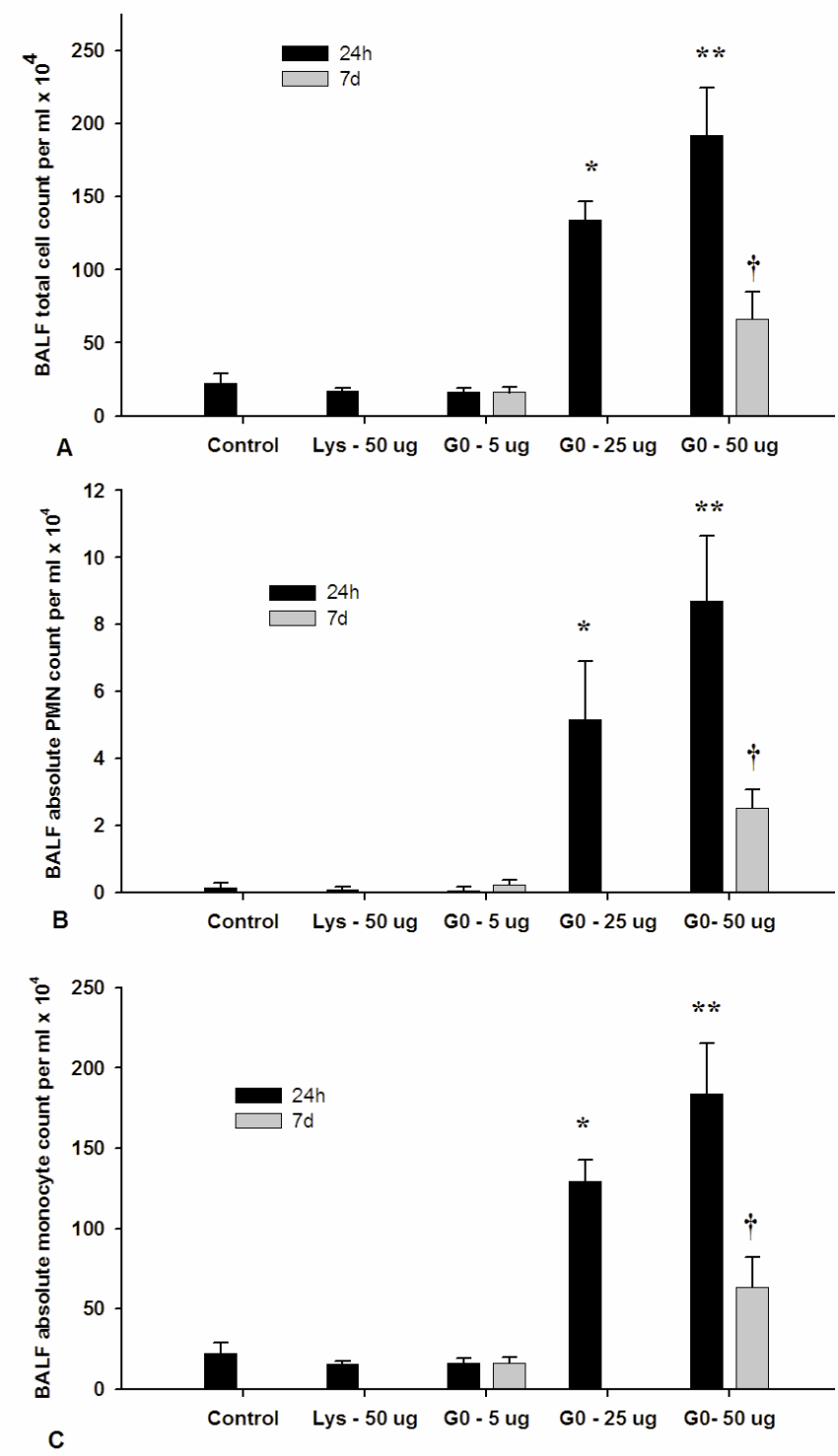

Figure 3.2 Total number (**A**) and differential cell counts (**B,C**) in bronchoalveolar lavage fluid from mice at 24h and 7d. Values represent means ± SD. * denotes significant difference from Control, Lysine and 5 µg groups at 24h ($P < 0.05$). ** denotes significant difference from all other groups at 24h. † denoted different from same treatment dose at 24h ($P < 0.05$).

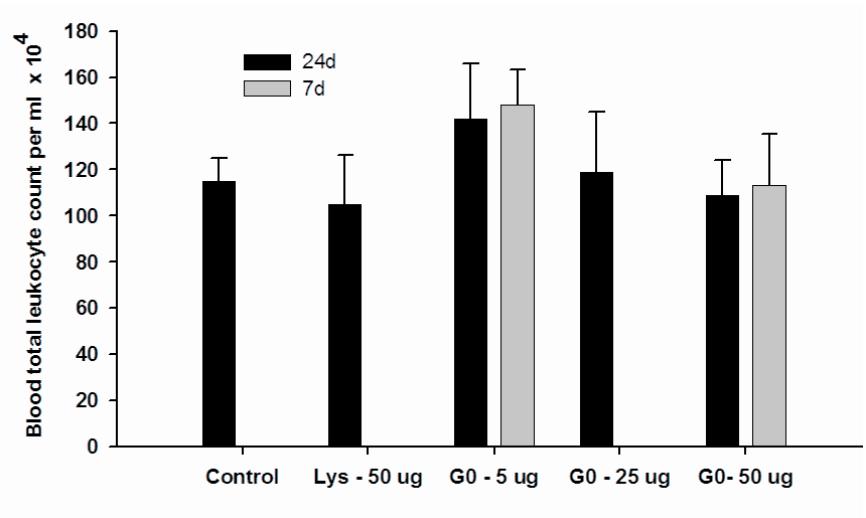

Figure 3.3 Blood total leukocyte count. Values represent means ± SD. Significance level was set at $P < 0.05$.

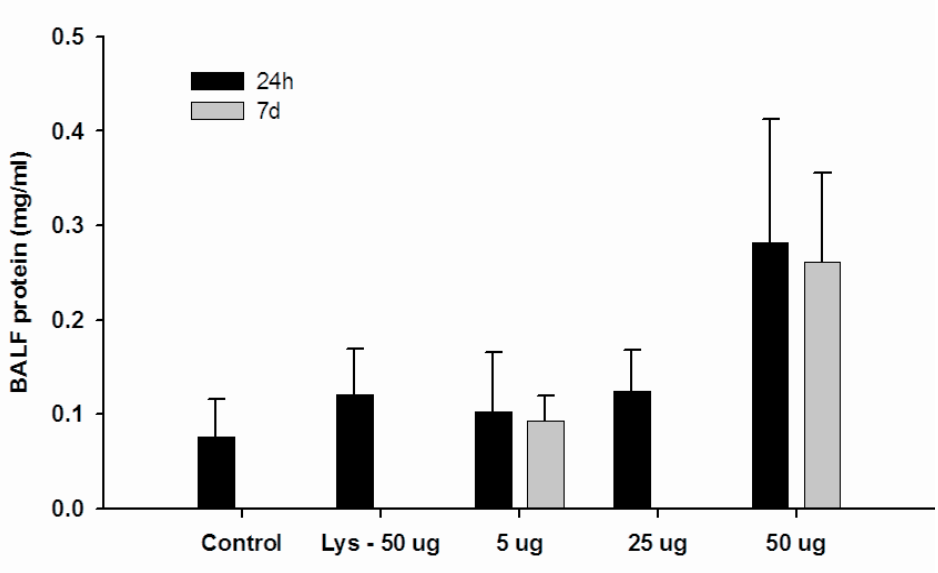

Figure 3.4 Total protein in bronchoalveolar lavage fluid. Values represent means ± SD. Significance level was set at $P < 0.05$.

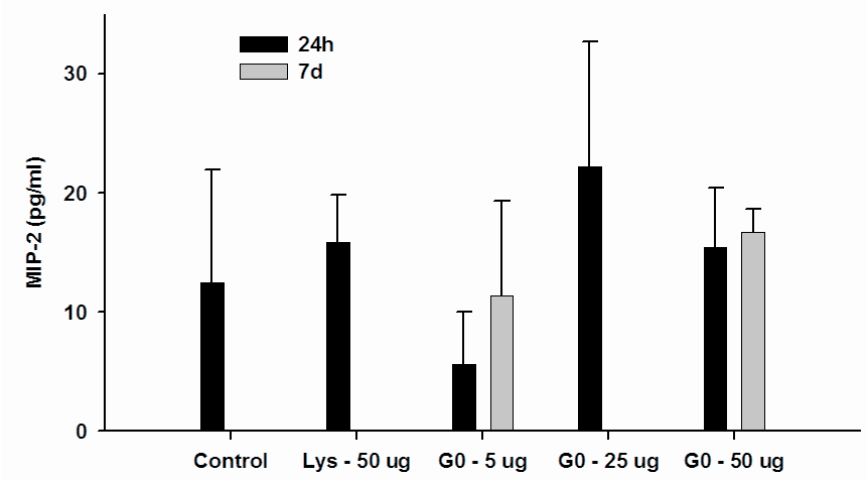

Figure 3.5 Enzyme linked- immunosorbent assay for Macrophage inflammatory protein-2 on bronchoalveolar lavage fluid. Values represent means ± SD. Significance level was set at $P < 0.05$

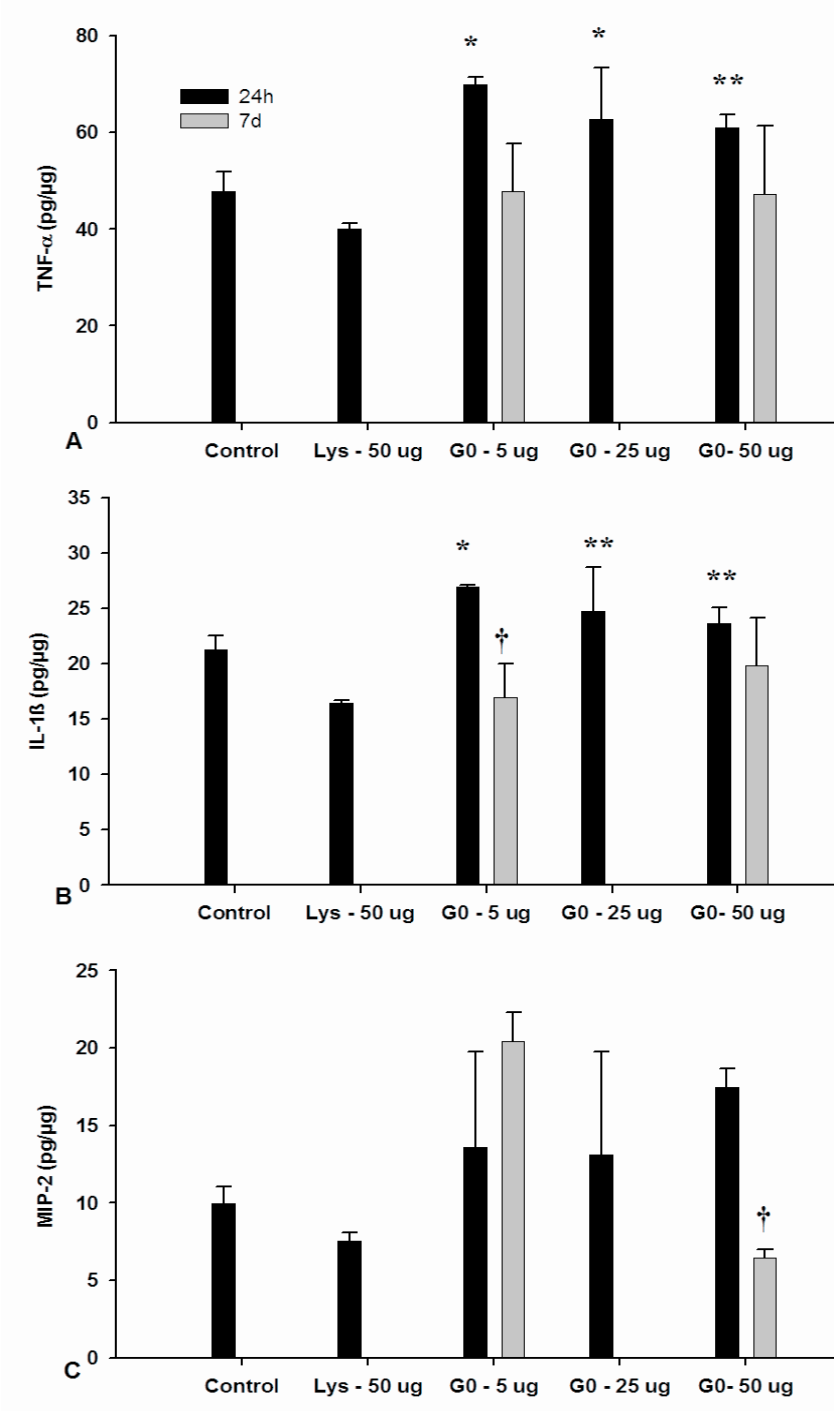

Figure 3.6 Enzyme linked- immunosorbent assay for Tumor necrosis factor-α (**A**), Interleukin-1β (**B**) and Macrophage inflammatory protein-2 (**C**) performed on lung homogenates. Values represent means ± SD. Values are presented as pg/µg of loaded protein as equal amounts of tissue protein (20 µg) were used in analysis. * denotes significant difference from Control and Lysine groups at 24h. ** denotes significant difference from Lysine group only. † denotes different from same treatment dose at 24h ($P < 0.05$).

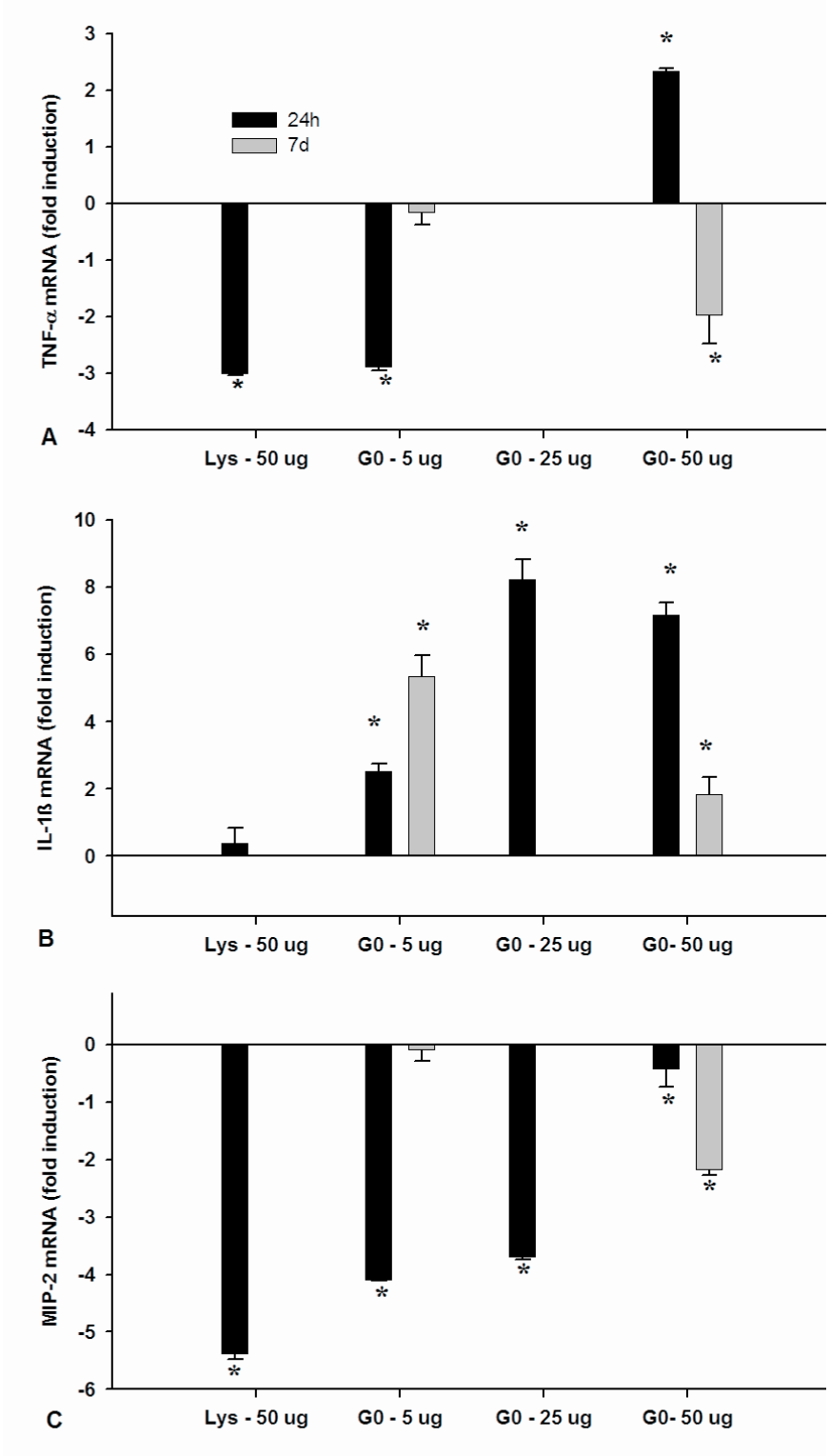

Figure 3.7 Quantitative real time reverse transcriptase polymerase chain reaction for Tumor necrosis factor-α (**A**), Interleukin-1β (**B**) and Macrophage inflammatory protein-2 (**C**) mRNA expression. * denotes significant difference from Control lungs ($P < 0.05$). Values represent means ± SD.

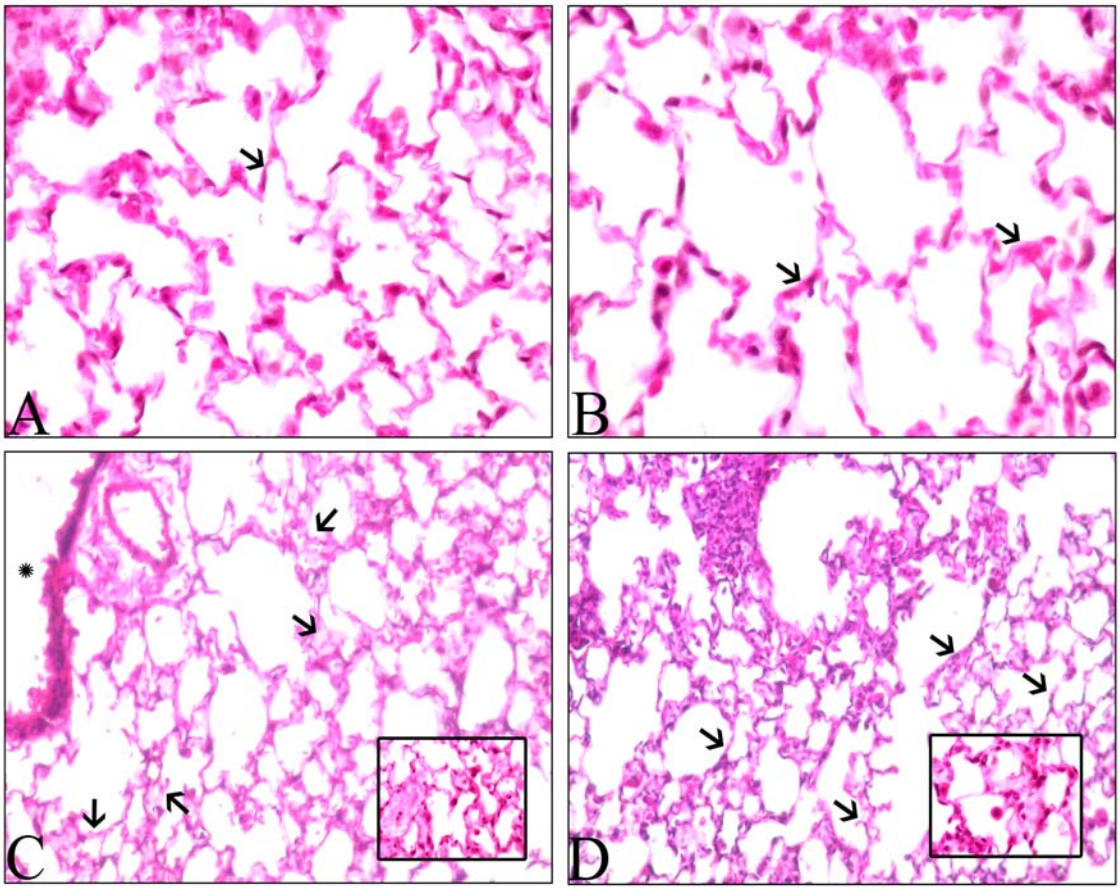

Figure 3.8 Hematoxylin-eosin stained lung sections. Lung sections from mice Control (**A**) and Lysine (**B**) show normal alveolar septa (arrows) while those from 50 µg at 24h (**C**) show septal congestion (inset), septal thickening and edema (arrows). Section of a lung collected 7d post-instillation of 50 µg of RNT(**1**)-G0 (**D**) shows nearly normal alveolar septa (arrows) and some congestion (arrows). Original magnification: X40

3.5 Discussion

I present the first *in vivo* data on the acute inflammatory potential of self-assembled rosette nanotubes in the lungs of C57/BL mice. Moreover, these are the first toxicity screening data on a synthetic organic nanomaterial and add to literature on the interaction of functionalized nanotubes with biological systems *in vitro* (Pantarotto *et al.*, 2003; Sayes *et al.*, 2005; Dumortier *et al.*, 2006). The key findings from this study are that C57/BL mice do not show signs of lung inflammation at the dose of 5 μg at 24h and no response is triggered by 7d. Additionally, while a dose of 50 μg triggered significant lung inflammatory responses at 24h, the effects are resolving by 7d.

The intratracheal instillation technique was chosen as an exposure method in this screening study of RNT. While there are advantages and disadvantages of this technique (Driscoll *et al.*, 2000; Oberdorster *et al.*, 2005a), instillation studies are qualitatively a positive predictor of particle induced pathology. Moreover, within the field of inhalation toxicology, a reliable method of delivering nanotubes via aerosol or inhalation chamber is still being devised and pulmonary deposition patterns of nanotubes upon inhalation remain unresolved. It should also be noted that the dose range used here is similar to previous work on SWNT where oropharyngeal aspiration was used to deliver the material to the lungs (Shvedova *et al.*, 2005).

My initial examination of the pulmonary response to instillation of the nanotubes included the evaluation of inflammatory cells in the bronchoalveolar lavage fluid (Henderson, 2005). A significant influx of total cells was observed in our 25 μg and 50 μg dose treatment groups at 24h compared with our control and lysine groups. The compound in this study is a lysine based rosette nanotube (Fig 3.1), and thus in an

attempt to delineate the possible role of lysine versus the nanotube structure, lysine was used as an additional control group. As lysine did not trigger an influx of inflammatory cells, we attribute the observed inflammation at 24h to an effect of the nanotube structure per se and not the lysine component.

While acute inflammatory responses are important in the study of particle toxicology, the resolution of such responses is crucial to understanding the longer-term effects. I tested whether the 5 μg dose triggered inflammation by 7d post treatment and additionally whether the inflammation observed at 24h in the 50 μg dose resolved. Of note, the 5 μg dose did not induce an influx of cells at 7d and the 50 μg treatment showed significant reduction in cell total number compared with 24h. The absolute PMN and monocyte count also paralleled the responses of the total cell count. It should be emphasized that while instillation of particles into the lungs may cause an acute inflammatory response due to the bolus nature of the exposure, the lung is a resilient organ that can resolve the effects of modest acute insults after exposure to such toxicants as particulate matter. Thus, particulate nanomedicine delivery systems such as functionalised nanotubes (Moghimi & Kissel, 2006) may be useful for non-chronic delivery of therapies to the lung (Hung, 2006; Pison *et al.*, 2006), provided no persistent pathology is caused. In addition to the lung response, I also determined whether nanotube instillation caused a peripheral immune response, as determined by blood total leukocyte count. Contrary to what is observed upon exposure to particulate matter where monocytes may be released from bone marrow (Goto *et al.*, 2004), I did not observe any differences in total leukocyte count in the blood between any treatment groups, and conclude that a peripheral response was not evoked by pulmonary exposure to the nanotubes. The BALF

cell counts were also supported through histological evidence of congestion, accumulation of inflammatory cells in alveolar septa and dilatation of perivascular spaces in lungs of mice treated with 25 and 50 μg of nanotubes at 24 hours but not at 7 days. Lung sections from 5 μg group did not show signs of inflammation at both 24 hours and 7 days of treatment. *In toto,* these data support induction of lung inflammation by 24 hours at the higher doses of RNT used in this study, which is resolving by 7 days.

As a marker of lung permeability changes I measured total protein in the lavage fluid. Of note, while a significant increase in BAL fluid total cell number was observed in both the 25 μg and 50 μg groups, neither group showed a significant change in lung permeability. When measured at 7d post-treatment total protein in the lavage fluid had not changed from 24h in the 5 or 50μg groups. The protein data are in contrast to evidence of edema in hematoxylin-eosin stained subjectively assessed lung sections collected at 24h from the high dose groups. The signs of edema, however, were resolving by 7d. Dailey and colleagues (Dailey *et al.*, 2006) observed a reduced level of BAL protein at 14d relative to 24h when they compared BAL protein levels at 24h and 14d after instillation of fine (220nm) polystyrene nanoparticles. They did observe however that treatment with ultrafine (75nm) polystyrene particles resulted in a persistent elevation in BAL protein levels at 14d when compared with 24h. Taken together with the reduction in total cell count in the present study, these responses are suggestive of resolution of inflammation occurring between 24h and 7d.

In order to assess the possible molecular contributors to the acute influx of cells I examined the expression of the cytokines TNF-α and IL-1β and the chemokine MIP-2 in both the lavage fluid and the lung tissues. I also studied mRNA expression of these

inflammatory mediators in lung tissues with qRT-PCR. While TNF-α and IL-1β are central players in acute lung inflammation (Goodman *et al.*, 2003), MIP-2 promotes migration of inflammatory cells (Driscoll, 2000; Kobayashi, 2006).

Mouse lungs treated with 5 μg of nanotubes showed higher TNF-α and IL-1β protein concentrations compared to Control and Lysine treated tissues at 24 hours while the 50 μg group differed from Lysine but not the Control group. Lung tissues from mice treated with 25 μg showed higher concentration of TNF-α compared to both Lysine and Control but IL-1β levels were more than the Lysine group only. While IL-1β mRNA was increased in all the nanotube treated groups compared to the Control, TNF-α mRNA was elevated in the 50 μg group only. The TNF-α mRNA levels were reduced in the 5 μg group compared to the control. Although there is a discrepancy in the expression of IL-1β protein and mRNA in the 5 μg group, we judge the protein data to be of more importance because protein is the functional product of gene transcription. Furthermore, it is well known that all of the mRNA may not be translated into a mature protein. Both TNF-α and IL-1β are released by lung macrophages, epithelium and endothelium in response to a variety of stimuli such as endotoxin and bacteria (Goodman *et al.*, 2003). These cytokines induce expression of adhesion molecules such as selectins and integrins to facilitate migration of inflammatory cells such as neutrophils and monocytes (Goodman *et al.*, 2003). Even though expression of the chemokine MIP-2 remained unaltered at 24 hours post-treatment, there was an increase in monocytes in BALF. It is well known that monocyte and neutrophil migration is promoted though a complex interplay of many chemokines and adhesion molecules such as MCP-1, IL-8 and integrin αvβ3 (Janardhan *et al.*, 2006; Kobayashi, 2006). The increased expression of cytokines in the 5 μg group

did not result in higher migration of inflammatory cells into lungs. Nevertheless, increased numbers of cells in the lungs of mice treated with 25 and 50 μg of nanotubes could be a functional outcome of increased expression of TNF-α and IL-1β and associated expression of adhesion molecules.

Acute lung inflammation induced by a single application of a stimulus normally resolves through migration of inflammatory cells out of the lung. Therefore, I examined lung tissues at 7d post-treatment. Histologic examination showed some resolution of inflammation in the 50 μg group along with a decrease in MIP-2 protein levels despite unaltered protein expression of TNF-α and IL-1β. Macrophage inflammatory protein-2 is a central chemokine in bacterial sepsis and oxidant-induced lung injury (Dailey *et al.*, 2006) and promotes recruitment of neutrophils and monocytes (Goodman *et al.*, 2003). Previous work on other classes of nanotubes has clearly indicated the role of metals used in the synthetic process and the associated oxidative stress response (Donaldson *et al.*, 2006). A critical aspect of the RNT studied here is the absence of metals in the synthetic process of the compound. Thus, the measurement of MIP-2 was considered an important end-point. Macrophage inflammatory protein-2 was detected in both the lavage fluid and the tissue homogenate, but no differences in MIP-2 were detected between treatment groups in the lavage fluid at 24h or 7d. Furthermore, while no changes were detected in the tissue at 24h, a statistically significant decrease in MIP-2 was detected at 7d compared to 24h in the 50 μg group. Despite few changes in MIP-2 protein among treatments, all groups showed a decrease in MIP-2 mRNA relative to control. This is in contrast to previous data (Dailey *et al.*, 2006) showing an increase in MIP-2 mRNA expression after treatment with biodegradable polymeric nanoparticles and non-

biodegradable polystyrene nanoparticles. A reduction in MIP-2 expression may be responsible for reduced numbers of inflammatory cells and suggest resolution of inflammation in RNT-treated animals. Taken together, these data show that 5 μg and 50 μg may represent non-inflammatory and inflammatory doses, respectively, of this nanotube and provide a framework for their further toxicity characterization.

The RNT are by design water-soluble and metal free. Thus their rapid synthesis and subsequent administration in water does not allow for easy visualization *in vivo* upon histological examination. However, the observed difference in responses between doses shows that the instillation method was successful in exposing the lung to this organic nanomaterial. A labelled version of the RNT is currently being developed for *in vitro* and *in vivo* uptake and distribution studies. Due to the fact that I could not visualize the tubes *in vivo*, the aggregation state in the lung could not be ascertained. While the aggregation state of this RNT is pH-dependent when studied under laboratory conditions, it is not known whether these observations can be extended to behaviour in physiological fluids such as lung surfactant. Indeed, a paucity of information exists on the interaction of nanomaterials with components of the physiological environment.

3.6 Summary

In summary, here I presented the first *in vivo* study on rosette nanotubes which is also the first of its kind for an organic nanomaterial obtained through self-assembly. Moreover, the biologically inspired design of the rosette nanotubes may confer toxicological advantages over other nanotube compounds for biomedical application.The data demonstrated that a 5 μg dose of RNT(**1**)-G0 is well tolerated in murine lungs up to

7d post-instillation, and that even with a 50 μg dose, inflammation is resolving by 7d. Future studies will examine the uptake and distribution kinetics of the RNT *in vitro* and *in vivo.* In light of many reports of nanomaterial induced toxicity, my study presents a much needed example of how a biologically inspired synthetic nanomaterial created on the principle of self-assembly can be introduced into the mammalian system without adverse effects. Moreover, my data may provide a framework to encourage future novel nanomaterials that are toxicologically favourable due to their biologically inspired and self-assembling architectures.

CHAPTER 4

Low inflammatory activation by self-assembling rosette nanotubes in human Calu-3 pulmonary epithelial cells

4.1 Abstract

Rosette nanotubes (RNT) are a class of organic nanotubes synthesized through the self-assembly. These water-soluble nanotubes are synthesized in the absence of any metals and have a range of biomedical applications including drug delivery. I have chosen to evaluate the potential *in vitro* toxicity of the RNT(**2**)-K1 compound in a Calu-3 pulmonary epithelial cell line. Cells were treated with: Control (media only), Lysine (50 ug/ml), 1, 5, 50 μg/ml of RNT(**2**)-K1 (nanotube with lysine residue composition), 80 μg/ml of Min-U-Sil® Quartz and 1 ug/ml of lipopolysaccharide. Cells and supernatants were collected for analysis at 1, 6, 24 h after treatment. Cellular viability determined with Trypan blue was significantly reduced in the quartz and 50 μg/ml nanotube treated groups. Enzyme linked- immunosorbent assay was conducted on cell supernatants for Interleukin-8 (IL-8), Tumour necrosis factor-α (TNF- α) and Endothelial monocyte activating polypeptide-II (EMAP-II). I observed no detectable levels of TNF-α or EMAP-II in the supernatant of any group. Although IL-8 concentrations did not differ between treatments its concentrations increased with time within each of the groups. Quantitative real-time reverse-transcriptase polymerase chain reaction (qRTPCR) was also performed for IL-8, and the adhesion molecule ICAM-1. Interleukin-8 mRNA showed increased expression in the 50 μg/ml RNT(**2**)-K1 treated groups at both 1 and 6h, while ICAM-1 showed the greatest increase at 6h in the quartz-treated group. In conclusion, RNT(**2**)-K1 neither reduces cell viability at moderate doses nor does it induce a dose-dependent inflammatory response in pulmonary epithelial cells *in vitro.*

4.2 Introduction

The field of nanotechnology continues to mature, holding the promise of new and value-added materials and devices that will potentially benefit all areas of society (Roco, 2004). One of the primary drivers of nanotechnology is the potential biomedical application of new nanomaterials. While nanomaterials have demonstrated fascinating 'proof of concept' displays of functionality, many fundamental questions remain in order to effectively interface nanotechnology with cellular and subcellular structures.

The general focus of nanoparticle toxicity has traditionally been on combustion derived materials and others with relevance to occupational health such as quartz (Donaldson *et al.*, 2005; Oberdorster *et al.*, 2005b; Oberdorster *et al.*, 2007). Modern versions of nanomaterials have been engineered to exploit novel properties at the nanoscale and have sparked interest in the potential toxicity secondary to particle-cell interactions. Our understanding of these interactions have far reaching implications for development of nanomedical applications, new biomaterials and also to better combat potential toxicity of such materials during human medical application or occupational exposure (Kagan *et al.*, 2005).

Recently, attention has been focused on engineered carbon nanomaterials and the properties which confer biocompatibility or toxicity to them (Cui *et al.*, 2005; Ding *et al.*, 2005; Jia *et al.*, 2005; Lanone & Boczkowski, 2006; Magrez *et al.*, 2006; Nel *et al.*, 2006; Worle-Knirsch *et al.*, 2006; Xia *et al.*, 2006; Yamawaki & Iwai, 2006). *In vitro* work has also been devoted to the cellular responses to carbon nanomaterials (Sayes *et al.*, 2004; Sayes *et al.*, 2005; Chlopek *et al.*, 2006; Magrez *et al.*, 2006; Davoren *et al.*, 2007; Unfried *et al.*, 2007). However, no work has been conducted on self-assembling

nanotubes, that are naturally water soluble and void of metals in the synthetic process (Fenniri *et al.*, 2001; Fenniri *et al.*, 2002a; Fenniri *et al.*, 2002b).

Self-assembling rosette nanotubes, are a novel class of nanotubes that are biologically inspired and naturally water soluble upon synthesis (Fenniri *et al.*, 2001; Fenniri *et al.*, 2002a; Fenniri *et al.*, 2002b). In brief, the nanotubes are formed from guanine-cytosine motif building blocks that undergo a rapid hierarchial self assembly process in water maintained by 18 H-bonds which then organize to form a nanotube with a central channel of 1.1 nm (Fenniri *et al.*, 2001; Fenniri *et al.*, 2002b) . The formed tubes are non-covalent, yet kinetically stable and maintained by electrostatic, hydrophobic and stacking interactions (Fenniri *et al.*, 2002b). The nanostructure studied here known as RNT(**2**)-K1, contains lysine at the G/C motif. However, one of the novel properties of the rosette nanotube is the ability to accept a variety of functional groups at the G/C site which imparts functional versatility to the nanotubes for specific nanomedical or biological applications. These nanotubes are in stark contrast to the widely studied SWNT or MWNT in that their synthesis requires no use of metals and they are naturally water soluble upon formation. The diameter of RNT(**2**)-K1 was shown to be in agreement with the calculated average diameter of 3.2 nm, TEM images of RNT(**2**)-K1 featured a diameter of 3.4 ± 0.3 nm (Moralez *et al.*, 2005). The key difference between these compounds is that RNT(**2**)-K1 has a single G∧C base whereas RNT(**1**)-G0 from Chapter 3 features two bases (See Figures 4.1 and 3.1 respectively).

Previous work has been conducted on the *in vivo* pulmonary responses to self-assembling rosette nanotubes. However, *in vivo* responses are complex and do not provide information on the contributions of individual cells. Airway epithelium is one of

the first lines of defense against inhaled pathogens or environmental pollutants (Nicod, 2005), and has been shown to play a direct role in airway inflammation (Beck-Schimmer *et al.*, 2004). Conversely, the epithelium is also a central target for delivery of pulmonary therapeutics due to its vast surface area and role in inflammation (Groneberg *et al.*, 2003). Upon interaction with foreign particulate material, the epithelium is activated through a cell signaling cascade resulting in secretion of inflammatory mediators and expression of adhesion molecules (Simon & Paine 3rd, 1995; Takizawa, 1998; Ning *et al.*, 2004; Barlow *et al.*, 2005; Gurr *et al.*, 2005; Bergamaschi *et al.*, 2006; Neff *et al.*, 2006). These events are critical for the host defense and can also lead to airway inflammation (Auger *et al.*, 2006). Therefore, it is important to assess the contributions of the epithelium to possible lung inflammatory responses after exposure to RNT. Thus, I used the Calu-3 epithelial cell line to study the effects of direct *in vitro* exposure to RNT(**2**)-K1.

4.3 Materials and methods

4.3.1 *Cell culture*

Calu-3 (human bronchial epithelial adenocarcinoma cell line) cells were procured from American Type Culture Collection (ATCC, Manassas,VA,USA) and cultured in 250ml plastic culture flasks. The cells were cultured and maintained in Minimal Essential Medium (MEM), with 10% Fetal Calf Serum, 4mM glutamine, 0.5ml Pen-strep at 10µg/ml. Cells were grown in an incubator at 37º C, 5% CO_2 and 100% humidity. Media was changed every 3-4 days or as required.

4.3.2 RNT(2)-K1 synthesis and characteristics.

The nanotubes were formed by mixing 1 mg of compound **2** in 1ml of nanopure, sterile water and heating at 90ºC for ~30 min. The self-assembly process is quantitative, thus 1mg of compound **2** yields 1 mg of RNT(**2**)-K1 (Figure 4.1). Scanning and transmission electron microscopy shows that the length of the nanotubes is polydisperse. The synthetic protocol employed here yields tubes that are several microns long. Without a heating protocol they range from 50-200 nm in length. Regardless of the length, RNT(**2**)-K1 has an outer diameter of ~4 nm. Their calculated surface area is ~10^4 m^2/g. The aggregation state of RNT(**2**)-K1 is pH-dependent: as the protonation state of the lysine changes, the nanotubes aggregate in a parallel fashion (Moralez *et al.*, 2005). At low pH they are well dispersed however their status upon being introduced into cell culture media is unknown.

Min-U-Sil 5 ® Quartz was used as a positive control and was procured from US Silica. The company supplied data sheet indicates the more than 98% of the crystalline silica particles were less than 5 μm in diameter and purity was listed at 99.4%. The *E. Coli* lipopolysaccharide (0127:B8) was purchased from Sigma.

4.3.3 ***Experimental overview***

Cells were seeded in 24 wells plates at 5x10^5 cells per well (2cm^2 wells) in 1 ml of media and were allowed to settle for 36h prior to exposure (Figure 4.2). Cells were then exposed to Control (media only), Lysine (50 μg/ml) 1 or 5 or 50 μg/ml of RNT(**2**)-K1, 80 μg/ml of Quartz, or LPS at 1 μg/ml. The Quartz particles were suspended in media and vortexed for 30s prior to exposure to cells. The cell treatment groups were then incubated at 37º C, 5% CO_2 and 100% humidity for 1, 6 or 24h at which time

Trypan blue counts were performed, supernatants were collected for analysis and RNA was isolated from cell pellets. Cells were exposed between passage numbers 8-10.

4.3.4 *Cell viability*

Cell viability was determined using the Trypan blue exclusion method (McAteer & Davis, 2002). Viability is expressed as percentage of non-viable cells.

4.3.5 *Enzyme linked- immunosorbent assay (ELISA) for Tumor necrosis factor-α, Interleukin-8, and Endothelial monocyte-activating polypeptide-II*

The ELISA was conducted on cell supernatants which were collected and stored at -80 ºC. For quantification, samples in duplicates, from triplicate exposures for each treatment were used. Tumor necrosis factor-α and IL-8 were quantified by sandwich ELISA using antibody pairs and recombinant standards purchased from R&D Systems. EMAP-II was quantified as described in section 2.3.5.

4.3.6 *RNA isolation and quantitative real time reverse-transcriptase polymerase chain reaction (qRTPCR) for, Interleukin-8 and ICAM-1*

Total RNA was extracted from the human lung epithelial cells (Calu-3 cell line) by using RNeasy mini kit (Qiagen, Ontario, Canada) according to the manufacturer's instructions. During the extraction process, RNA was treated with RNase-free DNase (Qiagen, Ontario, Canada) to rule out any DNA contamination in the samples. Integrity of RNA was confirmed by agarose gel electrophoresis and RNA was quantified by spectrophotometric analysis. The mRNA was reverse transcribed at 42 °C for 40 min by using QuantiTect reverse transcriptase kit (Qiagen, Ontario, Canada) as per the manufacturer's instructions. This cDNA was used for QRtPCR analysis for the expression of TNF-α (GenBank Accession No. NM_000594), IL-8 (GenBank Accession

No CAG46946) and ICAM-1 (GenBank Accession No. AF340038) genes using Quantifast SYBR green PCR kit (Qiagen, Ontario, Canada). The glyceraldehyde-3-phosphate dehydrogenase gene (GAPDH; GenBank Accession No. NM_002046) was used as the reference housekeeping gene. The reactions were performed using the primer pairs; 5'- ATG AGC ACT GAA AGC ATG-3' and 5'-GAG AGG TCC CTG GGG AAC-3' for TNF-α, 5'-ATG ACT TCC AAG CTG GCC-3' and 5'-ACA ATA ATT TCT GTG TTG GCG-3' for IL-8, 5'-ATG GCT CCC AGC AGC CCC-3' and 5'-TTA GGC AAC GGG GTC TCT-3' for ICAM-1 and 5'-ATG GGG AAG GTG AAG GTC-3' and 5'-GAC AAG CTT CCC GTT CTC-3' for GAPDH. A negative control reaction consisted of all the components of the reaction mixture except RNA. Real-time PCR analysis was performed using the MX3005PLightCycler (Stratagene). The cDNA was denatured at 95°C for 5 minutes. This was followed by amplification of the target DNA through 45 cycles of denaturation at 95°C for 30 seconds, annealing at 55°C for 30 seconds and elongation at 60°C for 30 seconds. Relative expression levels were calculated after correction for expression of GAPDH using MxPro software.

4.3.7 *Data analysis*

Statistical analysis was carried out with SigmaStat® statistical software. Values represent the means ± SD. Comparisons between treatment groups were performed using a two-way ANOVA. When significant main effects were observed, a Tukey's post hoc test was performed. Differences were considered significant when $P < 0.05$.

4.4 Results

4.4.1 *Cell viability*

The percentage of non-viable cells (Fig. 4.3) was increased in the 50 μg/ml RNT(**2**)-K1 and quartz treated cells ($P<0.05$) compared to all other groups at 1h. At 6h the 50 μg/ml RNT(**2**)-K1 and Quartz differed from the Control, Lysine and 1 μg/ml RNT(**2**)-K1 groups. At 24h, LPS treated cells showed a greater number of non-viable cells than Control, Lysine and 1 μg/ml groups, while Quartz treatment resulted in a greater reduction in the percentage of viable cells compared to all other treatment groups at 24h. Within the Quartz treated group cell viability was reduced at 24h more than both the 1h and 6h time-points indicating an effect of time ($P<0.05$). No interaction of time and treatment was indicated by the statistical model.

4.4.2 *Enzyme linked- immunosorbent assay (ELISA) for Interleukin-8, Tumor necrosis factor-α, Endothelial monocyte-activating polypeptide-II*

The levels of TNF-α and EMAP-II were below the limit of detection in the supernatant studied in this experiment. Interleukin-8 concentrations in the supernatant did not differ between treatment groups (Fig 4.4). However, an effect of time was observed within each treatment as IL-8 concentration in the supernatant at 24h was significantly greater than both 1h and 6h time-points.

4.4.3 *RNA isolation and real time reverse-transcriptase polymerase chain reaction (qRTPCR) for Interleukin-8(IL-8) and Intercellular adhesion molecule-1 (ICAM-1)*

The IL-8 mRNA expression was different between 1 and 6 h within each treatment group, with the exception of Quartz and Control cells which did not show an

effect of time (Fig 4.5). At 1h, the 1 and 5 μg/ml RNT(**2**)-K1 treated groups did not differ from LPS or from each other. The IL-8 mRNA expression in the Quartz group did not differ from the lysine treated cells. All other groups at 1 hour were different from each other. At 6 hours, the quartz treated group did not differ from the 1 and 5 μg/ml RNT(**2**)-K1 treated group, nor did the LPS and 50 μg/ml RNT(**2**)-K1 treated groups. All other groups had significantly different levels of IL-8 mRNA expression at 6h. There was a significant interaction effect of dose and time in this statistical model ($P<0.001$).

ICAM-1 mRNA expression was significantly different between 1 and 6 h within each treatment group. At the 1h time-point, all other groups differed from each other with the exception of the Lysine and 50 μg/ml RNT(**2**)-K1 treated cells. At 6h all treatment groups differed significantly from each other.

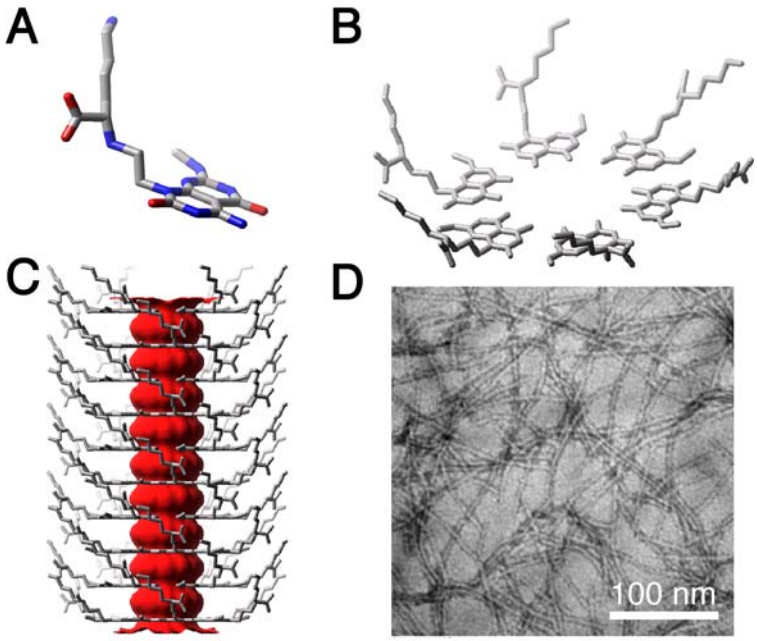

Figure 4.1 Rosette nanotube (RNT(**2**)-K1) assembled from compound **2** and corresponding molecular model and transmission electron micrographs.

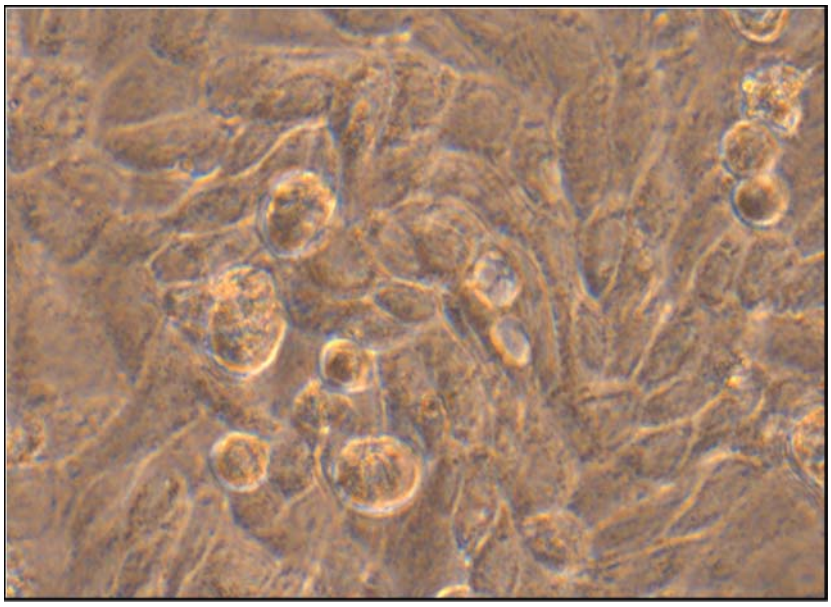

Figure 4.2. Inverted light micrograph of human Calu-3 epithelial cell line in culture. Original image taken at 40X

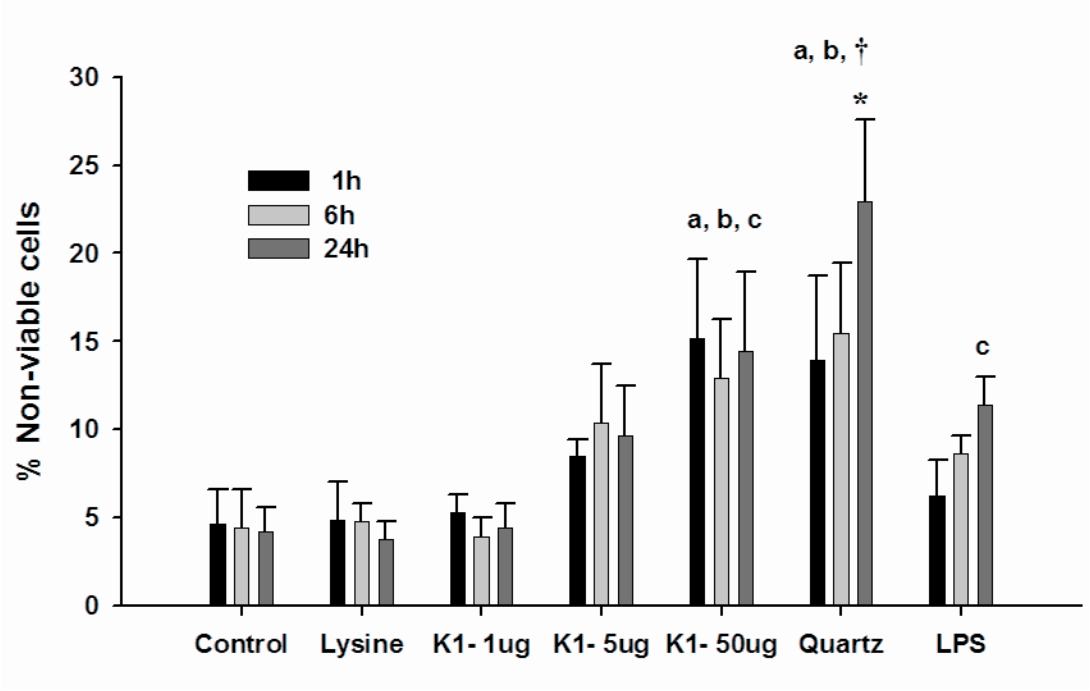

Figure 4.3. Trypan blue cell viability assay. Values are the mean percentage of non-viable cells ± SD of triplicate exposures. **a** denotes significantly greater than Control, Lysine,1 µg/ml RNT(**2**)-K1 and LPS groups at 1h; **b and c** denote significantly greater than Control, Lysine and 1 µg/ml groups at 6h and 24h respectively, ***** denotes greater than 1h and 6h within the Quartz treatment. † denotes greater than all other treatment groups at 24h ($P < 0.05$).

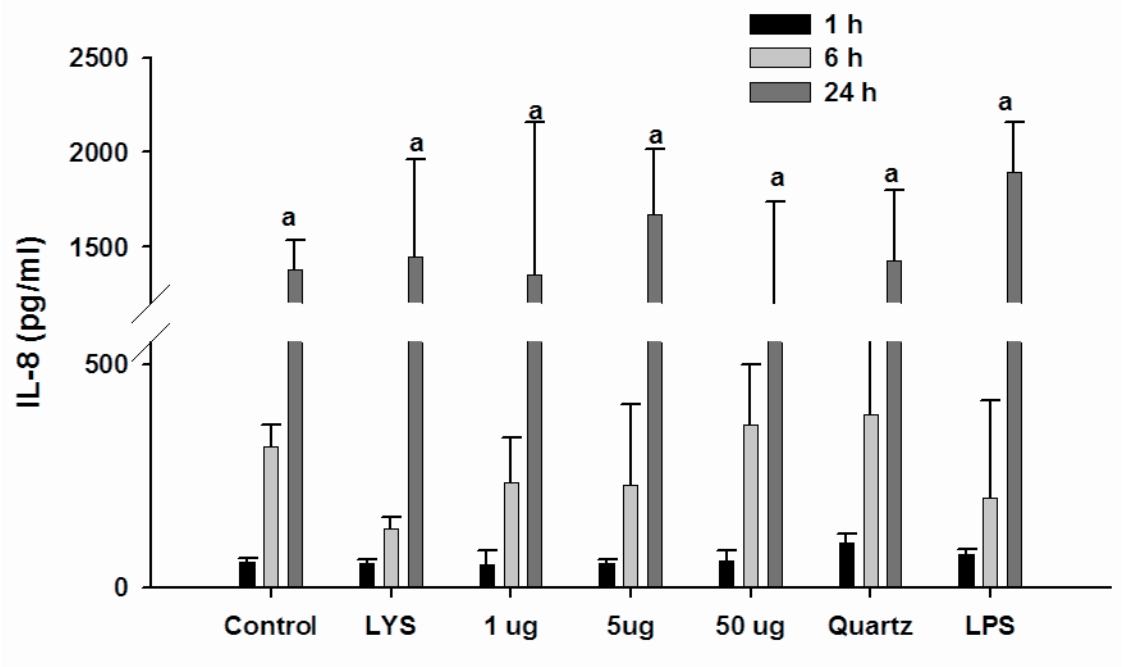

Figure 4.4. Enzyme linked- immunosorbent assay for Interleukin-8 on cell supernatant. '**a**' denotes significantly greater than 1 h and 6 h values within same treatment group ($P<0.05$) .Values represent means ± SD.

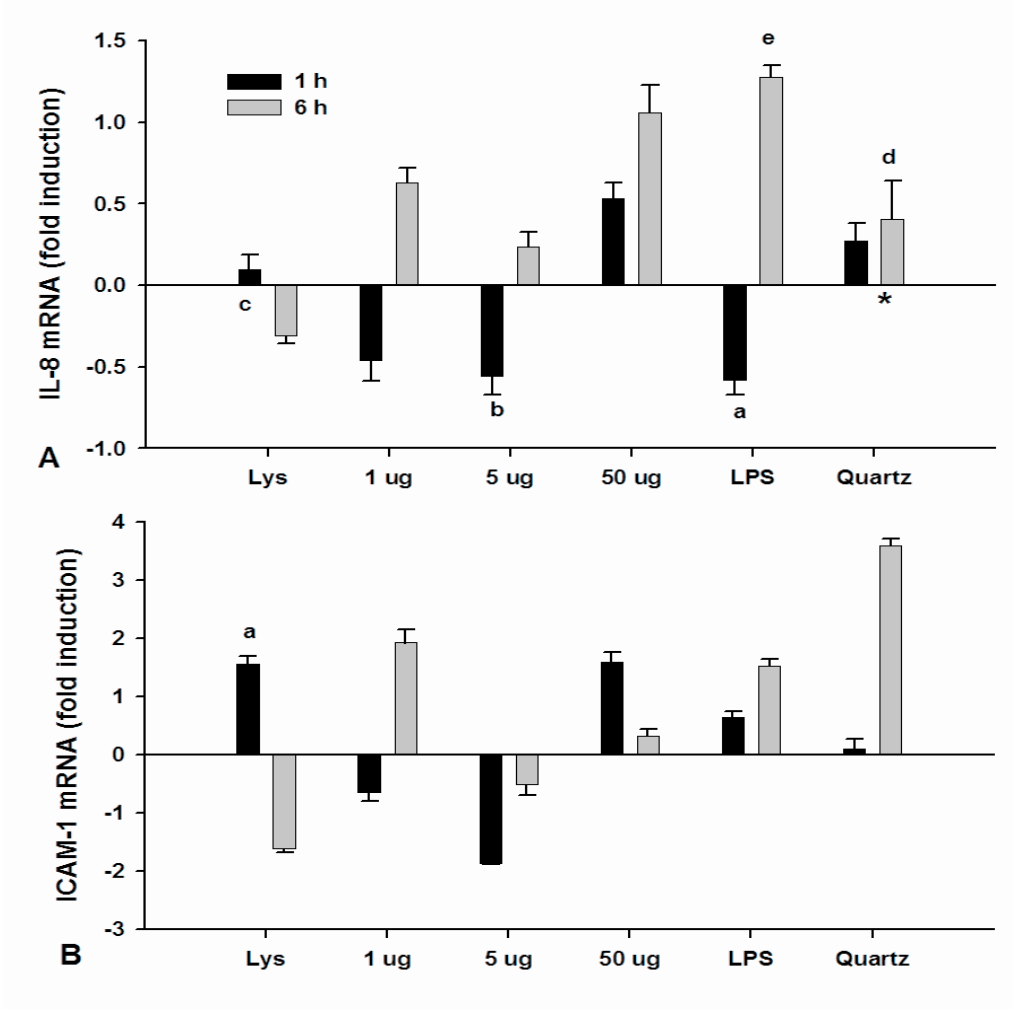

Figure 4.5. Quantitative real time reverse transcriptase polymerase chain reaction for Interleukin-8 (**A**) and Intercellular adhesion molecule-1 (**B**) mRNA expression. Values represent means ± SD fold change from control cells. Interleukin-8 **(A)**:***** denotes no difference between 1&6h. **a** denotes LPS at 1h not different from 1 and 5 µg/ml RNT(**2**)-K1 treated cells; **b** denotes no difference from 1 µg/ml RNT(**2**)-K1group at 1h; **c** denotes quartz not different from Lysine treated cells at 1h. **d** denotes no difference from 1 and 5 µg/ml RNT(**2**)-K1treated cells at 6h; **e** denotes no difference from 50 µg/ml RNT(**2**)-K1 treated cells. All other groups are significantly different from each other. Intercellular adhesion molecule-1 **(B)**: Within each treatment group mRNA expression differed between 1 and 6 h; **a** denotes no significant difference from 50 µg/ml RNT(**2**)-K1 treated cells at 1h. At 6h all treatment groups were significantly different from each other.

4.5 Discussion

The present work represents the first *in vitro* experiments on the interaction of self-assembling rosette nanotubes with a human epithelial cell line and add to our understanding of the lung response previously observed *in vivo* in mice (Journeay *et al.*, 2007b). The results of this study indicate exposure of human Calu-3 epithelial cells to rosette nanotubes can alter transcriptional activity of IL-8 and ICAM-1, but no differences between treatment groups are detected based on levels of IL-8 protein in the supernatant. This is despite changes in cell viability at the highest dose of nanotubes, and with Quartz and LPS treatment of the cells. Thus, Calu-3 human epithelial cells do not exhibit a robust inflammatory response upon exposure to rosette nanotubes, which is likely due to their water soluble and metal free design.

In an attempt to assess the wide spectrum of inflammatory activation of the cells in this study, a range of doses and treatment groups were studied. These doses are comparable to *in vitro* epithelial studies using single-walled nanotubes (Davoren *et al.*, 2007) and also reflect doses equal to the highest and below the lowest doses administered in our *in vivo* study (Journeay *et al.*, 2007b). While high phenomenological doses *in vitro* can provide useful data for comparison with other studies, caution should be used in making broad conclusions from this dose alone. However, the high dose data presented here underscore the biologically favorable toxicity profile of the rosette nanotubes. Distinct features of the present experiment included the use of the human Calu-3 epithelial cell line, and the use of lysine, LPS and Quartz as Control groups. Lysine was used as a control for the lysine component of the rosette nanotubes while LPS is a known activator of epithelial cells (Neff *et al.*, 2006). Other particle cellular toxicity studies have

commonly used the human A549 lung epithelial-like cell lines (Worle-Knirsch *et al.*, 2006; Davoren *et al.*, 2007). Thus, while Calu-3 cells have been used as a model for drug delivery and metabolism studies (Florea *et al.*, 2003; Forbes & Ehrhardt, 2005), this work is the first to examine responses of this cell line after exposure to a soluble engineered nanostructure.

I used Tyrpan blue to assess cell viability. Of note I saw the greatest effect on cell viability in the Quartz treated cells, but also observed a reduction in cell viability in the 50 μg/ml RNT(**2**)-K1 treated group. Quartz treatment was the only group that showed a time-dependent effect on cell viability and by 24h was greater than all other treatment groups. While Trypan blue counting is an accepted method for determining cell viability in a tiered toxicity screening approach (Oberdorster *et al.*, 2005a), it should be interpreted cautiously as this technique indicates grossly disrupted membranes (McAteer & Davis, 2002) and therefore is not specific to other forms of cell death or injury. It has also been shown with molecular nano-onions in skin fibroblasts that the mechanisms of cell death are affected by the dose used (Ding *et al.*, 2005). Nevertheless, I provide the first Trypan blue screening data on rosette nanotubes, and my Quartz data is in agreement with previous work on various forms of Quartz particles (Cakmak *et al.*, 2004). Moreover, the RNT(**2**)-K1 doses of 1 and 5 μg/ml were well tolerated by the cells. These findings are important as they lay a framework around which a non-toxic range of doses can be developed for future cellular uptake and biomedical application studies using the rosette nanotubes.

I also examined the potential secretion of three proinflammatory mediators known as IL-8, TNF-α and EMAP-II, which if secreted *in vivo* can amplify the inflammatory

response and activate other cell types in the lung. Indeed, carbon black has been shown to induce secretion of chemotaxins from type II epithelial cells which can potentially induce monocyte migration (Barlow *et al.*, 2005). It is also well known that particulate matter can directly induce cytokine release in bronchiolar epithelium (Fujii *et al.*, 2001). I did not see a treatment effect on IL-8 secretion in this cell line, but rather an effect of time on IL-8 levels in the supernatant of all groups. Similar to Mazzarella and colleagues (Mazzarella *et al.*, 2007) I also observed an increase in IL-8 in the supernatant over time even in the control cells. While it is somewhat surprising that our controls did not differ from the treatment groups, cytokines can play a role in autocrine and paracrine cellular processes involved with growth and development. Lipopolysaccharide was used as a positive control and was expected to produce large amounts of IL-8. But others have studied A549 cells and failed to induce IL-8 gene expression or protein secretion within 24 hours of using LPS doses ranging from 1pg to 10µg (Standiford *et al.*, 1990). While our LPS dose of 1µg/ml was considered significant I did not observe an effect on cytokine secretion and the reasons for lack of an effect are not apparent from these experiments. Interleukin-8 and its rodent analogue MIP-2 (Driscoll, 2000), are chemokines often associated with oxidative stress and can lead to significant cell recruitment *in vivo* (Dailey *et al.*, 2006; Kobayashi, 2006). Given the role of metals in nanostructure-induced oxidative stress (Ghio *et al.*, 1999; Donaldson *et al.*, 2006; Kagan *et al.*, 2006; Xia *et al.*, 2006; Shvedova *et al.*, 2007), it is a reasonable conclusion that the lack of treatment effect on IL-8 secretion may be due to the fact that the rosette nanotubes are void of metals.

While macrophages are generally accepted as a robust source of TNF-α (Rich *et al.*, 1989), little is know about secretion of this protein in the Calu-3 cell line. I did not detect TNF-α in the supernatant of any of the samples. This is in agreement with other work that treated epithelial cells with quartz (Driscoll *et al.*, 1997). Conversely quartz has been shown to trigger release of TNF-α in macrophages (Driscoll *et al.*, 1993). It is also well known that pulmonary epithelium can respond to exogenous TNF-α produced by macrophages (Driscoll *et al.*, 1997; Driscoll, 2000). However, my data suggest that Calu-3 cells do not produce detectable levels of the cytokine in response to the treatment doses used in these experiments.

In my previous work I identified upregulation of total EMAP-II (proEMAP/p43 and mature EMAP-II) in LPS-treated rat lungs and localized this protein intracellularly in the pulmonary epithelium (Journeay *et al.*, 2007a). Additionally, it has been shown in a meconium- aspiration induced model of lung injury that mature EMAP-II expression is increased (Lukkarinen *et al.*, 2004). Thus, it is possible that *in vitro*, mature EMAP-II could be secreted in response to particle exposure. However, similar to TNF-α, mature EMAP-II was not detected in the supernatant. Both proEMAP/p43 and mature EMAP-II are proinflammatory so the fact that I did not see secretion of this protein *in vitro* does not rule out the possibility that intracellular proEMAP/p43 is increased. While EMAP-II biology is still being investigated (van Horssen *et al.*, 2006) I show here that *in vitro* Calu-3 epithelial cell exposure to rosette nanotubes, quartz or LPS does not cause secretion of EMAP-II. It is possible that the concentration of TNF-α and EMAP-II in the supernatants were below the detection limit because of their dilution in the supernatant or lack of release of these cytokines from intracellular sites.

To better understand whether exposure to nanotubes was inducing transcription of proinflammatory molecules, I studied mRNA expression of IL-8 and ICAM-1. Recent work has shown an upregulation of IL-8 mRNA in an A549 human epithelial cell line at 4 h post-exposure to TiO_2 (Singh *et al.*, 2007). Our data show an increase in IL-8 mRNA in Quartz and 50 μg/ml RNT(**2**)-K1 treated cells at both 1h and 6h. Furthermore, LPS treated cells showed a significant increase by 6h. Of note all treatment groups except lysine treated cells showed an increase in IL-8 mRNA over controls, suggesting that for some treatments a time period of 1-6 hours is required for a significant transcriptional response. While the mRNA data do not parallel responses observed with protein secretion, it is possible that even though transcription of the IL-8 gene is activated, it may not necessarily lead to a greater level of protein secretion into the supernatant due to post-translational blocks. Furthermore, there could be intracellular accumulation of IL-8 protein and in future studies one could disrupt the cells to measure the intracellular pool of the protein as well (Standiford *et al.*, 1990).

Intercellular adhesion molecule-1 (ICAM-1) has previously been shown to be upregulated on the rat epithelial cell surface in response to LPS (Madjdpour *et al.*, 2000) and also in human bronchiolar epithelium subsequent to exposure to diesel particles (Takizawa *et al.*, 2000), or PM_{10} (Ishii *et al.*, 2005). However these are the first mRNA expression data in the Calu-3 epithelial cell line using an engineered nanomaterial and show modest differences in expression between treatment groups, with Quartz showing the most prominent increase in ICAM-1 mRNA transcription at 6h. The ICAM-1 is an adhesion protein that ligates β-2 integrins and its expression is critical for the recruitment of inflammatory cells such as neutrophils (Beck-Schimmer *et al.*, 2004). The modest

increases in ICAM-1 mRNA expression along with changes in IL-8 mRNA expression following RNT(**2**)-K1 treatment suggest proinflammatory activation of Calu-3 cells.

4.6 Summary

This study provides the first data in the human Calu-3 epithelial cell line on the inflammatory activation by water soluble, self-assembling nanotubes. While the pulmonary epithelium can be directly activated by particulate matter (Fujii *et al.*, 2001) diesel particles (Takizawa *et al.*, 2000), and LPS (Madjdpour *et al.*, 2000), the present data suggest a lack of a robust *in vitro* inflammatory response in the human Calu-3 epithelial cell line. It is likely that the novel metal free and water soluble nature of the rosette nanotubes plays a role in the observed lack of cytokine secretion in this study.

CHAPTER 5

Inflammatory activation of the human U937 monocytic cell line by self-assembled rosette nanotubes

5.1 Abstract

More information on the body's initial defense responses to nanomaterials are required due to possible exposures either through intentional medical and consumer application or unintentional airborne occupational materials. Here I have studied the inflammatory responses of the human U937 macrophage cell line to rosette nanotube exposure and also tested the effect of nanotube-length on cytokine levels in the supernatant. Cells were plated in the same number and treated in the same manner as per Chapter 4. The results indicate that RNT(**2**)-K1 can activate transcription of proinflammatory genes (IL-8 and TNF-α) as early as one hour, but this effect is not paralleled by protein secretion into the supernatant. Although both short and long nanotubes exhibit time-dependent effects on cytokine secretion, neither the dose nor nanotube length have a profound effect on inflammatory protein release. Moreover, 1 and 5 μg/ml of RNT(**2**)-K1 have no effect on cell viability by 24h. These data indicate that the U937 human macrophage cell line lacks a robust inflammatory response upon exposure to rosette nanotubes.

5.2 Introduction

Increasing activity in nanotechnology has elevated the demand for information on the interactions of biological systems with nanomaterials. The development of nanotechnology is leading to a wide array of nanostructures with novel physicochemical properties for applications in medicine, composite materials and electronics to name a few. As the field matures there is an increased probability of intentional exposure through medical or consumer products (Oberdorster *et al.*, 2005b; Oberdorster *et al.*, 2007) or unintentional exposure via occupational handling of commercial quantities of nanomaterials (Maynard & Aitken, 2007). Regardless of the exposure scenario, information on the toxicity and fate of nanomaterials within organisms is warranted.

Nanomaterials may gain access to the body via a number of routes of exposure but much of the literature has focused on inhalation exposure. Indeed, our initial understanding of nanotoxicology is rooted in studies on ultrafine particles (Oberdorster *et al.*, 2005b; Oberdorster *et al.*, 2007). Nanomaterials by the nature of their size are considered to have a greater propensity to become airborne and moreover, particles less than <100nm have a greater deposition potential and can reach the alveolar region of the lung (ICRP, 1994). As a result, pulmonary nanotoxicology studies may have applications from two perspectives (Medina *et al.*, 2007). The first being to better understand uptake and clearance for particulate nanomedicines to harness the large surface area and highly vascular nature of the deep lung (Hung, 2006; Moghimi & Kissel, 2006; Pison *et al.*, 2006), and the second being to better understand the disposition of nanoscale particles in the lung and how their unique properties may trigger disease processes (Bergamaschi *et al.*, 2006).

Once an agent reaches the lung environment one of the first cellular defenses to be encountered is the macrophage population. Typically, macrophages engulf foreign particulate and transport the material to the mucociliary escalator for clearance (Lehnert, 1992). Indeed this clearance mechanism is a crucial aspect in determining retention of particles in the lung and possible translocation to the interstitium or the blood. When a macrophage engulfs foreign agents or inert particles it produces a proinflammatory signal (Duffield, 2003). An understanding of this inflammatory activation of macrophages is central to understanding the lung response to nanomaterial exposure.

Cytotoxicity has been shown to be attenuated when carbon nanomaterials such as single-walled nanotubes and fullerenes are made soluble with the addition of surface molecules (Sayes *et al.*, 2004; Sayes *et al.*, 2005; Dumortier *et al.*, 2006; Nimmagadda *et al.*, 2006). Self-assembling rosette nanotubes however, are a novel class of nanotubes that are biologically inspired and naturally water soluble upon synthesis (Fenniri *et al.*, 2001; Fenniri *et al.*, 2002a; Fenniri *et al.*, 2002b). We have previously examined their proinflammatory potential *in vivo* using mice and *in vitro* using a pulmonary epithelial cell line. Alveolar macrophages are credited with clearance of inhaled particles and to keep the alveolar epithelium clear for gas exchange (Lehnert *et al.*, 1985; Dorger & Krombach, 2000). These cells, however, can be activated by bacteria, endotoxins and particles which initiates inflammation in the alveolar region (Driscoll *et al.*, 1993; Oberdorster *et al.*, 1994; Olivieri & Scoditti, 2005). Given the strategic location and inflammatory activity of the alveolar macrophages and the potential biomedical implications of their interactions with RNT, I used a human macrophage cell line to investigate their responses following exposure to RNT.

5.3 Materials and Methods

5.3.1 *Cell culture*

U937 human monocytic cells (Sundstrom & Nilsson, 1976) were procured from American Type Culture Collections (ATCC, Manassas,VA,USA) and cultured in 250ml plastic culture flasks. The cells were cultured and maintained in RPMI-1640, with 10% Fetal calf serum, 1% Pen-Strep at 100 U penicillin and 100 μg/ml Streptomycin, 4.5 mM glucose, 1mM sodium pyruvate, 15mM HEPES. Cells were grown in an incubator at 37º C, 5% CO_2 and 100% humidity and maintained between 2 x 10^5 and 2 x 10^6 cells/ml of media. Media was changed every 3-4 days or as required. See Figure 5.1 for cell images.

The cells were induced to differentiate into macrophages by adding 12-*O*-tetradecanoylphorbol 13-acetate (TPA) at 5 μg/ml after which the cells were allowed to adhere for 48h prior to exposure.

5.3.2 *RNT(2)-K1 synthesis and characteristics.*

See section 4.2.2 for RNT(**2**)-K1, Quartz and LPS characteristics. See Figure 4.1 for RNT(**2**)-K1 image. The short RNT(**2**)-K1, were synthesized in water at 18°C, which as been shown to reduce the self-assembled length of the nanotubes relative to synthesis at 90°C (Fenniri *et al.*, 2002b).

5.3.3 *Experimental overview*

Cells were seeded at 5x10^5 cells in 24 well plates (2cm^2). Cells were then exposed to Control (media only), Lysine (50 μg/ml) 1 ,5 or 50 μg/ml of RNT(**2**)-K1 ,80 μg/ml of Quartz or LPS at 1 μg/ml The Quartz particles were suspended in media and vortexed for 30s prior to exposure to cells. The cell treatment groups were then incubated at 37º C, 5% CO_2 and 100% humidity for 1, 6 or 24h at which time Trypan blue counts

were performed, supernatants were collected for analysis and RNA was isolated from cell pellets.

5.3.4 *Cell viability*

Cell viability was determined as per section 4.3.4.

5.3.5 *Enzyme linked- immunosorbent assay (ELISA) for Tumor necrosis factor-α, Interleukin-8 and Endothelial monocyte-activating polypeptide-II*

This was performed as per section 4.3.5.

5.3.6 *RNA isolation and real time reverse-transcriptase polymerase chain reaction (qRTPCR) for TNF-α, Interleukin-8 and Intercellular adhesion molecule-1*

This was performed as per section 4.3.6.

5.3.7 *Data analysis*

Statistical analysis was carried out with SigmaStat statistical software. Values represent the means ± SD. Comparisons between treatment groups were performed using a two-way ANOVA. When significant main effects were observed, a Tukey's post hoc test was performed. Differences were considered significant when $P < 0.05$.

5.4 Results

5.4.1 *Cell Viability*

Cell viability results are displayed in Figure 5.2. Within the Quartz treated group, cell viability was significantly different between all time points. In the 50 μg/ml RNT(**2**)-K1 treated cells a significant reduction in cell viability was observed at 24h relative to the 1h and 6h groups. Within the 1h time-point no reduction in cell viability was observed between any treatments. At 6h Quartz treated cells showed reduced viability as

compared to Control, Lysine and 1 and 5 μg/ml RNT(**2**)-K1treated cells. At 24h, quartz treated cells showed reduced viability over all other treatments at 24h.

5.4.2 *Enzyme linked- immunosorbent assay (ELISA) for Tumor necrosis factor-α and Endothelial monocyte-activating polypeptide-II on cell supernatant*

Within the control, lysine and 1 μg/ml RNT treated groups levels of TNF-α did not change over time (Figure 5.3A). Within the LPS, quartz, 5 and 50 μg/ml RNT(**2**)-K1 treated groups an effect of time on cytokine level was observed. At 1h, TNF-α concentration did not differ between treatments. At 6h, the Quartz samples contained significantly less TNF-α concentrations than the LPS, Lysine, 5 and 50μg/ml RNT(**2**)-K1 treated groups. LPS-treated cells showed more TNF-α than the 50 μg/ml RNT(**2**)-K1 treated groups at 6h. At 24h, lysine treated cells showed significantly less cytokine compared to 5 and 50 μg/ml RNT(**2**)-K1 treated groups.

Endothelial monocyte-activating polypeptide-II was only detected in the LPS and Quartz treated groups at 24h of exposure. Interleukin-8 data was inconclusive and therefore not reported here (Figure 5.3B).

Short nanotubes (Figure 5.4) induced a time-dependent effect among the different doses. Within the 5 and 50 μg/ml RNT(**2**)-K1 treated cells, supernatant levels of TNF-α at 1h were lower than both 6 and 24h time-points. In the 1 μg/ml RNT(**2**)-K1 treated cells levels of TNF-α only differed between 1h and 24h samples.

5.4.3 *Quantitative real time reverse-transcriptase polymerase chain reaction (qRTPCR) for TNF-α, Interleukin-8 and ICAM-1*

TNF-α mRNA induction was different in all groups between 1h and 6h except in the LPS treated cells (Figure 5.5A). At 1h, all treatment groups exhibited increased

mRNA expression relative to control cells except the Lysine and LPS groups in which mRNA levels were suppressed below control. Quartz treated cells showed greater TNF-α mRNA expression than all of the other treatment groups. At 6h, the quartz treated cells showed a higher level of mRNA expression that all other treatment groups. The RNT(**2**)-K1 treated groups did not differ in their mRNA expression as function of dose.

Within each treatment group IL-8 mRNA was significantly different between 1h and 6h (Figure 5.5B). At the 1h time point, in the 1 μg/ml RNT(**2**)-K1 treated group, mRNA did not differ from the 5μg/ml and 50 μg/ml RNT(**2**)-K1 groups. The 5 and 50 μg/ml RNT(**2**)-K1 groups did not differ from each other or the quartz treated group. All other groups were significantly different from each other at 1h. At 6h, the level of induction did not differ between nanotubes treated groups, nor did LPS differ from Lysine treated cells. All other groups were significantly different from each other at 6h. The level of induction demonstrated significant interaction between time and treatment.

For ICAM-1 expression (Figure 5.5C) only the LPS, 5 and 50 μg/ml RNT(**2**)-K1 treated groups differed between 1 and 6h. At 1h, the Lysine, Quartz, 1 and 5 μg/ml RNT(**2**)-K1treated groups did not differ from each other. At 6h, the Lysine, Quartz, 1 and 5 μg/ml RNT(**2**)-K1 treated groups did not differ from each other, nor did the 5 and 50 μg/ml RNT(**2**)-K1 treated groups. All other groups were significantly different from each other at 6h. The level of ICAM-1 induction demonstrated significant interaction between time and treatment.

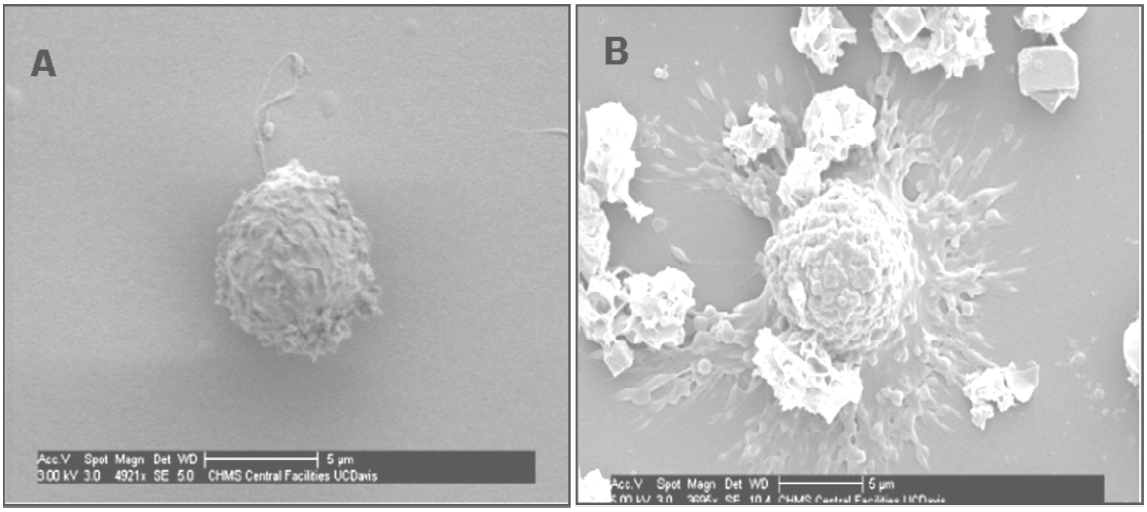

Figure 5.1 Scanning electron micrograph (SEM) images of U937 cell line. **A**: Undifferentiated U937 monocyte and **B**: differentiated U937 macrophage. Images are from work published by Vogel et al. *Cardiovascular Toxicology* 4: 363-73, 2004 (Vogel *et al.*, 2004). **Permission to use granted on 08-13-2007 (See Appendix A).**

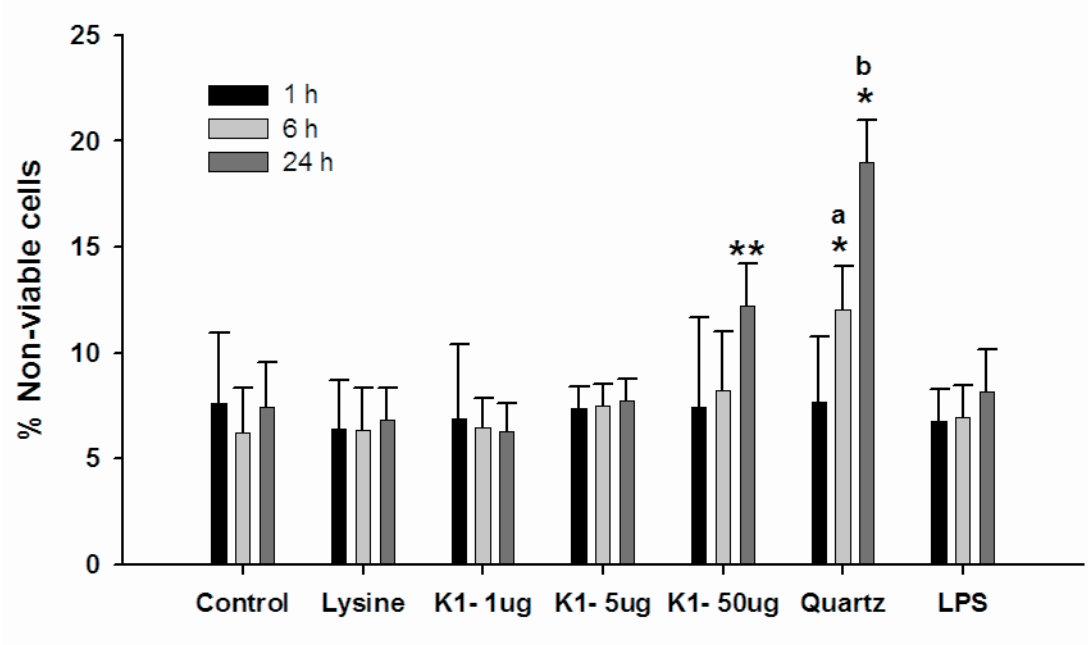

Figure 5.2. Trypan blue cell viability assay. Values are the mean percentage of non-viable cells ± SD of triplicate exposures. ***** denotes difference between other time-points within the Quartz treatment ($P < 0.05$). ****** denotes significantly different from 1 and 6h time points within 50 µg/ml RNT(**2**)-K1 treated cells. **a** denotes reduced viability as compared to Control, Lysine and 1 and 5 µg/ml RNT(**2**)-K1 treated cells at 6h. **b** denotes significantly different from all other treatments at 24 h.

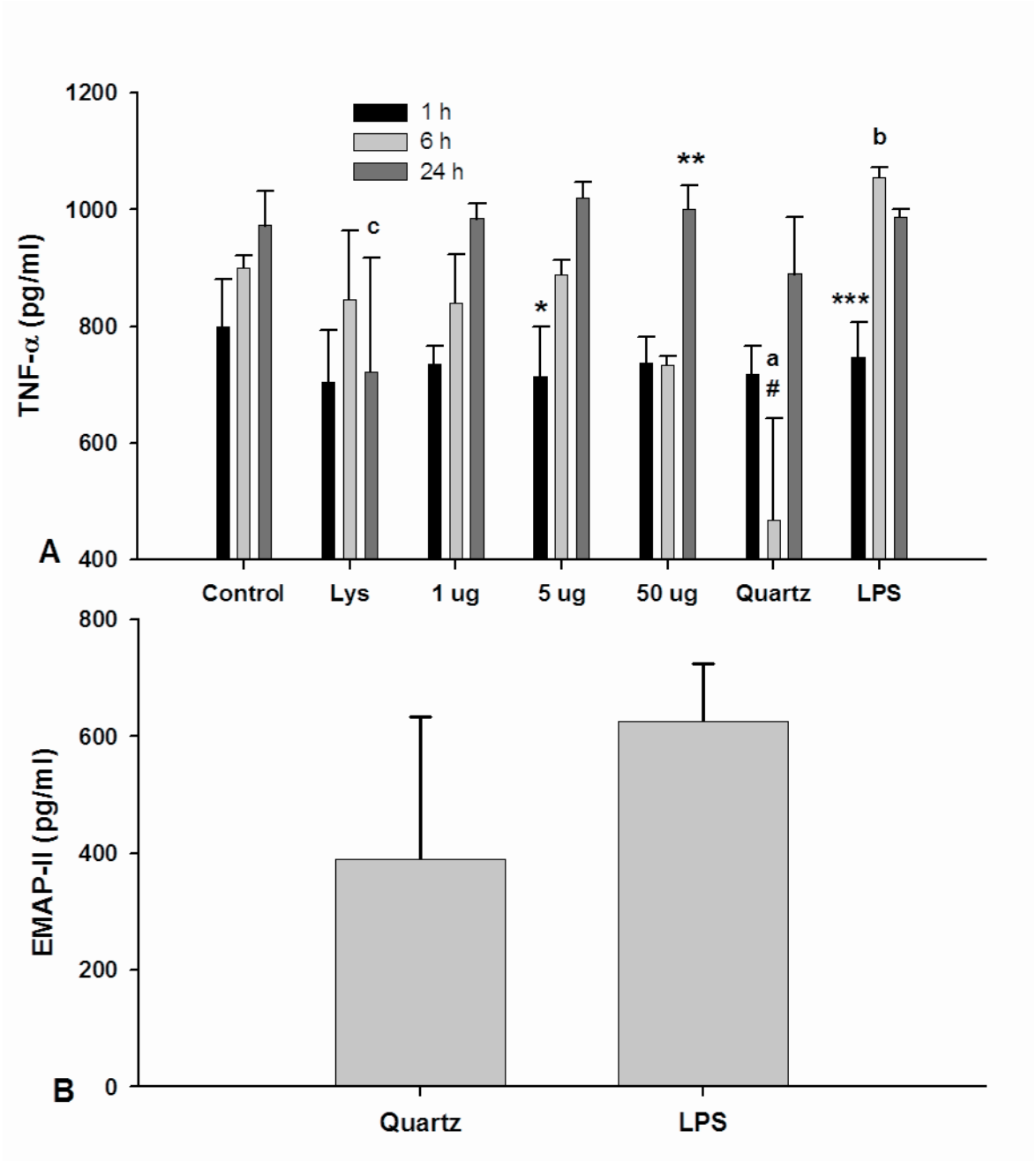

Figure 5.3 Enzyme linked-immunosorbent assay for tumor necrosis factor-α (**A**), and Endothelial monocyte-activating polypeptide-II (**B**) on cell supernatant. Values represent means ± SD. **A**: ***** denotes different from same group at 24h. ****** denotes greater than same group at both 1 and 6h. # denotes less than both 1 and 24h levels. ******* 1h LPS values are less than both 6 and 24h. **a** denotes Tumor necrosis factor-α was lower than all other treatment groups at 6h, except the 50 µg/ml RNT(**2**)-K1 group. **b** indicates higher than all groups at 6h. **c** indicates lysine treated cells showed less Tumor necrosis factor-α in the supernatant than both the 5 and 50 µg/ml RNT(**2**)-K1 treated cells at 24h. **B:** No difference in Endothelial monocyte-activating polypeptide-II concentration was detected in the Quartz and LPS groups.

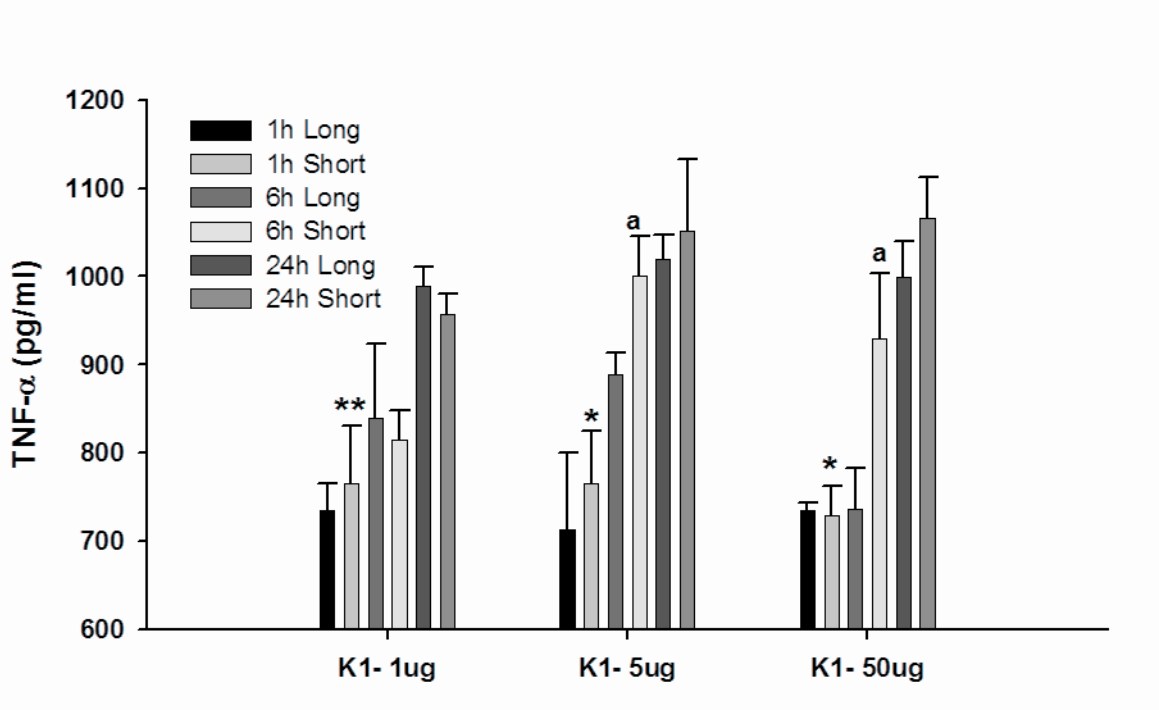

Figure 5.4 Effect of RNT(**2**)-K1 length on tumor necrosis factor-α levels in supernatant as determined by Enzyme linked-immunosorbent assay. Effect of time for long RNT(**2**)-K1 is depicted in Fig. 5.3. ****** denotes lower level than same dose of short tubes at 24h. ***** indicates lower than both 6 and 24h time points. **a** indicates significant difference from long RNT(**2**)-K1 at 6h.

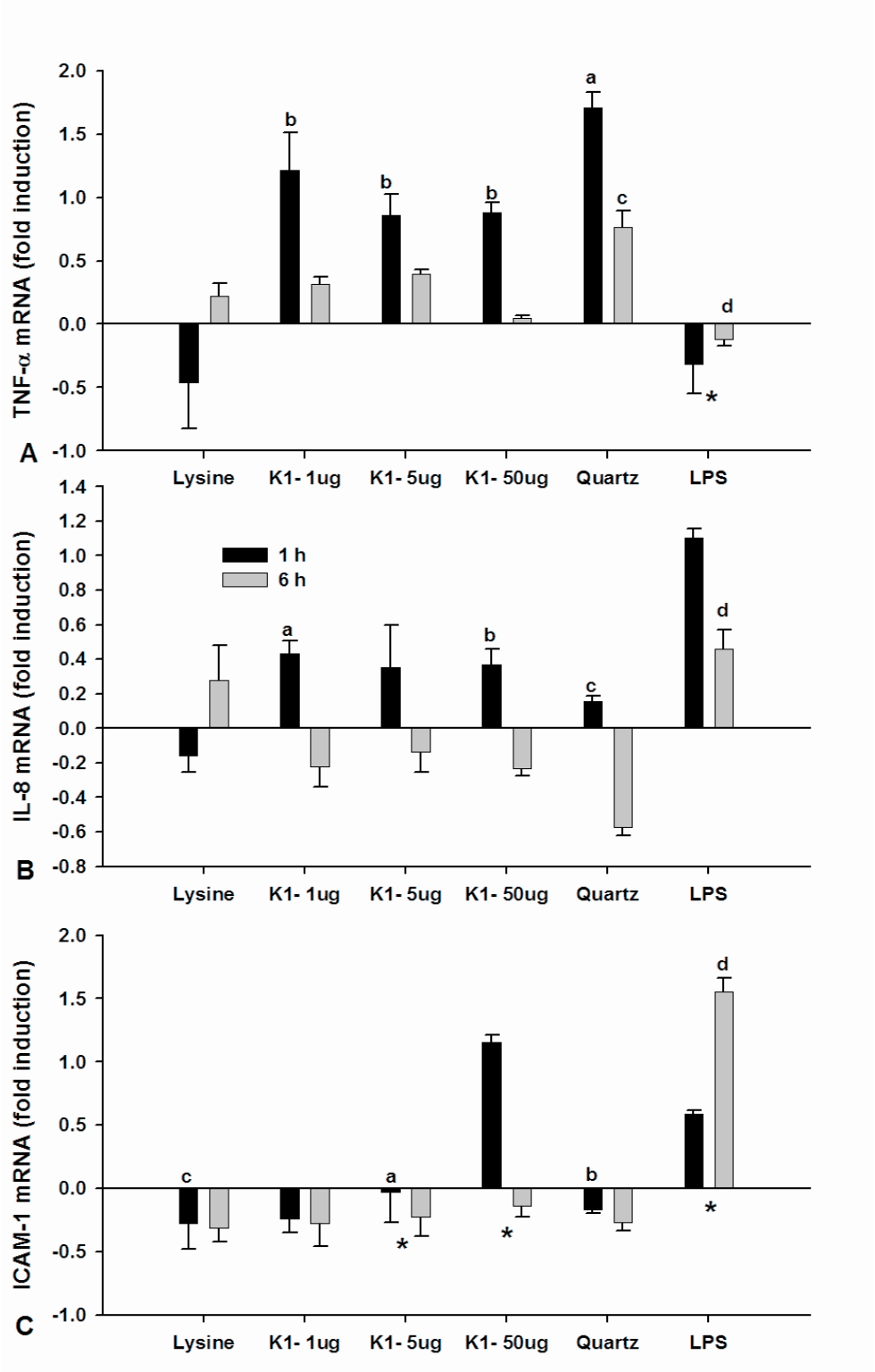

Figure 5.5. Quantitative real time reverse transcriptase polymerase chain reaction for tumor necrosis factor-α (**A**) Interleukin-8 (**B**) and intercellular adhesion molecule-1 (**C**) mRNA expression. Values represent means ± SD fold change from control cells. **A: *** indicates values for LPS treated cells did not differ

between 1 and 6h. All other groups demonstrated an effect of time. **a** indicates quartz treated cells expressed greater levels of mRNA than all other treatment groups at 1h. **b** indicates greater mRNA expression than Lysine and LPS groups at 1h. **c** indicates the quartz value was higher than all other treatment groups at 6h. **d** indicated lower mRNA expression than both the 1 and 5 μg/ml RNT(**2**)-K1 treated cells at 6h. **B:** Within each treatment all values differed between and 1 and 6h. **a** indicates no difference from 5 and 50 μg/ml RNT at 1h. **b** indicates not different from Quartz or 5 μg/ml RNT at 1h. **c** indicates not different from 5 μg/ml RNT at 1h. **d** LPS did not differ from Lysine at 6h. None of the RNT(**2**)-K1 treated groups differed from each other 6h. All other treatment groups were significantly different at 6h. **C: *** indicates values are different between 1 and 6h. **a** indicates at 1h, 5 μg/ml RNT(**2**)-K1 did not differ from Lysine, Quartz, or 1 μg/ml RNT treated cells. **b** indicates Quartz did not differ from Lysine or 1 μg/ml at 1h. **c** indicates no difference between Lysine and 1 μg/ml RNT(**2**)-K1 treated cells. **d** indicated LPS treated cells had greater Intercellular adhesion molecule-1 mRNA expression than all other treatments at 6h. No other differences between groups were detected.

5.5 Discussion

This work demonstrates that human U937 macrophages lack a robust inflammatory response upon exposure to rosette nanotubes. Such information is important because macrophages are a pivotal cell type for recognition and removal of engineered nanostructures from the lung environment. Moreover, by altering the temperature conditions of self-assembly I have studied the effect of nanotube length on inflammatory activation. Of note, the rosette nanotubes only reduce cell viability at 24h under the highest dose conditions, which is in contrast to that of quartz which reduced cell viability more prominently.

Previous studies have examined macrophage responses to the single-walled carbon nanotubes (Jia *et al.*, 2005; Dumortier *et al.*, 2006; Kagan *et al.*, 2006; Pulskamp *et al.*, 2007). Additionally, the U937 cell line has been employed to study the induction of proinflammatory cytokines by air pollution particulate (Vogel *et al.*, 2005). While Dumortier et al.(Dumortier *et al.*, 2006) studied functionalized water soluble carbon nanotubes in macrophages additional *in vitro* work has been conducted on other water solubilized nanostructures (Sayes *et al.*, 2004; Sayes *et al.*, 2005). The present work is however the first work peformed on a naturally water-soluble and self-assembling nanotube with 'length-tunable' characteristics.

Cell viability was studied using the Trypan blue exclusion method and indicated that only at 24h did the highest dose of rosette nanotubes reduce viability. This is in contrast to the quartz treated cells which showed a significant reduction in cell viability by 6h and also a greater magnitude of effect over all other treatment groups. The quartz data are similar to other work using the Trypan blue method in this cell line whereby

urban dust and diesel exhaust particulate reduced cell viability by 24h (Vogel *et al.*, 2005). As discussed in the previous chapter, Trypan blue detects only gross disruption of the membrane (McAteer & Davis, 2002) and therefore does not discriminate among other forms of cell death.

As markers of inflammatory activation, the supernatant levels of cytokines TNF-α and EMAP-II were measured. Tumour necrosis factor-α is produced by a number of cell types but the alveolar macrophages are a particularly robust source of this protein (Rich *et al.*, 1989). It is a key initiator of the lung inflammatory cascade as it induces a number of proinflammatory effects in other cellular targets in the lung (Driscoll, 2000). I noticed higher concentrations of secreted TNF-α in the LPS treated cells than all other treatment groups at the 6h time-point. This difference however was no longer apparent by 24h. Conversely, TNF-α concentration in the Quartz treated group was the lowest at 6h but not at 24h. This coincides with the reduction in cell viability observed at 6h which would suggest fewer viable cells were available to produce and secrete the protein. Quartz treated cells showed the greatest induction of TNF-α mRNA at both 1 and 6h and therefore suggests that while the gene is being transcribed other factors are contributing to the lack of differences in protein level in the supernatant.

The rosette nanotubes are synthesized via a self-assembly mechanism, in which the length of the nanotubular structures has been shown to be influenced by temperature of the solvent (Fenniri *et al.*, 2002b). I leveraged this temperature dependent effect to study the effect of nanotube length on TNF-α release. Previously, Sato and colleagues (Sato *et al.*, 2005) studied the influence of multi-walled carbon nanotube length on responses of a THP-1 leukemia cell line and on subcutaneous inflammatory responses.

They concluded that the degree of inflammation in cutaneous tissue was greater for 825nm-MWCNT than for 225nm-MWNT. They attributed this observation to the likelihood that the shorter MWNT would be more readily enveloped. The present experiments differ from that of Sato et al. in that the short RNT(**2**)-K1 ranged from 50-200nm while the long RNT were microns long. I observed an effect of length only at 6h in the 5 and 50 μg/ml RNT groups and contrary to Sato and colleagues I noticed a greater response in the short RNT treated cells as measured by TNF-α secretion. This response may reflect differences in the phagocytic action towards different sized structures. The effect of nanostructure size on uptake and the time-course of proinflammatory activation has not yet been fully elucidated (Oberdorster *et al.*, 1994; Lucarelli *et al.*, 2004; Moss & Wong, 2006).

I also report the first data on secretion of mature EMAP-II from a human macrophage cell line *in vitro*. In rats, I have previously shown that total EMAP-II is upregulated in LPS induced acute lung inflammation and using immuno-gold electron microscopy localized EMAP-II in monocytes (See Fig 2.2G). The present data indicate that rosette nanotubes do not induce secretion of mature EMAP-II at any dose or time-point. However, I did observe an increase in EMAP-II concentration in macrophages treated with LPS and quartz at 24h. This finding adds to my data on EMAP-II upregulation *in vivo* and for the first time identifies Quartz exposure as a possible stimulant for EMAP-II release *in vitro*. Elaboration of EMAP-II by macrophages *in vivo* in response to inhaled particulate matter would lead to recruitment of monocytes/macrophages to promote lung inflammation as shown by intratracheal instillation of pure EMAP-II (Journeay *et al.*, 2007a).

I also studied the induction of gene expression for the proinflammatory mediators. Tumour necrosis factor-α gene transcription was quickly activated upon exposure to all nanotube doses as well as Quartz at 1h. This effect was not observed in the Lysine and LPS treated cells. The fold change in TNF-α mRNA was less apparent by 6h in the RNT groups but remained the most elevated in Quartz treated cells. It is logical that transcription of the TNF-α is induced rapidly in response to foreign particulate. This is supported by studies showing TNF-α is one of the central proinflammatory mediators produced by macrophages (Rich *et al.*, 1989) and that its secretion is also a hallmark of particle induced inflammation (Driscoll *et al.*, 1997; Driscoll, 2000).

All treatment groups demonstrated a divergent transcriptional response between 1 and 6h relative to control cells for IL-8 mRNA. At 1h, all treatment groups with the exception of lysine showed an increased transcriptional response relative to controls, while at 6 h the opposite was true for all groups except LPS where mRNA levels remained elevated above the control cells. While few data exist on engineered nanostructures and the induction of proinflammatory cytokine transcription (Gojova *et al.*, 2007), previous work using carbon black, urban and diesel exhaust particulate have reported such responses *in vitro* using the U937 cell line (Vogel *et al.*, 2005). They observed comparable IL-8 mRNA changes using carbon black, with much larger changes being observed for atmospheric particulate types. A key difference in my study is the measurement of mRNA induction at much earlier time points (1 and 6h) and the fact that the atmospheric particles contain many contaminants which are metallic in nature (Ghio *et al.*, 1999). The increased expression of IL-8 has important implications *in vivo* because

this cytokine is a central chemotactic molecule for neutrophil migration into the lung (Goodman *et al.*, 2003; Kobayashi, 2006).

Intercellular adhesion molecule-1 (ICAM-1) mRNA changes were also studied. ICAM-1 mRNA is suppressed below control levels in all groups except the 50 μg/ml RNT(**2**)-K1 group and the LPS treated cells at 1h. At 6h, however only LPS treated cells have increased levels of ICAM-1 mRNA over control cells. Once again few data exist on soluble engineered nanomaterials and their ability to induce adhesion molecules. It has been shown that alveolar macrophage expression of ICAM-1 can be increased after 24h of exposure to PM_{10} (Ishii *et al.*, 2005), however no effect was seen when measured at 2h. Given that rosette nanotubes are drastically different structures from PM_{10} and the time course of our measures was different, I can conclude that ICAM-1 is not induced at low doses of RNT(**2**)-K1 before 6h *in vitro*. However, LPS which is a well known inducer of ICAM-1 did show an increase at both 1 and 6h.

5.6 Summary

I provide the first data in a human macrophage cell line after exposure to rosette nanotubes. The results indicate that RNT(**2**)-K1 can activate transcription of proinflammatory cytokine genes as early as one hour, but this effect is not paralleled by protein secretion into the supernatant. Both short and long nanotubes exhibit an effect of time on cytokine secretion. However, neither dose nor nanotube length has a profound effect on inflammatory cytokine release. Moreover, 1 and 5 μg/ml doses of RNT(**2**)-K1 have no effect on cell viability by 24h. While the macrophage inflammatory activation has been studied in this work, future studies must be conducted to examine the intracellular uptake of the RNT.

CHAPTER 6

Discussion and Synthesis

6.1 General commentary and conclusions

Nanotechnology is continuing to develop rapidly as an economic and scientific force secondary to both market pull and technology push. Regardless of whether the drivers of nanotechnology are scientific or economic, addressing the environmental health and safety aspects of this technology are crucial to its societal acceptance and economic prosperity. Indeed, the scaling up of nanomaterial production to commercial levels might be limited only by a lack of information on human health and environmental handling of nanostructures. As with any new substance the science of toxicology is being applied to address possible risk associated with exposure to nanomaterials. However, assessment of human health risks of nanomaterials presents some unique barriers when studying both the exposure and hazard elements of the risk equation (Maynard *et al.*, 2006). For example, the nature of the rosette nanotube self-assembly process has made it difficult to label the structures for uptake and biodistribution studies, whereas more traditional materials can be rendered radioactive or tagged fluorescently with greater utility. Nevertheless, this dissertation represents some of the first work in the field of nanotoxicology. Moreover, it provides an early framework of terminology and research design considerations for future nanotoxicology research in Canada and internationally.

'Nanotoxicology', which has been defined as the 'science of engineered nanodevices and nanostructures that deals with their effects in living organisms' (Oberdorster *et al.*, 2005b), has been launched on a platform upon our understanding of ultrafine particle research. This has raised the issue of whether conventional toxicology

approaches are sufficient to establish the relative toxicity of engineered nanostructures with traditional particulate toxicants. The answer to this remains to be determined, but recent work has highlighted the difficulties in working with nanostructures which include characterization, batch variation, aggregation state and the most appropriate dose metric (Oberdorster *et al.*, 2005a; Oberdorster *et al.*, 2005b; Powers *et al.*, 2007; Wittmaack, 2007). The rosette nanotube starting compounds studied here are produced using standard operating procedures and the resulting nanotube chemical structures have been well characterized (Fenniri *et al.*, 2001; Fenniri *et al.*, 2002a; Fenniri *et al.*, 2002b; Moralez *et al.*, 2005).

At present, a tiered testing strategy (Oberdorster *et al.*, 2005a) is being encouraged due to the lack of toxicity data currently available, however the interpretation of the data must recognize the unique properties of nanostructures before making general conclusions. These considerations are in stark contrast to the well established toxicity data and mechanisms of response to contaminants such endotoxin used in Chapter 1 (Thorn, 2001; Rylander, 2002). Regardless of the toxicant, pulmonary toxicity studies have many well accepted end-points for measuring the degree of response. One hallmark end-point is analysis of the bronchoalveolar lavage fluid (Henderson, 2005). Influx of inflammatory cells into the airspace is a sensitive marker of inflammation with physiological significance. It should be emphasized however that when using the accepted screening method of intratracheal instillation (Driscoll *et al.*, 2000), the bolus nature of the dose can lead to an inflammatory response being observed early which later resolves. In support of this mechanism I have reported an inflammatory response at 24h post-instillation which is resolving by 7d. These data are in agreement with recent

pulmonary toxicity data on water soluble C_{60}, which showed a response as measured by bronchoalveaolar lavage cell counts that later dissipated (Sayes *et al.*, 2007a). Characterizing the acute response by 24h is of toxicological importance particularly if it is severe, however the long-term outcome is also integral to understanding the possible health effects of nanomaterials.

When studying the lungs as a target organ, distinct differences exist between the inflammatory response to nanomaterials and endotoxin. Therefore, in the present body of work I began by studying a well established model of acute lung inflammation and identified the upregulation of a novel cytokine known as EMAP-II. This is the first study to identify a role for EMAP-II in the lung inflammation literature and provides a new foundation to further our understanding of the cell recruitment cascade. Using techniques and approaches similar to Chapter 1, I conducted an *in vivo* pulmonary toxicity screening study of self-assembling rosette nanotubes, in which EMAP-II was not detected in the bronchoalveolar lavage fluid. Endotoxin induces a robust inflammatory response as part of an innate defense via receptors such as Toll-like receptor-4 (TLR-4) (Thorn, 2001; Rylander, 2002). In contrast, the general mechanisms by which engineered nanostructures induce inflammation are still being elucidated. Until now, no data existed on the pulmonary responses to water soluble self-assembling nanotubes. Deriving the precise mechanisms of nanostructure induced inflammation is complex given the range of compositions and our evolving understanding of the role of oxidative stress and aspect ratio in toxicity (Xia *et al.*, 2006; Oberdorster *et al.*, 2007; Unfried *et al.*, 2007). The traditional model for understanding ultrafine particle toxicity is grounded in an oxidative stress paradigm (Seaton *et al.*, 1995; Donaldson *et al.*, 2001; Donaldson & Stone, 2003;

Donaldson *et al.*, 2005). Therefore, depending upon the synthetic process employed and the subsequent chemical content of a nanostructure it is reasonable to test the hypothesis that oxidative stress is the primary mechanism of toxicity (Xia *et al.*, 2006). Based on this line of reasoning and the observed chemical composition, one would not expect the rosette nanotubes studied here to act via a similar mechanism. Although these experiments were not designed to test this specific hypothesis, the rosette nanotubes are biologically inspired, water soluble and metal free (Fenniri *et al.*, 2001; Fenniri *et al.*, 2002a) and therefore unlikely to generate reactive oxygen species in a manner similar to combustion derived carbon particles or metal oxides (Ghio *et al.*, 1999; Unfried *et al.*, 2007). Additionally, there is no evidence to suggest that rosette nanotubes would act through innate receptor responses such as Toll-like receptors, although other innate immune recognition responses can be modulated by nanoscale particles (Lucarelli *et al.*, 2004).

In an attempt to probe the potential of the rosette nanotubes to directly activate specific cells I applied *in vitro* methods to look at the human pulmonary epithelial and macrophage responses. These data establish important approaches for evaluating rosette nanotube toxicity and are the first comprehensive data on the proinflammatory potential of the rosette nanotubes in human cell lines. *In vitro* models to screen for possible *in vivo* toxicity are presently in demand as the development of new nanomaterials is out-pacing the capacity to test their toxicity or biocompatibility. The unique issues associated with nanostructure dosimetry (Wittmaack, 2007) have made it difficult to develop a suite of *in vitro* tests with comparative capacity to *in vivo* responses (Sayes *et al.*, 2007b). From a risk assessment standpoint, *in vitro* studies should be used in combination with an

evaluation of exposures scenarios, epidemiology and *in vivo* toxicity studies (Devlin *et al.*, 2005). Unfortunately, inadequate consideration of dosing and experimental design has led to artefacts and some poor interpretations of *in vitro* data in nanotoxicology research (Worle-Knirsch *et al.*, 2006). Nevertheless, *in vitro* work is extremely valuable in isolating responses of specific cell types, as has been conducted in this work, as well as for studying subcellular localization and mechanisms of uptake of other nanostructures (Stearns *et al.*, 2001; Chithrani *et al.*, 2006; Chithrani & Chan, 2007; Unfried *et al.*, 2007).

Due to the fact that my studies were not designed for the purpose of studying possible *in vitro* correlates of *in vivo* responses, the cellular results are discordant with the *in vivo* mouse study. This is likely due to the complex biology of the lung environment. For example, as discussed in Chapter 4, while pulmonary epithelium can be activated directly to contribute to the inflammatory response, it is also responsive to exogenous TNF-α which can amplify the inflammatory cascade in epithelium as well as other cell types (Driscoll *et al.*, 1997; Driscoll, 2000). Conversely, macrophages are a robust source of TNF-α (Rich *et al.*, 1989) and can also interact directly with epithelium and in concert with neutrophils influence inflammatory cell recruitment (Janardhan *et al.*, 2006). Thus, the disagreement between the acute responses at 24h in my mouse study and the lack of a robust response observed *in vitro* may be attributed to a number of factors. Firstly, the bolus nature of administering material via intratracheal instillation has been known to cause acute responses which may or may not be an artefact. Moreover, the incredibly complex interrelationship among cell populations in the lung and the redundant physiological nature of the inflammatory response can make it difficult to find

accordance between *in vivo* and *in vitro* toxicity data. To this end, water soluble C_{60} has been shown to cause no difference in lung toxicity relative to control animals which is in contrast to *in vitro* data (Sayes *et al.*, 2007a). One noteworthy difference between C_{60} and the rosette nanotubes studied here is that of aspect ratio. High-aspect ratio nanoparticles such as nanotubes may be more of an irritant for lungs than spherical C_{60}. While speculative, there is long history of differences between the inflammation and toxicokinetics of fibres in the lung relative to those without a large aspect ratio (Donaldson & Tran, 2002; Oberdorster, 2002).

6.2 Future directions

Nanotoxicology is presently in its infancy and thus the potential directions it can take are wide open. This is particularly true in Canada as this work is the first of its kind domestically. With respect to the rosette nanotubes a few logical areas have been identified for future directions. The determination of possible inflammation caused by nanomaterials is an important element of establishing their toxicity. However, the mere size of nanoscale particulate has created a demand to better understand the factors influencing the cellular uptake and *in vivo* toxicokinetics of nanoparticles. In this body of work, the complex nature of the rosette nanotube self-assembly process has made it difficult to develop a means by which they can be imaged, tracked, and quantified *in vitro* or *in vivo*. To date, only a few papers exists on the biodistribution of carbon nanotubes *in vivo* (Wang *et al.*, 2004; Singh *et al.*, 2006b; Guo *et al.*, 2007). Moreover, the nanotubes studied in these papers had to undergo considerable surface functionalization to be rendered soluble. Therefore, in order for self-assembling rosette nanotubes to be a viable

biomedical alternative to single-walled carbon nanotubes, biodistribution and uptake studies must be performed.

Aggregration of nanomaterials is a common problem in nanotoxicity research (Oberdorster *et al.*, 2005a; Oberdorster *et al.*, 2005b), and can indeed alter the toxicity of a given nanotube (Wick *et al.*, 2007). The rosette nanotubes studied in this work aggregate in a pH-dependent fashion as the protonation state of the surface lysine group changes (Moralez *et al.*, 2005). The aggregation state has tremendous implications for the interpretation of biodistribution data but even more so for *in vivo* and *in vitro* toxicity assessment. Solving the issue of aggregation of the nanotubes will be a key to moving forward with work on biomedical applications, because at present little is known about aggregation state in the physiologic milieu.

Finally, while the *in vivo* responses observed in the my mouse study appeared promising, longer term end-points such as 28 and 90 days should be studied to extend these results. Additionally, once a labeled rosette nanotube compound is developed, pulmonary clearance studies can be performed and a more detailed understanding of uptake into the lung cellular architecture and possible translocation can be assessed.

In toto, these novel nanotoxicology studies present an opportunity to establish experimental benchmarks in a rapidly growing area of research and to address some truly fundamental questions on the handling of nanostructures by living organisms.

CHAPTER 7

References

ABRAHAM, E., ARCAROLI, J., CARMODY, A., WANG, H. & TRACEY, K. J. (2000a). Cutting edge: HMG as a Mediator of Acute Lung Inflammation. *Journal of Immunology* **165,** 2950-2954.

ABRAHAM, E., CARMODY, A., SHENKAR, R. & ARCAROLI, J. (2000b). Neutrophils as early immunologic effectors in hemorrhage- or endotoxemia-induced acute lung injury. *American Journal of Physiology Lung Cellular and Molecular Physiology* **279,** L1137-L1145.

AITKEN, R. J., CHAUDHRY, M. Q., BOXALL, A. B. & HULL, M. (2006). Manufacture and use of nanomaterials: current status in the UK and global trends. *Occupational Medicine* **56,** 300-306.

AJAYAN, P. M. (1999). Nanotubes from Carbon. *Chemical Reviews* **99,** 1787-1800.

AUGER, F., GENDRON, M. C., CHAMOT, C., MARANO, F. & DAZY, A. C. (2006). Responses of well-differentiated nasal epithelial cells exposed to particles: role of the epithelium in airway inflammation. *Toxicology and Applied Pharmacology* **215,** 285-294.

AWASTHI, K., SRIVASTAVA, A. & SRIVASTAVA, O. N. (2005). Synthesis of carbon nanotubes. *Journal of Nanoscience and Nanotechnology* **5,** 1616-1636.

BARLOW, P. G., CLOUTER-BAKER, A., DONALDSON, K., MACCALLUM, J. & STONE, V. (2005). Carbon black nanoparticles induce type II epithelial cells to release chemotaxins for alveolar macrophages. *Particle and Fibre Toxicology* **2**.

BARNETT, G., JAKOBSEN, A. M., TAS, M., RICE, K., CARMICHAEL, J. & MURRAY, J. C. (2000). Prostate adenocarcinoma cells release the novel proinflammatory polypeptide EMAP-II in response to stress. *Cancer Research* **60,** 2850-2857.

BECK-SCHIMMER, B., SCHIMMER, R. C. & PASCH, T. (2004). The Airway compartment: Chambers of secrets. *News in Physiological Sciences* **19,** 129-132.

BERGAMASCHI, E., BUSSOLATI, O., MAGRINI, A., BOTTINI, M., MIGLIORE, L., BELLUCCI, S., IAVICOLI, I. & BERGAMASCHI, A. (2006). Nanomaterials and lung toxicity: Interactions with airway cells and relevance for occupational health risk assessment. *International Journal of Immunopathology and Pharmacology* **19,** 3-10.

BIANCO, A. (2004). Carbon nanotubes for the delivery of therapeutic molecules. *Expert Opinion in Drug Delivery* **1,** 57-65.

BIANCO, A. & PRATO, M. (2003). Can carbon nanotubes be considered useful tools for biological applications? *Advanced Materials* **15,** 1765-1768.

BORM, P. J. A. (2002). Particle toxicology: From coal mining to nanotechnology. *Inhalation Toxicology* **14,** 311-324.

BORM, P. J. A. & TRAN, C. L. (2002). From quartz hazard to quartz: the coal mines revisited. *Annals of Occupational Hygiene* **46,** 25-32.

BOWDEN, D. (1984). The Alveolar macrophage. *Environmental Health Perspectives* **56,** 327-341.

CAKMAK, G. D., SCHINS, R. P., SHI, T., FENGOLIO, I., FUBINI, B. & BORM, P. J. A. (2004). In vitro genotoxicity assessment of commercial quartz flours in comparison to standard DQ12 quartz. *International Journal of Hygiene and Environmental Health* **207,** 105-113.

CHITHRANI, B. D. & CHAN, W. C. W. (2007). Elucidating the mechanism of cellular uptake and removal of protein-coated gold nanoparticles of different sizes and shapes. *Nano Letters* **7,** 1542-1550.

CHITHRANI, B. D., GHAZANI, A. A. & CHAN, W. C. W. (2006). Determining the size and shape dependence of gold nanoparticle uptake into mammalian cells. *Nano Letters* **6,** 662-668.

CHLOPEK, J., CZAJKOWSKA, B., SZARANIEC, B., FRACKOWIAK, E., SZOSTAK, K. & BEGUIN, F. (2006). In vitro studies of carbon nanotubes biocompatibility. *Carbon* **44,** 1106-1111.

CHRISTENSEN, C. M. (1997). *The Innovator's Dilemma: When technologies cause great firms to fail*. Harvard Business School Press.

CHUN, A. L., JOMHA, N. M., WEBSTER, T. J. & FENNIRI, H. (2005). Localized articular cartilage defects: A Review on current modes of treatment and how nanotechnology can play a role. *NanoBiotechnology* **1,** 43.

CHUN, S., MORALEZ, J., FENNIRI, H. & WEBSTER, T. (2004). Helical rosette nanotubes: a more effective orthopedic implant material. *Nanotechnology* **15,** S234-239.

COOKE, W. E. (1924). Fibrosis of the lungs due to inhalation of asbestos. *British Medical Journal* **2,** 147.

CUI, D., TIAN, F., OZKAN, C. S., WANG, M. & GAO, H. (2005). Effect of single wall carbon nanotubes on human HEK293 cells. *Toxicology Letters* **155,** 73-85.

DAILEY, L. A., JEKEL, N., FINK, L., GESSLER, T., SCHMEHL, T., WITTMAR, M., KISSEL, T. & SEEGER, W. (2006). Investigation of the proinflammatory potential of biodegradable nanoparticle drug delivery systems in the lung. *Toxicology and Applied Pharmacology* **215,** 100-108.

DANIEL, M. C. & ASTRUC, D. (2004). Gold nanoparticles: Assembly, supramolecular chemistry, quantum-size-related properties, and applications toward biology, catalysis and nanotechnology. *Chemical Reviews* **104,** 293-346.

DAVOREN, M., HERZOG, E., CASEY, A., COTTINEAU, B., CHAMBERS, G., BYRNE, H. J. & LYNG, F. M. (2007). *In vitro* toxicity evaluation of single walled carbon nanotubes on human A549 lung cells. *Toxicology in Vitro* **21,** 438-448.

DEVLIN, R. B., FRAMPTON, M. W. & GHIO, A. J. (2005). In vitro studies: What is their role in toxicology? *Experimental and Toxicologic Pathology* **57,** 183-188.

DING, L., STILWELL, J., ZHANG, T., ELBOUDWARE, O., JIANG, H., SELEGUE, J. P., COOKE, P. A., GRAY, J. W. & CHEN, F. F. (2005). Molecular characterization of the cytotoxic mechanism of multiwall carbon nanotubes and nano-onions on human skin fibroblasts. *Nano Letters* **5,** 2448-2464.

DONALDSON, K., AITKEN, R., TRAN, L., STONE, V., DUFFIN, R., FORREST, G. & ALEXANDER, A. (2006). Carbon nanotubes: A review of their properties in relation to pulmonary toxicology and workplace safety. *Toxicological Sciences* **92,** 5-22.

DONALDSON, K. & STONE, V. (2003). Current hypotheses on the mechanisms of toxicity of ultrafine particles. *Ann Ist Super Santia* **39,** 405-410.

DONALDSON, K., STONE, V., CLOUTER, A., RENWICK, L. & MACNEE, W. (2001). Ultrafine particles. *Occupupational and Environmental Medicine* **58,** 211-216.

DONALDSON, K., STONE, V., TRAN, C., KREYLING, W. & BORM, P. (2004). Nanotoxicology. *Occupational and Environmental Medicine* **61,** 727-728.

DONALDSON, K. & TRAN, C. L. (2002). Inflammation caused by particles and fibers. *Inhalation Toxicology* **14,** 5-27.

DONALDSON, K., TRAN, L., JIMENEZ, L. A., DUFFIN, R., NEWBY, D. E., MILLS, N., MACNEE, W. & STONE, V. (2005). Combustion-derived nanoparticles: A review of their toxicology following inhalation exposure. *Particle and Fibre Toxicology* **2,** 1-14.

DORGER, M. & KROMBACH, F. (2000). Interaction of alveolar macrophages with inhaled mineral particulates. *Journal of Aerosol Medicine* **13,** 369-380.

DORGER, M. & KROMBACH, F. (2002). Response of aleveolar macrophages to inhaled particulates. *European Surgical Research* **34,** 47-52.

DRESSELHAUS, M. S., DRESSELHAUS, G. & EKLUND, P. C. (1996). *Science of Fullerenes and Carbon Nanotubes*. Academic Press, New York.

DRISCOLL, K., COSTA, D., HATCH, G., HENDERSON, R., OBERDORSTER, G., SALEM, H. & SCHLESINGER, R. (2000). Intratracheal instillation as an exposure technique for the evaluation of respiratory tract toxicity: Uses and limitations. *Toxicological Sciences* **55,** 24-35.

DRISCOLL, K. E. (2000). TNFalpha and MIP-2: role in particle-induced inflammation and regulation by oxidative stress. *Toxicology Letters* **112-113,** 177-183.

DRISCOLL, K. E., CARTER, J. M., HASSENBEIN, D. G. & HOWARD, B. (1997). Cytokines and particle-induced inflammatory cell recruitment. *Environmental Health Perspectives* **105,** 1159-1164.

DRISCOLL, K. E., HASSENBEIN, D. G., CARTER, J., POYNTER, J., ASQUITH, T. N., GRANT, R. A., WHITTEN, J., PURDON, M. P. & TAKIGIKU, R. (1993). Macrophage inflammatory proteins 1 and 2: expression by rat alveolar macrophages, fibroblasts, epithelial cells in rat lung after mineral dust exposure. *American Journal of Respiratory Cell and Molecular Biology* **8,** 311-328.

DUFFIELD, J. S. (2003). The inflammatory macrophage: a story of Jekyll and Hyde. *Clinical Science* **104,** 27-38.

DUMORTIER, H., LACOTTE, S., PASTORIN, G., MAREGA, R., WU, W., BONIFAZI, D., BRIAND, J. P., PRATO, M., MULLER, S. & BIANCO, A. (2006). Functionalized carbon nanotubes are non-cytotoxic and preserve the functionality of primary immune cells. *Nano Letters* **6,** 1522-1528.

FENNIRI, H., DENG, B. L. & RIBBE, A. E. (2002a). Helical rosette nanotubes with tunable chiroptical properties. *Journal of the American Chemical Society* **124,** 11064-11072.

FENNIRI, H., DENG, B. L., RIBBE, A. E., HALLENGA, K., JACOB, J. & THIYAGARAJAN, P. (2002b). Entropically driven self-assembly of multichannel rosette nanotubes. *Proceedings of the National Academy of Sciences USA* **99,** 6487-6492.

FENNIRI, H., MATHIVANAN, P., VIDALE, K. L., SHERMAN, D. M., HALLENGA, K., WOOD, K. V. & STOWELL, J. G. (2001). Helical rosette nanotubes: design, self-assembly, and characterization. *Journal of the American Chemical Society* **123,** 3854-3855.

FIORITO, S., SERAFINO, A., ANDREOLA, F., TOGNA, A. & TOGNA, G. (2006). Toxicity and biocompatibility of carbon nanoparticles. *Journal of Nanoscience and Nanotechnology* **6,** 591-599.

FLOREA, B. I., CASSARA, M. L., JUNGINGER, H. E. & BORCHARD, G. (2003). Drug transport and metabolism characteristics of the human airway epithelial cell line Calu-3. *Journal of Controlled Release* **87,** 131-138.

FORBES, B. & EHRHARDT, C. (2005). Human respiratory epithelial cell culture for drug delivery applications. *European Journal of Pharmaceutics and Biopharmaceutics* **60,** 193-2005.

FUJII, T., HAYASHI, S., HOGG, J. C., VINCENT, R. & VAN EEDEN, S. F. (2001). Particulate matter induces cytokine expression in human bronchial epithelial cells. *American Journal of Respiratory Cell and Molecular Biology* **25,** 265-271.

FUJITA, M., KUWANO, K., KUNITAKE, R., HAGIMOTO, N., MIYAZAKI, H., KANEKO, Y., KAWASAKI, M., MAEYAMA, T. & HARA, N. (1998). Endothelial cell apoptosis in lipopolysaccharide-induced lung injury in mice. *International Archives of Allergy and Immunology* **117,** 202-208.

GEORGAKILAS, V., TAGMATARCHIS, N., PANTAROTTO, D., BIANCO, A., BRIAND, J. P. & PRATO, M. (2002). Amino acid functionalisation of water soluble carbon nanotubes. *Chemical Communications***,** 3050-3051.

GHIO, A. J. & BENNETT, W. D. (2007). Metal particles are inappropriate for testing a postulate of extrapulmonary transport. *Environmental Health Perspectives* **115,** A70.

GHIO, A. J., STONEHUERNER, J., DAILEY, L. A. & CARTER, J. D. (1999). Metals associated with both the water-soluble and insoluble fractions of an ambient air pollution particle catalyze an oxidative stress. *Inhalation Toxicology* **11,** 37-49.

GOJOVA, A., GUO, B., KOTA, R. S., RUTLEDGE, J. C., KENNEDY, I. M. & BARAKAT, A. I. (2007). Induction of inflammation in vascular endothelial cells by metal oxide nanoparticles: Effect of particle composition. *Environmental Health Perspectives* **115,** 403-409.

GOODMAN, R. B., PUGIN, J., LEE, J. S. & MATTHAY, M. A. (2003). Cytokine-mediated inflammation in acute lung injury. *Cytokine & Growth Factor Reviews* **14,** 523-535.

GOTO, Y., ISHII, H., HOGG, J. C., SHIH, C. H., YATERA, K., VINCENT, R. & VAN EEDEN, S. F. (2004). Particulate matter air pollution stimulates monocyte release from the bone marrow. *American Journal of Respiratory and Critical Care Medicine* **170,** 891-897.

GRONEBERG, D. A., WITT, C., WAGNER, U., CHUNG, K. F. & FISCHER, A. (2003). Fundamentals of pulmonary drug delivery. *Respiratory Medicine* **97,** 382-387.

GUO, J., ZHANG, X., LI, Q. & LI, W. (2007). Biodistribution of functionalized multiwall carbon nanotubes in mice. *Nuclear Medicine and Biology* **34,** 579-583.

GURR, J. R., WANG, A. S. S., CHEN, C. H. & JAN, K. Y. (2005). Ultrafine titanium dioxide particles in the absence of photoactivation can induce oxidative damage to human bronchial epithelial cells. *Toxicology* **213,** 66-73.

HENDERSON, R. F. (2005). Use of bronchoalveolar lavage to detect respiratory tract toxicity of inhaled material. *Experimental and Toxicologic Pathology* **57 Suppl 1,** 155-159.

HOOD, E. (2004). Nanotechnology: Looking as we leap. *Environmental Health Perspectives* **112,** A741-749.

HUDSON, J. L., CASAVANT, M. J. & TOUR, J. M. (2004). Water-soluble exfoliated nonroping single-wall carbon nanotubes. *Journal of the American Chemical Society* **126,** 11158-11159.

HUNG, O. (2006). Drug transformation: Advances in drug delivery systems. *Canadian Journal of Anesthesia* **53,** 1074-1077.

INTERNATIONAL COMMISSION ON RADIOLOGICAL PROTECTION. (1994). *International commission on radiological protection. Human respiratory tract model for radiological protection.* Elsevier Science Ltd, Tarrytown,NY.

ISHII, H., HAYASHI, S., HOGG, J. C., FUJII, T., GOTO, Y., SAKAMOTO, N., MUKAE, H., VINCENT, R. & VAN EEDEN, S. F. (2005). Alveolar macrophage-epithelial cell interaction following exposure to atmospheric particles induces the release of mediators involved in monocyte mobilization and recruitment. *Respiratory Research* **6,** 87.

IVAKHNO, S. S. & KORNELYUK, A. I. (2004). Cytokine-like activities of some aminoacyl-tRNA synthetases and auxiliary p43 cofactor of aminoacylation reaction and their role in oncogenesis. *Experimental Oncology* **26,** 250-255.

JANARDHAN, K., APPLEYARD, G. & SINGH, B. (2004). Expression of integrin subunits $\alpha_v\beta_3$ in acute lung inflammation. *Histochemistry and Cell Biology* **121,** 383-390.

JANARDHAN, K. S., SANDHU, S. K. & SINGH, B. (2006). Neutrophil depletion inhibits early and late monocyte/macrophage increase in lung inflammation. *Frontiers in Bioscience* **11,** 1569-1576.

JIA, G., WANG, H., YAN, L., WANG, X., PEI, R., YAN, T., ZHAO, Y. & GUO, X. (2005). Cytotoxicity of carbon nanomaterials: Single-wall nanotube, multi-wall nanotube and fullerene. *Environmental Science and Technology* **39,** 1378-1383.

JOHNSON, R. S., YAMAZAKI, T., KOVALENKO, A. & FENNIRI, H. (2007). Molecular basis for water-promoted supramolecular chirality inversion in helical rosette nanotubes. *Journal of the American Chemical Society* **129,** 5735-5743.

JOURNEAY, W. S., JANARDHAN, K. S. & SINGH, B. (2007a). Expression and function of endothelial monocyte activating polypeptide-II in acute lung inflammation. *Inflammation Research* **56,** 175-181.

JOURNEAY, W. S., SURI, S. S., MORALEZ, J. G., FENNIRI, H. & SINGH, B. (2007b). Novel self-assembling nanotubes show low acute pulmonary toxicity *in vivo*. *ACS Nano***,** Submitted August 2007.

KAGAN, V. E., BAYIR, H. & SHVEDOVA, A. A. (2005). Nanomedicine and nanotoxicology: two sides of the same coin. *Nanomedicine* **1,** 313-316.

KAGAN, V. E., TYURINA, Y. Y., TYURIN, V. A., KONDURU, N. V., POTAPOVICH, A. I., OSIPOV, A. N., KISIN, E. R., SCHWEGLER-BERRY, D., MERCER, R., CASTRANOVA, V. & SHVEDOVA, A. A. (2006). Direct and indirect effects of single walled carbon nanotubes on RAW 264.7 macrophages: role of iron. *Toxicology Letters* **165,** 88-100.

KAO, J., HOUCK, K., FAN, Y., HAEHNEL, I., LIBUTTI, S. K., KAYTON, M. L., GRIKSCHEIT, T., CHABOT, J., NOWYGROD, R., GREENBERG, S., KUANG, W. J., LEUNG, D. W., HAYWARD, J. R., KISIEL, W., HEATH, M., BRETT, J. & STERN, D. M. (1994). Characterization of a novel tumour-derived cytokine. *Journal of Biological Chemistry* **269,** 25106-25119.

KAO, J., RYAN, J., BRETT, J., CHEN, J., SHEN, H., FAN, Y., GODMAN, G., FAMILLETTI, P. C., WANG, F., PAN, Y. C. E., STERN, D. & CLAUSS, M. (1992). Endothelial monocyte-activating polypeptide II - A novel tumour-derived polypeptide that activates host-response mechanisms. *Journal of Biological Chemistry* **267,** 20239-20247.

KARLUSS, T. & SAYRE, P. (2005). Research strategies for safety evaluation of nanomaterials, Part I: Evaluating the human health implications of exposure to nanoscale materials. *Toxicological Sciences* **87,** 316-321.

KNIES, U. E., BEHRENSDORF, H. A., MITCHELL, C. A., DEUTSCH, U., RISAU, W., DREXLER, H. C. & CLAUSS, M. (1998). Regulation of endothelial monocyte-activating polypeptide II release by apoptosis. *Proceedings of the National Academy of Sciences USA* **95,** 12322-12327.

KO, Y. G., PARK, H., KIM, T., LEE, J. W., PARK, S. G., SEOL, W., KIM, J. E., LEE, W. H., KIM, S. H., PARK, J. E. & KIM, S. (2001). A cofactor of tRNA synthetase, p43, is secreted to up-regulate proinflammatory genes. *Journal of Biological Chemistry* **276,** 23028-23033.

KOBAYASHI, Y. (2006). Neutrophil infiltration and chemokines. *Critical Reviews in Immunology* **26,** 307-316.

KOBZIK, L. (1995). Lung macrophage uptake of unopsonized environmental particulates. *Journal of Immunology* **155,** 367-376.

KREYLING, W., SEMMIER, M., ERBE, F., MAYER, P., TAKENAKA, S. & SCHULZ, H. (2002). Translocation of ultrafine insoluble iridium particles from lung epithelium to extrapulmonary organs is size dependent but very low. *Journal of Toxicology and Environmental Health Part A* **65,** 1513-1530.

KREYLING, W. G., SEMMLER-BEHKNKE, M. & MOLLER, W. (2006). Ultrafine particle-lung interactions: Does size matter? *Journal of Aerosol Medicine* **19,** 74-83.

LAM, C., JAMES, J., MCCLUSKEY, R. & HUNTER, R. (2004). Pulmonary toxicity of single-wall carbon nanotubes in mice 7 and 90 days after intratracheal instillation. *Toxicological Sciences* **77,** 126-134.

LAM, C. W., JAMES, J. T., MCCLUSKEY, R., AREPALLI, S. & HUNTER, R. L. (2006). A Review of carbon nanotube toxicity and assessment of potential occupational and environmental health risks. *Critical Reviews in Toxicology* **36,** 186-217.

LANONE, S. & BOCZKOWSKI, J. (2006). Biomedical applications and potential health risks of nanomaterials: Molecular mechanisms. *Current Molecular Medicine* **6,** 651-663.

LASKIN, D. L. & PENDINO, K. J. (1995). Macrophages and inflammatory meditators in tissue injury. *Annual Reviews in Pharmacology Toxicology* **35,** 655-677.

LEHNERT, B. E. (1992). Pulmonary and thoracic macrophage subpopulations and clearance of particles from the lung. *Environmental Health Perspectives* **97,** 17-46.

LEHNERT, B. E., VALDEZ, Y. E. & HOLLAND, L. M. (1985). Pulmonary macrophages: Alveolar and interstitial populations. *Experimental Lung Research* **9,** 177-190.

LIN, Y., TAYLOR, S., LI, H., FERNANDO, K. A. S., QU, L., WANG, W., GU, L., ZHOU, B. & SUN, Y. P. (2004). Advances toward bioapplications of carbon nanotubes. *Journal of Materials Chemistry* **14,** 527-541.

LUCARELLI, M., GATTI, A., SAVARINO, G., QUATTRONI, P., MARTINELLI, L., MONARI, E. & BORASCHI, D. (2004). Innate defence functions of macrophages can be biased by nano-sized ceramic and metallic particles. *European Cytokine Network* **15,** 339-346.

LUKKARINEN, H., LAINE, J., LEHTONEN, J., ZAGARIYA, A., VIDYASAGAR, D., AHO, H. & KAAPA, P. (2004). Angiotensin II receptor blockade inhibits pneumocyte apoptosis in experimental meconium aspiration. *Pediatric Research* **55,** 326-333.

MADJDPOUR, C., OERTIL, B., ZIEGLER, U., BONVINI, J. M., PASCH, T. & BECK-SCHIMMER, B. (2000). Lipopolysaccharide induced functional ICAM-1 expression in rat alveolar epithelial cells in vitro. *American Journal of Physiology Lung Cellular and Molecular Physiology* **278,** L572-579.

MAGREZ, A., KASAS, S., SALICIO, V., PASQUIER, N., SEO, J. W., CELIO, M., CATSICAS, S., SCHWALLER, B. & FORRO, L. (2006). Cellular toxicity of carbon-based nanomaterials. *Nano Letters* **6,** 1121-1125.

MANGUM, J. B., TURPIN, E. A., ANTAO-MENEZES, A., CESTA, M. F., BERMUDEZ, E. & BONNER, J. C. (2006). Single-walled carbon nanotube (SWCNT)- induced interstitial fibrosis in the lungs of rats is associated with increased levels of PDGF mRNA and the formation of unique intercellular carbon structures that bridge alveolar macrophages *in situ*. *Particle and Fibre Toxicology* **3,** 15.

MARTIN, C. R. & KOHLI, P. (2003). The emerging field of nanotube biotechnology. *Nature Reviews. Drug Discovery* **2,** 29-37.

MATSCHURAT, S., KNIES, U. E., PERSON, V., FINK, L., STOELCKER, B., EBENEBE, C., BEHRENSDORF, H. A., SCHAPER, J. & CLAUSS, M. (2003). Regulation of EMAP II by hypoxia. *American Journal of Pathology* **162,** 93-103.

MAUS, U., HUWE, J., EMERT, L., EMERT, M., SEEGER, W. & LOHMEYER, J. (2002). Molecular pathways of monocyte emigration into the alveolar air space of intact mice. *American Journal of Respiratory and Critical Care Medicine* **165,** 95-100.

MAUS, U., HUWE, J., MAUS, U., SEEGER, W. & LOHMEYER, J. (2001). Alveolar JE/MCP-1 and endotoxin synergize to provoke lung cytokine upregulation, sequential neutrophil and monocyte influx, and vascular leakage in mice. *American Journal of Respiratory and Critical Care Medicine* **164,** 406-411.

MAYNARD, A. D. & AITKEN, R. J. (2007). Assessing exposure to airborne nanomaterials: Current abilities and future requirements. *Nanotoxicology* **1,** 26-41.

MAYNARD, A. D., AITKEN, R. J., BUTZ, T., COLVIN, V., DONALDSON, K., OBERDORSTER, G., PHILBERT, M. A., RYAN, J., SEATON, A., STONE, V., TINKLE, S. S., TRAN, L., WALKER, N. J. & WARHEIT, D. B. (2006). Safe handling of nanotechnology. *Nature* **444,** 267-269.

MAYNARD, A. D., BARON, P. A., FOLEY, M., SHVEDOVA, A. A., KISIN, E. R. & CASTRANOVA, V. (2004). Exposure to carbon nanotube material: aerosol release during the handling of unrefined single-walled carbon nanotube material. *Journal of Toxicology and Environmental Health Part A.* **67,** 87-107.

MAZZARELLA, G., FERRARACCIO, F., PRATI, M. V., ANNUNZIATA, S., BIANCO, A., MEZZOGIORNO, A., LIGUORI, G., ANGELILLO, I. F. & CAZZOLA, M. (2007). Effects of diesel exhaust particles on human lung epithelial cells: An in vitro study. *Respiratory Medicine* **101,** 1155-1162.

MCATEER, J. A. & DAVIS, J. M. (2002). Basic cell culture technique and the maintenance of cells lines. In *Basic Cell Culture: A Practical approach*. ed. DAVIS, J. M. Oxford University Press, New York.

MEDINA, C., SANTOS-MARTINEZ, M. J., RADOMSKI, A., CORRIGAN, O. I. & RADOMSKI, M. W. (2007). Nanoparticles: pharmacological and toxicological significance. *British Journal of Pharmacology* **150,** 552-558.

MEYER, M., PERSSON, O. & POWER, Y. (2001). Mapping excellence in nanotechnologies: preparatory study. European Commission.

MOGHIMI, S. M. & KISSEL, T. (2006). Particulate nanomedicines. *Advanced Drug Delivery Reviews* **58,** 1451-1455.

MOLLER, W., HOFER, T., ZIESENIS, A., KARG, E. & HEYDER, J. (2002). Ultrafine particles cause cytoskeletal dysfunction in macrophages. *Toxicology and Applied Pharmacology* **182,** 197-207.

MORALEZ, J. G., RAEZ, J., YAMAZAKI, T., MOTKURI, R. K., KOVALENKO, A. & FENNIRI, H. (2005). Helical rosette nanotubes with tunable stability and hierarchy. *Journal of American Chemical Society* **127,** 8307-8309.

MOSS, O. R. & WONG, V. A. (2006). When nanoparticles get in the way: Impact of projected area on in vivo and in vitro macrophage function. *Inhalation Toxicology* **18,** 711-716.

MURRAY, J. C., BARNETT, G., TAS, M., JAKOBSEN, A., BROWN, D., POWE, D. & CLELLAND, C. (2000). Immunohistochemical analysis of endothelial-monocyte-activating polypeptide-II expression in vivo. *American Journal of Pathology* **157,** 2045-2053.

MURRAY, J. C., HENG, Y. M., SYMONDS, P., RICE, K., WARD, W., HUGGINS, M., TODD, I. & ROBINS, R. A. (2004). Endothelial monocyte-activating polypeptide- II (EMAP II): a novel inducer of lymphocyte apoptosis. *Journal of Leukocyte Biology* **75,** 772-776.

NANOTOXICOLOGY. (2004). Developing experimental approaches for the evaluation of toxicological interactions of nanoscale materials, pp. 1-37. University of Florida, Gainesville,FL.

NEFF, S. B., ROTH-Z'GRAGGEN, B., NEFF, T. A., JAMNICKI-ABEGG, M., SUTER, D., SCHIMMER, R. C., BOOY, C., JOCH, H., PASCH, T., WARD, P. A. & BECH-SCHIMMER, B. (2006). Inflammatory response of tracheobronchial epithelial cells to endotoxin. *American Journal of Physiology Lung Cellular and Molecular Physiology* **290,** L86-L96.

NEL, A., XIA, T., MADLER, L. & LI, N. (2006). Toxic potential of materials at the nanolevel. *Science* **311,** 622-627.

NEMMAR, A., HOET, P., VANQUICKENBORNE, B., DINSDALE, D., THOMEER, M., HOYLAERTS, M., VANBILLOEN, H., MORTELMANS, L. & NEMERY, B. (2002). Passage of inhaled particles into the blood circulation in humans. *Circulation* **105,** 411-414.

NEMMAR, A., VANBILLOEN, H., HOYLAERTS, M., HOET, P., VERBRUGGEN, A. & NEMERY, B. (2001). Passage of intratracheally instilled ultrafine particles from the lung into the systemic circulation in hamster. *American Journal of Respiratory and Critical Care Medicine* **164,** 1665-1668.

NICOD, L. P. (2005). Lung defences: an overview. *European Respiratory Review* **14,** 45-50.

NIMMAGADDA, A., THURSTON, K., NOLLERT, M. U. & MCFETRIDGE, P. S. (2006). Chemical modification of SWNT alters *in vitro* cell-SWNT interactions. *Journal of Biomedical Materials Research A.* **76A,** 614-625.

NING, Y., TAO, F., QIN, G., IMRICH, A., GOLDSMITH, C., YANG, Z. & KOBZIK, L. (2004). Particle epithelial interaction. Effect of priming and bystander neutrophils on interleukin-8 release. *American Journal of Respiratory Cell and Molecular Biology* **30,** 744-750.

OBERDORSTER, G. (2000). Toxicology of ultrafine particles: in vivo studies. *Philosophical Transactions of the Royal Society of London A* **358,** 2719-2740.

OBERDORSTER, G. (2002). Toxicokinetics and effects of fibrous and nonfibrous particles. *Inhalation Toxicology* **14,** 29-56.

OBERDORSTER, G. & ELDER, A. (2007). Metal particles and extrapulmonary transport: oberdorster and elder respond. *Environmental Health Perspectives* **115,** A70-71.

OBERDORSTER, G., FERIN, J. & LEHNERT, B. (1994). Correlation between particle size *In Vivo* particle persistence and lung injury. *Environmental Health Perspectives* **102(Suppl 5),** 173-179.

OBERDORSTER, G., GELEIN, R., FERIN, J. & WEISS, B. (1995). Association of particulate air pollution and acute mortality: involvement of ultrafine particles. *Inhalation Toxicology* **7,** 111-124.

OBERDORSTER, G., MAYNARD, A., DONALDSON, K., CASTRANOVA, V., FITZPATRICK, J., AUSMAN, K. D., CARTER, J., KARN, B., KREYLING, W., LAI, D., OLIN, S., MONTEIRO-RIVIERE, N., WARHEIT, D. & YANG, H. (2005a). Principles for characterizing the potential human health effects from exposure to nanomaterials: elements of a screening strategy. *Particle and Fibre Toxicology* **2,** 1-35.

OBERDORSTER, G., OBERDORSTER, E. & OBERDORSTER, J. (2005b). Nanotoxicology: An Emerging discipline evolving from studies of ultrafine particles. *Environmental Health Perspectives* **113,** 823-839.

OBERDORSTER, G., SHARP, Z., ATUDOREI, V., ELDER, A., GELEIN, R., LUNTS, A., KREYLING, W. & COX, C. (2002). Extrapulmonary translocation of ultrafine carbon particles following whole body inhalation exposure of rats. *Journal of Toxicology and Environmental Health Part A* **65,** 1531-1543.

OBERDORSTER, G., STONE, V. & DONALDSON, K. (2007). Toxicology of nanoparticles: A historical perspective. *Nanotoxicology* **1,** 2-25.

OLIVIERI, D. & SCODITTI, E. (2005). Impact of environmental factors on lung defences. *European Respiratory Review* **14,** 51-56.

PANTAROTTO, D., PARTIDOS, C. D., GRAFF, R., HOEBEKE, J., BRIAND, J. P., PRATO, M. & BIANCO, A. (2003). Synthesis, structural characterization and immunological properties of carbon nanotubes functionalized with peptides. *Journal of the American Chemical Society* **125,** 6160-6164.

PARK, H., PARK, S. G., LEE, J. W., KIM, T., KIM, G., KO, Y. G. & KIM, S. (2002). Monocyte cell adhesion induced by a human aminoacyl-tRNA synthetase-associated factor, p43: identification of the related adhesion molecules and signal pathways. *Journal of Leukocyte Biology* **71,** 223-230.

PARK, S. G., SHIN, H., SHIN, Y. K., LEE, Y., CHOI, E. C., PARK, B. J. & KIM, S. (2005). The novel cytokine p43 stimulates dermal fibroblast proliferation and wound repair. *American Journal of Pathology* **166,** 387-398.

PIANTADOSI, C. A. & SCHWARTZ, D. A. (2004). The Acute respiratory distress syndrome. *Annals of Internal Medicine* **141,** 460-470.

PISON, U., WELTE, T., GIERSIG, M. & GRONEBERG, D. A. (2006). Nanomedicine for respiratory diseases. *European Journal of Pharmacology* **533,** 182-194.

POLIZU, S., SAVADOGO, O., POULIN, P. & YAHIA, L. (2006). Applications of carbon nanotubes-based biomaterials in biomedical nanotechnology. *Journal of Nanoscience and Nanotechnology* **6,** 1883-1904.

POWERS, K. W., PALAZUELOS, M., MOUDGIL, B. M. & ROBERTS, S. M. (2007). Characterization of the size, shape, and state of dispersion of nanoparticles for toxicological studies. *Nanotoxicology* **1,** 42-51.

PULSKAMP, K., DIABATE, S. & KRUG, H. F. (2007). Carbon nanotubes show no sign of acute toxicity but induce intracellular reactive oxygen species in dependence on contaminants. *Toxicology Letters* **168,** 58-74.

QUEVILLON, S., AGOU, F., ROBINSON, J. C. & MIRANDE, M. (1997). The p43 component of the mammalian multi-synthetase complex is likely to be the precursor of endothelial monocyte-activating polypeptide II cytokine. *Journal of Biological Chemistry* **272,** 32573-32579.

QUINTOS-ALAGHEBAND, M. L., WHITE, C. W. & SCHWARZ, M. A. (2004). Potential role for antiangiogenic proteins in the evolution of bronchopulmonary dysplasia. *Antioxidants and Redox Signaling* **6,** 137-145.

RAEZ, J., MORALEZ, J. G. & FENNIRI, H. (2004). Long-range flow-induced alignment of self-assembled rosette nanotubes on Si/SiOx and poly(methyl methacrylate)-coated Si/SiOx. *Journal of the American Chemical Society* **126,** 16298-16299.

RENWICK, L., BROWN, D., CLOUTER, A. & DONALDSON, K. (2004). Increased inflammation and altered macrophage chemotactic responses caused by two ultrafine particle types. *Occupational and Environmental Medicine* **61,** 442-447.

RENWICK, L., DONALDSON, K. & CLOUTER, A. (2001). Impairment of alveolar macrophage phagocytosis by ultrafine particles. *Toxicology and Applied Pharmacology* **172,** 119-127.

RICH, E. A., PANUSKA, J. R., WALLIS, R. S., WOLF, C. B., LEONARD, M. L. & ELLNER, J. J. (1989). Dyscoordinate expression of tumour necrosis factor-alpha by human blood monocytes and alveaolar macophages. *American Review of Respiratory Disease* **139,** 1010-1016.

ROCO, M. C. (2004). Science and technology integration for increased human potential and societal outcomes. *Annals of the New York Academy of Sciences* **1013,** 1-16.

ROYAL SOCIETY. (2004). Nanoscience and Nanotechnologies: Opportunities and Uncertainties, pp. 116. Royal Society and Royal Academy of Engineering, London,UK.

RYLANDER, R. (2002). Endotoxin in the environment--exposure and effects. *Journal of Endotoxin Research* **8,** 241-252.

SATO, Y., YOKOYAMA, A., SHIBATA, K., AKIMOTO, Y., OGINO, S., NODASAKA, Y., KOHGO, T., TAMURA, K., AKASAKA, T., UO, M., MOTOMIYA, K., JEYADEVAN, B., ISHIGURO, M., HATAKEYAMA, R., WATARIB, F. & TOHJIA, K. (2005). Influence of length on cytotoxicity of multi-walled carbon nanotubes against human acute monocytic leukemia cell line THP-1 in vitro and subcutaneous tissue of rats *in vivo*. *Molecular Biosystems* **1,** 176-182.

SAVILL, J. S., WYLLIE, A. H., HENSON, J. E., WALPORT, M. J., HENSON, P. M. & HASLETT, C. (1989). Macrophage phagocytosis of aging neutrophils in inflammation. Programmed cell death in the neutrophil leads to its recognition by macrophages. *Journal of Clinical Investigation* **83,** 865-867.

SAYES, C. M., FORTNER, J. D., GUO, W., LYON, D., BOYD, A. M., AUSMAN, K. D., TAO, Y. J., SITHARAMAN, B., WILSON, L. J., HUGHES, J. B., WEST, J. L. & COLVIN, V. L. (2004). The differential cytotoxicity of water-soluble fullerenes. *Nano Letters* **4,** 1881-1887.

SAYES, C. M., LIANG, F., HUDSON, J. L., MENDEZ, J., GUO, W., BEACH, J. M., MOORE, V. C., DOYLE, C. D., WEST, J. B., BILLUPS, W. E., AUSMAN, K. D. & COLVIN, V. L. (2005). Functionalization density dependence of single-walled carbon nanotubes cytotoxicity in vitro. *Toxicology Letters* **161,** 135-142.

SAYES, C. M., MARCHIONE, A. A., REED, K. L. & WARHEIT, D. B. (2007a). Comparative pulmonary toxicity assessments of C_{60} water suspensions in rats: Few differences in fullerene toxicity in vivo contrast to in vitro profiles. *Nano Letters* **E-pub July 14**.

SAYES, C. M., REED, K. L. & WARHEIT, D. B. (2007b). Assessing toxicity of fine and nanoparticles: comparing in vitro measurements to in vivo pulmonary toxicity profiles. *Toxicological Sciences* **97,** 163-180.

SCHLUESENER, H. J., SEID, K., ZHAO, Y. & MEYERMANN, R. (1997). Localization of endothelial-monocyte activating polypeptide-II (EMAP II), a novel proinflammatory cytokine, to lesions of experimental autoimmune encephalomyelitis, neuritis and uveitis: Expression by monocytes and activated microglial cells. *GLIA* **20,** 365-372.

SCHWARZ, M. A., LEE, M., ZHANG, F., ZHAO, J., JIM, Y., SMITH, S., BHUVA, J., STERN, D., WARBURTON, D. & STARNES, V. (1999). EMAP II: a modulator of neovascularization in the developing lung. *American Journal of Physiology Lung Cellular and Molecular Physiology* **276,** L365-L375.

SEATON, A., MACNEE, W., DONALDSON, K. & GODDEN, D. (1995). Particulate air pollution and acute health effects. *Lancet* **345,** 176-178.

SEMMLER-BEHKNKE, M., TAKENAKA, S., FERTSCH, S., WENK, A., SEITZ, J., MAYER, P., OBERDORSTER, G. & KREYLING, W. G. (2007). Evidence for institial uptake and subsequent reentrainment onto airways epithelium. *Environmental Health Perspectives* **115,** 728-733.

SHALAK, V., KAMINSKA, M., MITNACHT-KRAUS, R., VANDENABEELE, P. & CLAUSS, M. (2001). The EMAP-II cytokine is released from the mammalian multisynthetase complex after cleavage of its p43/proEMAP-II component. *Journal of Biological Chemistry* **276,** 23769-23776.

SHVEDOVA, A. A., KISIN, E. R., MERCER, R., MURRAY, A. R., JOHNSON, V. J., POTAPOVICH, A. I., TYURINA, Y. Y., GORELIK, O., SEVARAM, A., SCHWEGLER-BERRY, D., HUBBS, A. F., ANTONINI, J., EVANS, D. E., KU, B. K., RAMSEY, D., MAYNARD, A., KAGAN, V. E., CASTRANOVA, V. & BARON, P. (2005). Unusual inflammatory and fibrogenic pulmonary responses to single-walled carbon nanotubes in mice. *American Journal of Physiology Lung Cellular and Molecular Physiology* **289,** L698-L708.

SHVEDOVA, A. A., KISIN, E. R., MURRAY, A. R., GORELIK, O., AREPALLI, S., CASTRANOVA, V., YOUNG, S. H., GAO, F., TYURINA, Y. Y., OURY, T. D. & KAGAN, V. E. (2007). Vitamin E deficiency enhances pulmonary inflammatory response and oxidative stress induced by single-walled carbon nanotubes in C57BL/6 mice. *Toxicology and Applied Pharmacology* **221,** 339-348.

SIMON, R. H. & PAINE 3RD, R. (1995). Participation of pulmonary alveolar epithelial cells in lung inflammation. *Journal of Laboratory and Clinical Medicine* **126,** 108-118.

SINGH, P., GONZALEZ, M. J. & MANCHESTER, M. (2006a). Viruses and their uses in nanotechnology. *Drug Development Research* **67,** 1-19.

SINGH, R., PANTAROTTO, D., LACERDA, L., PASTORIN, G., KLUMPP, C., PRATO, M., BIANCO, A. & KOSTARELOS, K. (2006b). Tissue biodistribution and blood clearance rates of intravenously administered carbon nanotube radiotracers. *Proceedings of the National Academy of Sciences USA* **103,** 3357-3362.

SINGH, S., SHI, T., DUFFIN, R., ALBRECHT, C., VAN BERLO, D., HOHR, D., FUBINI, B., MARTRA, G., FENOGLIO, I., BORM, P. J. & SCHINS, R. P. (2007). Endocytosis, oxidative stress and IL-8 expression in human lung epithelial cells upon treatment with fine and ultrafine TiO(2): Role of the specific surface area and of surface methylation of the particles. *Toxicology and Applied Pharmacology* **E-pub May 18,** PMID: 17599375.

SMART, S. K., CASSADY, A. I., LU, G. Q. & MARTIN, D. J. (2006). The biocompatibility of carbon nanotubes. *Carbon* **44,** 1034-1047.

STANDIFORD, T. J., KUNKEL, S. L., BASHA, M. A., CHENSUE, S. W., LYNCH III, J. P., TOEWS, G. B., WESTWICK, J. & STRIETER, R. M. (1990). Interleukin-8 gene expression by a pulmonary epithelial cell line. *Journal of Clinical Investigation* **86,** 1945-1953.

STEARNS, R., PAULAUSKIS, J. & GODLESKI, J. (2001). Endocytosis of ultrafine particles by A549 cells. *American Journal of Cellular and Molecular Biology* **24,** 108-115.

SUNDSTROM, C. & NILSSON, K. (1976). Establishment and characterization of a human histiocytic lympphoma cell line (U937). *International Journal of Cancer* **17,** 565-577.

TAKIZAWA, H. (1998). Airway epithelial cells as regulators of airway inflammation. *International Journal of Molecular Medicine* **1,** 367-378.

TAKIZAWA, H., ABE, S., OHTOSHI, T., KAWASAKI, S., TAKAMI, K., DESAKI, M., SUGAWARA, I., HASHIMOTO, S., AZUMA, A., NAKAHARA, K. & KUDOH, S. (2000). Diesel exhaust particles up-regulate expression of intercellular adhesion molecule-1 (ICAM-1) in human bronchial epithelial cells. *Clinical and Experimental Immunology* **120,** 356-362.

TAS, M. P. R. & MURRAY, J. C. (1996). Endothelial-monocyte-activating polypeptide II. *International Journal of Biochemistry and Cell Biology* **28,** 837-841.

THOMPSON, J. L., RYAN, J. A., BARR, M. L., FRANC, B., STARNES, V. A. & SCHWARZ, M. A. (2004). Potential role for antiangiogenic proteins in the myocardial infarction repair process. *Journal of Surgical Research* **116,** 156-164.

THORN, J. (2001). The inflammatory response in humans after inhalation of bacterial endotoxin: a review. *Inflammation Research* **50,** 254-261.

TSAI, B. M., WANG, M., CLAUSS, M., SUN, P. & MELDRUM, D. R. (2004). Endothelial monocyte-activating polypeptide II causes NOS-dependent pulmonary artery vasodilation: A novel effect for a proinflammatory cytokine. *American Journal of Physiology Regulatory Integrative and Comparative Physiology* **287,** R767-771.

UNFRIED, K., ALBRECHT, C., KLOTZ, L., VON MIKECZ, A., GRETHER-BECK, S. & SCHINS, R. P. F. (2007). Cellular responses to nanoparticles: Target structures and mechanisms. *Nanotoxicology* **1,** 52-71.

VAN HORSSEN, R., EGGERMONT, A. M. & TEN HAGEN, T. L. (2006). Endothelial monocyte-activating polypeptide-II and its functions in (patho)physiological processes. *Cytokine and Growth Factor Reviews* **17,** 339-348.

VERNOOY, J. H., DENTENER, M. A., VAN SUYLEN, R. J., BUURMAN, W. A. & WOUTERS, E. F. (2001). Intratracheal instillation of lipopolysaccharide in mice induces apoptosis in bronchial epithelial cells: no role for tumor necrosis factor-alpha and infiltrating neutrophils. *American Journal of Respiratory Cell and Molecular Biology* **24,** 569-576.

VOGEL, C. F., SCIULLO, E. & MATSUMURA, F. (2004). Activation of inflammatory mediators and potential role of Ah-receptor ligands in foam cell formation. *Cardiovascular Toxicology* **4,** 363-373.

VOGEL, C. F. A., SCIULLO, E., WONG, P., KUZMICKY, P., KADO, N. & MATSUMURA, F. (2005). Induction of proinflammatory cytokines and C-reactive protein in human macrophage cell line U937 exposed to air pollution particulates. *Environmental Health Perspectives* **113,** 1536-1541.

WANG, F., WANG, J., DENG, X., SUN, H., SHI, Z., GU, Z., LIU, Y. & ZHAO, Y. (2004). Biodistribution of carbon single-wall carbon nanotubes in mice. *Journal of Nanoscience and Nanotechnology* **4,** 1019-1024.

WARHEIT, D. B., LAURENCE, B. R., REED, K. L., ROACH, D. H., REYNOLDS, G. A. M. & WEBB, T. R. (2004). Comparative pulmonary toxicity assessment of single wall carbon nanotubes in rats. *Toxicological Sciences* **77,** 117-125.

WICK, P., MANSER, P., LIMBACH, L. K., DETTLAFF-WEGLIKOWSKA, U., KRUMEICH, F., ROTH, C., STARK, W. J. & BRUININK, A. (2007). The degree and kind of agglomeration affect carbon nanotube cytotoxicity. *Toxicology Letters* **168,** 121-131.

WITTMAACK, K. (2007). In search of the most relevant parameter for quantifying lung inflammatory response to nanoparticle exposure: Particle number, surface area, or what? *Environmental Health Perspectives* **115,** 187-194.

WORLE-KNIRSCH, J. M., PULSKAMP, K. & KRUG, H. F. (2006). Oops they did it again! Carbon nanotubes hoax scientists in viability assays. *Nano Letters* **6,** 1161-1168.

XIA, T., KOVOCHICH, M., BRANT, J., HOTZE, M., SEMPF, J., OBERLEY, T., SIOUTAS, C., YEH, J. I., WIESNER, M. R. & NEL, A. E. (2006). Comparison of the abilities of ambient and manufactured nanoparticles to induce cellular toxicity according to an oxidative stress paradigm. *Nano Letters* **6,** 1794-1807.

YAMAWAKI, H. & IWAI, N. (2006). Cytotoxicity of water-soluble fullerene in vascular endothelial cells. *American Journal of Physiology Cell Physiology* **290,** C1495-1502.

Appendix A

Date: Mon, 13 Aug 2007 09:28:42 +0200
From: Permissions Europe/NL <permissions.dordrecht@springer.com>
To: Shane Journeay <shane.journeay@usask.ca>

With reference to your request (copy herewith) to reprint material on which Springer Science and Business Media control the copyright, our permission is granted, free of charge, for the use indicated in your enquiry.

This permission

* allows you non-exclusive reproduction rights throughout the World.

* excludes use in an electronic form. Should you have a specific project in mind, please reapply for permission.

* requires a full credit (Springer/Kluwer Academic Publishers book/journal title, volume, year of publication, page, chapter/article title, name(s) of author(s), figure number(s), original copyright notice) to the publication in which the material was originally published, by adding: with kind permission of Springer Science and Business Media.

- Material may not be republished until at least one year after our publication date.

- The material can only be used for the purpose of defending your dissertation, and with a maximum of 30 extra copies in paper.

Permission free of charge on this occasion does not prejudice any rights we might have to charge for reproduction of our copyrighted material in the future.

Sincerely yours

Inge Weijman
-
Inge Weijman
Springer
Special Licensing Department
-
Van Godewijckstraat 30 | 3311 GX
Office Number: 04C16b
P.O. Box 17 | 3300 AA
Dordrecht | The Netherlands
tel +31 (0) 78 657 6130

fax +31 (0) 78 657 6300
Inge.Weijman@springer.com
www.springeronline.com
-

-----Original Message-----
From: Shane Journeay [mailto:shane.journeay@usask.ca]
Sent: Thursday, August 02, 2007 7:12 PM
To: Permissions Europe/NL
Subject: RE: figure request

I am inquiring about the steps required to gain permission to use a figure from an article published in 'Cardiovascular Toxicology'.The journal article I am referring to is:

Vogel CF, Sciullo E, Matsumura F.
Activation of inflammatory mediators and potential role of ah-receptor ligands in foam cell formation. Cardiovascular Toxicology. 2004;4(4):363-73.
PMID: 15531779,,, DOI 10.1385/CT:4:4:363

I would like to use Figure 3A,B to show the U937 cells in a PhD dissertation only.

Please let me know what is required of me to gain permission for the use of these 2 images, in the dissertation.

I look forward to hearing from you again so I can proceed.

Shane Journeay

Appendix B

Invited Presentations, Awards, Professional Activities related to this research work:

Invited presentations

1) Journeay, W.S. *Pulmonary toxicity studies of the helical rosette nanotubes: Implications for nanomedicine and nanotoxicology.* Presentation to Canadian Federation of Biological Sciences / CIHR Nanomedicine workshop - Nanotoxicology and potential health effects symposium. Waterloo, ON, June 20-21, 2007

2) Journeay, W.S. *Nanoparticles and occupational health – What's the big deal about something so small?* Presentation to: Alberta Occupational Health Nurses Association – Education Day. Edmonton, AB, May 9th, 2007.

3) Journeay, W.S. *Occupational Health Issues for Nanotechnology*. Presentation and workshop participation: Health Canada – Workshop on Nanotechnology Strategy Development for the Health Portfolio. Ottawa, ON March 19-20, 2007.

4) Journeay, W.S. *Nanotoxicology and Industry*. Presentation and expert panel participation to: United States Environmental Protection Agency – Workshop on Nanotechnology Risk Assessment and Human Health. Chicago, IL, USA, September 7, 2006

5) Journeay, W.S. *Health impacts of nanomaterials: A crash course in nanotechnology and the life sciences*. Veterinary Biomedical Sciences seminar series -University of Saskatchewan, Saskatoon,SK, February 2005

6) Journeay, W.S. *Nanotechnology: Implications for occupational hygiene*. Full day professional development course delivered to Alberta Chapter of American Industrial Hygienists Association. Calgary,AB, Canada November 6th, 2005.

Awards

1) International Space University – Summer Session Program Scholarship CFISU 2006 $27000 - *Represented Canada at this program of 104 people from 27 countries*

2) PerkinElmer Life Science Toxicology Innovation & Leadership Award 2004-05 $500

3) BioContact-CIHR Next Generation Research Competition - 1 of 12 National Finalists

4) Dick Martin National Scholarship Award – Canadian Centre for Occupational Health and Safety $1000
- Essay title: *Nanotechnology: A new challenge for occupational health and safety*.

5) Canadian Institutes of Health Research Doctoral Award - $22 000 (National Award)

- Project title: *Nanoparticle uptake and toxicity in the lung*

6) 1st prize Graduate Student Poster – American Association of Anatomists - $400
- Experimental Biology / IUPS – San Diego,CA 2005

7) 2nd Prize poster award in the Cardiovascular/ Respiratory Sciences section - $50
- University of Saskatchewan Life Sciences Research Conference 2005

8) Pfizer award for best poster in basic sciences - $100
- Western College of Veterinary Medicine Research Day 2005

9) Travel award - 3rd Annual Nanomedicine symposium, Edmonton, AB 2005 - $500

10) Late-breaking abstract Travel Award – American Association of Anatomists
- Experimental Biology - Washington,DC 2004 - $150

11) Trudeau Foundation Scholar Nominee for the University of Saskatchewan 2004

Non-peer reviewed work:

1) ***Nanotoxicology and Industry –*** Presentation summary for US EPA Workshop on Human and Environmental Health Risk Assessment of Nanotechnology. Chicago, IL, USA, September 2007

2) ***MiNI: Micro and nanotechnology initiative – From Tiny to Infinity.*** International Space University Summer Session Program Team Project. 39 authors from 19 countries. A report assessing the use of micro and nanotechnologies in the space industry

3) ***Nanotechnology: A new challenge for occupational health and safety.*** Essay published in Canadian Centre for Occupational Health and Safety website as part of the Dick Martin Scholarship Award http://www.ccohs.ca/scholarship/winners/2004-05.html

Workshops:

1) ***Developing Experimental Approaches for the Evaluation of Toxicological Interactions of Nanoscale Materials -****A workshop addressing the challenges of conducting and interpreting studies of potential toxic effects of nanoscale materials.* Nov 2-4, 2004. University of Florida, Gainesville, FL, USA

2) ***US EPA Workshop on Human and Environmental Health Risk Assessment of Nanotechnology***. Chicago, IL, USA, September 2007

3) ***Towards a Nanotechnology Strategy for the Health Portifolio.*** Health Canada. Ottawa, ON. March 2007

Professional Activity

1) Member of Canadian Standards Association working group on Nanotechnologies. June 2007- Present.
2) TOX 412 – Nanotoxicology lecture, University of Saskatchewan 2006 & 2007